Targeting neoepitopes derived from KRAS mutations for cancer-specific immunotherapy

A dissertation submitted to attain the academic degree of

Doctor of Philosophy (Ph.D.)

from the Faculties
University Medical Center,
Social Sciences, Media, and Sports,
Chemistry, Pharmaceutical Sciences, Geography, and Geosciences,
and
Biology
of the Johannes Gutenberg University Mainz

Saber Ebrahimi
Born on 21.03.1988 in Karaj, Iran

This present work was performed from August 2019 to July 2024 in the Department of Internal Medicine Ⅲ, University Medical Center of the Johannes Gutenberg University Mainz.

First Supervisor: PD Dr. rer. physiol. et med. habil. Udo Hartwig

Second Supervisor: PD Dr. rer. nat. et med. habil. Ernesto Bockamp

Examination committee:

1. PD Dr. Udo F. Hartwig
2. PD Dr. Ernesto Bockamp
3. PD Dr. Matthias Bros
4. Prof. Dr. Bodo Plachter
5. PD Dr. Borhane Guezguez

Date of oral examination: 26/August/2024

Zusammenfassung

Hintergrund: Bei soliden Tumoren sind Mutationen im Proto-Onkogen Kristen Rat Sarcoma (*KRAS*) sehr häufig. Eine der vorherrschenden onkogenen Mutationen von *KRAS* ist eine singuläre Mutation im Codon 12, die z.B. in 28% aller Fälle zum Austausch der Amonsäre Glycin in Valin (G12V) führt. Trotz jahrelanger Bemühungen konnte bisher kein Medikament oder Impfstoff entwickelt werden, intrazelluläre mutierte Proteine wirksam anzugreifen, die von humanen Krebszellen mit *KRAS* G12V Mutation exprimiert werden. Trotzdem können Peptide, die von den intrazellulären mutierten Proteinen stammen, verarbeitet und über humane Leukozyten-Antigen-Klasse-I Moleküle auf der Oberfläche von Krebszellen als Peptid-HLA Komplex (pHLA) exprimiert werden. Diese mutationsassoziierten Neoantigene (MANA) sind attraktive intrazelluläre Ziele für die Immuntherapie.

Methoden: Einzelkettige variable Fragmente, die für $KRAS^{G12V}$ pHLA Komplexe spezifisch sind, wurden in die TCR-mimetischen chimären Antigenrezeptoren (TCRm CAR) und die T-Zell-bindenden bispezifischen Antikörper umkonstruiert. Zwei neuartige Methoden namens CAR-J-Repoter- und bispezifische T-Zell-Engagrs (BiTEs)-Assays wurden verwendet, um die Spezifität von den konstruierten TCRm CARs und den bispezifischen Antikörpern zu optimieren.

Ergebnisse: Wir haben gezeigt, dass sowohl die bispezifischen Antikörper als auch die TCR-mimetischen CAR in der Lage sind, T-Zellen zu aktivieren und Tumorzellen abzutöten, die mutiertes $KRAS^{G12V}$ Peptid in verwandten HLA-Komplexen beherbergen. Usere Ergebnisse zeigen, dass T-Zellen rekrutierende bispezifische Antikörper bie der Abtötung von Tumorzellen effizienter als TCRm CARs sind. Die Jurkat-NFAT- Reporterzellen haben ebenfalls Beweise geliefert, die diese Ergebniss stützen.

Konklusion: Wir konnten sowohl eine “TCR-like“ CAR T-Zell - als auch eine bispezifische Antikörper-basierte Immuntherapie entwickeln, um $KRAS^{G12V}$ Neoantigene im Kontext einer HLA-Allel-spezifischen Expression auf Krebszellen anzugreifen. Damit ist dieser Immuntherapieansatz prinzipiell in der Lage, Peptide intrazellulärer Proteine zu erkennen, die von mutierten Genen stammen und die mit klassischen monoklonalen Antikörpern oder einer klassischen CAR T-Zelltherapie nicht erreicht werden.

Abstract

Background: In solid tumors, mutations in the proto-oncogene Kristen Rat Sarcoma (*KRAS*) are highly common. One of the predominant oncogenic mutations of *KRAS* is a single amino acid mutation at codon 12, especially G12V, which accounts for 28% of all mutations in G12. In spite of decades of effort, no drug or vaccine has been able to effectively target intracellular mutated proteins expressed by human cancer cells with *KRAS* G12V mutation. Nevertheless, peptides derived from intracellular mutant proteins can be processed and presented by human leukocyte antigen class I molecules and expressed on the surface of cancer cells as peptide-HLA complexes (pHLA). These mutation-associated neoantigens (MANAs) are attractive intracellular targets for immunotherapy.

Methods: Single-chain variable fragments (scFvs) specific for $KRAS^{G12V}$ pHLA complexes were converted into TCR-mimic chimeric antigen receptors (TCRm CARs) and T-cell engaging bispecific antibodies. Two novel methods called CAR-J reporter and bispecific T-cell engager (BiTE) assays were used to optimize the specificity of engineered TCRm CARs and bispecific antibodies.

Results: We demonstrated that both bispecific antibodies and CARs derived from TCR-mimics were capable of activating T cells and killing tumor cells harboring mutant $KRAS^{G12V}$ peptide in cognate HLA complexes. Our results indicate that T cells-recruiting bispecific antibodies are more efficient in lysing tumor cells than TCRm CARs. Jurkat-NFAT reporter cells have also provided evidence to support these findings.

Conclusion: We developed both antibody-based immunotherapy and cellular immunotherapy approaches for targeting $KRAS^{G12V}$ neoantigens on cancer cell surfaces. In addition, this immunotherapy approach is capable of targeting intracellular proteins that originate from mutated genes and that are difficult to target with conventional monoclonal antibodies (mAbs) or classical CAR T cell therapy.

List of Abbreviations

°C	Celsius
µg	Microgram
µl	Microliter
µM	Micromolar
ABC	Avidin-biotin complex
ACT	Adoptive T-cell therapy
AEC	3-Amino-9-ethylcarbazole
α-MEM	Minimum Essential Medium Eagle Alpha Modification
AP-1	Activator Protein-1
APC	Antigen presenting cell
BiTE	Bispecific T-cell engager
bp	Base pair
BSA	Bovine serum albumin
CAR	Chimeric antigen receptor
CD	Cluster of differentiation
CLP	Common lymphoid progenitor
CRC	Colorectal adenocarcinoma
CTL	Cytotoxic T lymphocyte
CTLA-4	Cytotoxic T-lymphocyte-associated protein 4
dH2o	Distilled water
DMEM	Dulbecco's Modified Eagles Medium
DMSO	Dimethyl sulfoxide
DNA	Deoxyribonucleic acid
dNTP	Deoxynucleotide triphosphate
EDTA	Ethylendiamintetraacetat
ELISpot	Enzyme-linked immune spot assay
ER	Endoplasmic reticulum
E:T	Effector: Target
FACS	Fluorescence-activated cell sorting
FBS	Fetal bovine serum
FcγR	Fc gamma receptor
FDA	Food and Drug Administration
Fluc	Firefly luciferase
GAPs	GTPase-activating proteins
GEFs	Guanine nucleotide-exchange factors
G12V	Glycine amino acid at position 12 is substituted by Valine amino acid
hr	Hour
HA-tag	Hemagglutinin-tag
His-tag	Hexahistidin-tag
HLA	Human leukocyte antigen
H2O	Water
HSCs	Hematopoietic stem cells
ICIs	Immune checkpoint inhibitors
IFN-γ	Interferon gamma
IL	Interleukin

IRES	Internal ribosomal entry site
JNL	Jurkat-NFAT reporter cell
kb	Kilo base
KRAS	Kristen Rat Sarcoma
L	Liter
LTR	Long terminal repeat
M	Molar
mAb	Monoclonal antibody
MANAs	Mutation-associated neoantigens
MHC	Major histocompatibility complex
Min	Minute
ml	Milliliter
mM	Millimolar
MPPs	Multipotent progenitors
NEB	New England Biolabs
NFAT	Nuclear Factor of Activated T cells
NF-κB	Nuclear Factor kappa B
ng	Nanogram
NK cell	Natural killer cell
NSCLC	Non-small-cell lung carcinoma
PBL	Peripheral blood lymphocyte
PBMC	Peripheral blood mononuclear cell
PCR	Polymerase chain reaction
PD-1	Programmed death-1
PDAC	Pancreatic ductal adenocarcinoma
PD-L1	Programmed death-Ligand 1
PFA	Paraformaldehyde
pHLA	Peptide-Human leukocyte antigen
pMHC	Peptide-Major histocompatibility complex
rpm	Revolutions per minute
RT	Room temperature
scFv	Single-chain variable fragment
SDS	Sodium Dodecyl Sulfate
sec	Second
TAAs	Tumor-associated antigens
TAE	Tris-acetate-EDTA
TAP1, 2	Transporter associated with antigen processing type1, 2
TCR	T-cell receptor
TCR-like CAR	T-cell receptor-like chimeric antigen receptor
TCRm	T-cell receptor mimic
TIL	Tumor-infiltrating lymphocyte
TNF-α	Tumor necrosis factor alpha
TSAs	Tumor-specific antigens
V	Volt
VH	Variable heavy
VL	Variable light

List of Figures

List of Tables

Table of Contents

1. Introduction

1.1 T lymphocytes

T cells play a pivotal role in the adoptive immune response. They derive from common lymphoid progenitors (CLP) which originate from hematopoietic stem cells (HSCs) located in the bone marrow (Alberts et al., 2002). Beside T cells, CLPs differentiate into B and NK cells to constitute the lymphoid lineage of the hematopoietic system (Kondo & Motonari, 2016). Developing T cell precursor then migrate to the thymic gland for maturation. A crucial step in their maturation reflects the rearrangement of a functional T-cell receptor (TCR). Mature T cells are endowed with unique TCRs, which allows the immune system to recognize a vast variety of antigens. Upon expression, T cells must prove that their TCR can recognize individual alleles of the major histocompatibility complex (MHC) (positive selection) but do not react to self-proteins (negative selection). After leaving the thymus, T cells continue to differentiate into the periphery. T lymphocytes express either the CD4 or CD8 co-receptors and are divided into subsets based on their function to mediate cytokine support for T, B and NK cells, and execute immune-mediated cell death.

$CD4^+$ T cells are also referred to as T helper (Th) cells and comprise different Th-subsets. They assist other lymphocytes, including maturation of B cells into plasma cells and memory B cells, induce activation of cytotoxic $CD8^+$ T cells and regulate macrophage activity. Helper T cells are stimulated by antigen-presenting cells (APCs) upon recognition of peptide antigens presented by MHC class II molecules (Gutcher & Becher, 2007) and activation occurs as a result of simultaneous engagement of the TCR and co-stimulatory molecules (such as CD28) by the peptide-MHC II complex and co-stimulatory molecules on APCs. Both signals are necessary for an effective immune response. The only co-stimulatory receptor expressed constitutively by naive T cells is CD28, which interacts with its ligands CD80 and CD86 (B7.1 and B7.2, respectively) on the APC. Activated $CD4^+$T cells secrete various cytokines such as e.g. interleukin (IL)-2 and IL-4, which promote T cell proliferation and differentiation of T and B cells (Croft & Dubey, 2017). The expression of a wide variety of proteins changes on the surface of a T cell after full activation. Checkpoint molecules such as cytotoxic T-lymphocyte-associated protein 4 (CTLA-4) expression is increased on activated T cells, which outcompetes CD28 for binding to CD80/CD86. It is a

mechanism that prevents T cells from becoming overactivated (Maverakis et al., 2015). $CD8^+$ cytotoxic T cells (CTLs), destroy tumor and virus-infected cells, and are responsible for transplant rejection. They recognize target cells by binding to peptides presented by MHC I molecules, expressed on the surface of all nucleated cells. Cytotoxic T cells are capable of producing e.g. the cytokines IFN-γ and TNF-α, which influence other immune cells and induce receptor-mediated apoptosis.

In response to their cognate peptide/MHC interaction, antigen-naive T cells develop into CD45RA memory and CD45RO effector T cells (Akbar et al., 1988). Upon re-exposure to a known antigen, memory T cells develop into large numbers of effector T cells. Hence, they provide the immune system with memories of previously encountered pathogens. A remarkable feature of T cells is their ability to distinguish healthy from abnormal cells (cancer). Healthy cells express a large number of self-derived peptide-MHC complexes on their cell surface, but do not cause T cell stimulation. However, T cells respond to the same cell containing cancer-derived peptide-MHC complexes. This intrinsic feature of T cells, which is termed antigen discrimination, is mediated by the T cell receptor (TCR). Mammalian T cells express a unique TCR with distinct binding parameters for pMHCs. Variations in the receptors of T cells emerge from a random process in the thymus during T cell development, called V(D)J recombination (Vrisekoop et al., 2014). The result of this process is the formation of more than 10^{15} distinct receptors (Zarnitsyna et al., 2013). Despite the benefits of this diversity to the host, it poses the risk of reacting against self-pMHCs. To prevent reacting of recombined TCRs with self-pMHCs, T cells undergo layers of control in thymus, namely ′positive selection′ and ′negative selection′. As a result of these forms of selection, T cells are generated and educated with TCR signaling machinery in a way that limits future responsiveness to closely related self-antigens, while maintaining their responsiveness to foreign pMHCs (Wong et al., 2021).

1.2 Cancer and focus on *RAS* family of proto-oncogenes

Cancer is fundamentally a disease of tissue growth deregulation. The genes that regulate cell growth and differentiation must be altered in order to transform a normal cell into a cancer cell (Croce, 2008). The affected genes are divided into a broad range of categories. Oncogenes are genes that promote cell growth and reproduction. Cancer suppressor genes inhibit cell division and proliferation. Approximately 19.3

million new cancer cases and almost 10 million cancer deaths occurred worldwide in 2020. The global cancer burden is expected to increase by 47% from 2020 to 28.4 million cases in 2040. In 2020, lung cancer was estimated to account for 2.2 million new cancer cases and 1.8 million cancer-related deaths, representing approximately one in 10 (11.4%) cancers diagnosed and one in five (18%) cancer deaths (Sung et al., 2021).

In human cancers, the first proto-oncogenes discovered were *HRAS*, *NRAS*, and *KRAS*, which are members of the *RAS* family. All three subfamily members trigger three major cell signaling pathways- RAF/MEK/ MAPK, PI3K/AKT, and RAL-GDS- and play pivotal roles in mediating signals related to proliferation, differentiation, regulation of growth, and survival of cells (Fernández-Medarde & Santos, 2011). In the presence of somatic single-point mutations within these *RAS* proto-oncogenes, they become oncogenes that have been associated with cancer prognosis and carcinogenesis. Such alterations are evidently found in 27% of all human cancers, predominantly by mutated *KRAS* isoforms (85%), followed by mutated *NRAS* (11%) and *HRAS* (1% to 4%) isoforms (Hobbs et al., 2016; Kodaz et al., 2017). The mechanism by which RAS isoforms are regulated and distributed across different types of tissues is unknown, but mutations in *RAS* are tissue-specific among cancer cells. *KRAS* mutations are highly prevalent in lung, pancreatic, and colorectal adenocarcinomas. Mutated *NRAS* is commonly found in cutaneous melanoma, while *HRAS* mutations are frequently observed in neck and head squamous cell carcinomas (Fernández-Medarde et al., 2011; Hobbs et al., 2016; Cox et al., 2014).

1.2.1 *KRAS* proto-oncogene and its role in cell signaling

The proto-oncogene Kristen Rat Sarcoma (*KRAS*) encodes a GTP-binding protein that binds to the plasma membrane and acts as a GTPase switch to activate downstream signaling pathways for cell proliferation (Rajasekharan & Raman, 2013; Jancík et al., 2010). The *KRAS* gene contains 6 exons and has 2 alternative splice variants namely, KRASA4 and KRASB4. Unlike the more commonly expressed KRASB4 variant, the KRAS4A mRNA contains all 6 coding regions. Its translated product, termed KRAS, is a 188 amino acid protein with a molecular weight of 21.6 kDa (Simanshu et al., 2017; Zeitouni et al., 2016). By binding to GTP and GDP, the KRAS protein switches between active and inactive states (Bos et al., 2007). Transition between two states is

controlled by guanine nucleotide-exchange factors (GEFs) and GTPases-activating proteins (GAPs) (Fig. 1.1). GDP-bound KRAS is inactive in quiescent cells until it is activated by extracellular stimuli such as growth factors, cytokines, or hormones.

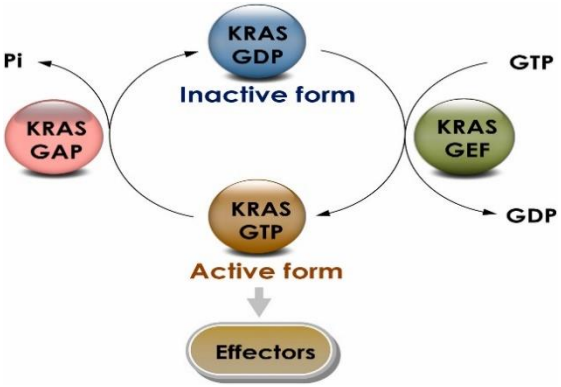

Figure 1.1: KRAS regulation cycle. Regulation of this cycle occurs through the opposing actions of guanine nucleotide-exchange factors (GEFs), which catalyze the exchange of GDP for GTP, and GTPase-activating proteins (GAPs), which increase the rate of GTP hydrolysis to GDP. (Pingyu Liu et al., 2019)

1.3 *KRAS* mutations in cancer

KRAS mutations are drivers of oncogenesis, and occur frequently in the codons 12, 13, and less often in the codons 61, 63, 117, 119, and 146. Although the codon 13 mutation implicates a shift from glycine (G) to aspartic acid (D), codon 12 mutations include G12D, G12A, G12R, G12S, and G12V shifts. The most common substitution mutations are G12D, G12V, and G13D, which result in the KRAS protein remaining continuously active (Jancík et al., 2010; Porru et al., 2018). Approximately 80%, 40%, and 25% of all cancers diagnosed are related to *KRAS* mutations such as pancreatic ductal adenocarcinoma (PDAC), colorectal adenocarcinoma (CRC), and non-small-cell lung carcinoma (NSCLC). (Jancík et al., 2010; Magliano & Logsdon, 2013). Furthermore, *KRAS* mutations can be found in biliary tract cancer (31%), endometrium cancer (14%), ovarian cancer (14%), prostate cancer (8%), cervical cancer (7%), stomach cancer (6%), and other organs. The *KRAS* positive cancers that bear a gain-of-function substitution usually have lower survival rates than their unmutated counterparts (Jinesh et al., 2018).

1.4 Therapeutic advances for *KRAS* mutated cancers over the past decades

Surgery remains the most common first-line method of treating cancer; however, its effectiveness is limited to early-stage cancers. The use of chemotherapy in combination with other regimens such as e.g. immune checkpoint blockade (ICB, see below) to enhance therapeutic responses for *KRAS* positive cancers is increasingly being applied. Despite these advances, therapeutic efficacy has been limited due to toxicity and partial responses of ICB. There are several adverse effects associated with the use of chemotherapeutic drugs (Goffin et al., 2010; Zeichner et al., 2016; Ranpura et al., 2011) as for example the expression of key DNA repair proteins results in resistance to platinum agents and poor outcomes in patients with non-small-cell lung cancer (NSCLC) (Olaussen et al., 2006; Lord et al., 2002).

In the treatment of *KRAS* positive cancer, targeted therapies can be viewed as an evolved form of non-specific chemotherapy. A number of mAbs that inhibit ligand-induced receptor activation, including antibodies to VEGFR and EGFR, have been developed (Lau et al., 2014; Hansen & Jakobsen, 2011; Miyamoto et al., 2017). Recently, it has been reported that mutated *KRAS* cancers are resistant to anti-VEGFR and anti-EGFR therapies, while only wild-type *KRAS* patients respond to these therapies (Masoud & Pagès, 2017; Shaib et al., 2013). In addition to antagonistic mAbs, thymidine kinase inhibitors (TKIs) such as e.g. Afatinib or Sotorasib have been developed to block phosphorylation of ADP or GDP by kinases either associated with EGRF activity or mutated $KRAS^{G12C}$ signaling In particular, Sotorasib has recently been demonstrated in several clinical studies to effectively inhibit of $KRAS^{G12C}$ signaling leading to partial remission (Lee, 2022). However, tumors frequently develop resistance to TKIs during treatment which results in loss of therapeutic efficacy. (Ostrem & Shokat, 2016; Patricelli et al., 2016; Lito et al., 2016). The development of inhibitors targeting pathways downstream of KRAS, e.g. MEK1/MEK2 inhibitor, PI3K inhibitors approved for advanced *KRAS* mutated NSCLC (Fig. 1.2). A recent study, however, reported that MEK and PI3K inhibitions were ineffective in mutant *KRAS* lung models (Chan & Hughes, 2015; Engelman et al., 2008; Hata et al., 2014). Hence, using our immune system to combat cancer is considered a future treatment.

Cancer patients with *KRAS* mutations may benefit from immunotherapy, which harnesses the host's immune system to fight tumor cells. Targeted programmed-death ligand-1/programmed death-1 (PD-L1/PD-1) immunotherapy is an attractive cancer

treatment (Jiang et al., 2019). A high level of expression of PD-L1 has been found on the surface of many tumor cells (Qin et al., 2015; Lin et al., 2015). To remove immunosuppression and restore immune function, ICB antibodies designed to block the PD-L1/PD-1 pathway. ICBs have a good therapeutic effect in patients with high expression of PD-L1, whereas the therapeutic effect is low in treatment of NSCLC patients with low expression of PDL-1 (Carbone, 2017). It has recently become possible to use immunotherapy-based treatments to activate the host immune system to respond to tumor-specific antigens (TSAs). Cancer vaccines and T cell-based immunotherapy are two approaches that are being developed for targeting mutant *KRAS*. For instance, DNA vaccines deliver plasmid DNA encoding and expressing desired tumor-specific antigens (TSAs) to cause antitumor immunity (Fioretti et al., 2010; Yang et al., 2014). A DNA vaccine targeting the mutant *KRAS* was administered by Weng et al. in 2014 and demonstrated effective anti-tumor activity against transgenic mouse lung cancer models (Weng et al., 2014). T cell-based immunotherapy targets mutant KRAS neoantigens by creating T cells that are highly reactive to tumor cells with relevant *KRAS* mutations.

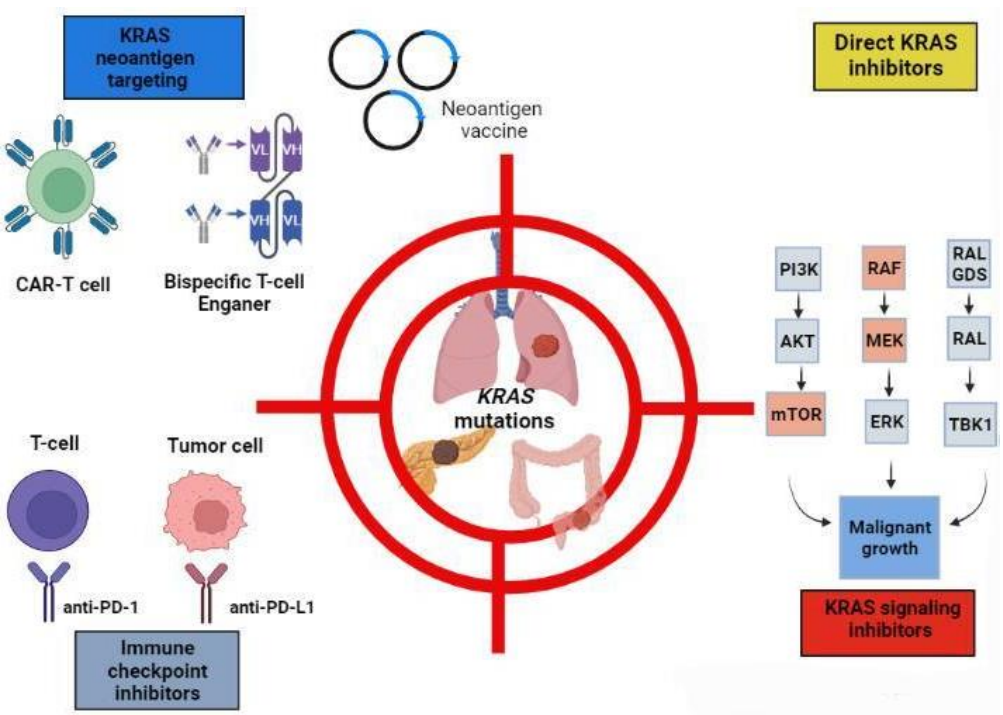

Figure 1.2: Current and future treatments for cancers with *KRAS* mutation. KRAS-targeted drugs, as well as immunological approaches targeting mutant KRAS neoantigens. The illustration was created with https://BioRender.com.

1.5 Adoptive T-cell immunotherapy

Typically, three types of cancer treatment are available: surgery, radiotherapy, and chemotherapy. The field of immunotherapy has recently emerged as a powerful and potentially curative therapy to target malignant tumors using the immune system. Historically, the concept of using immune cells to treat cancer cells dates back to the nineteenth century, when Wilhelm Busch and Friedrich Fehleisen observed that tumor regression declined following the development of a superficial skin infection. Later, they described an association between immune cells and cancer (Oiseth & Aziz, 2017).

Given the anti-leukemic effect of donor-derived T lymphocytes transferred into patients following allogeneic hematopoietic stem cell transplantation, termed donor lymphocyte infusion (DLI) (Weiden, 1979), and the reinfusion of ex vivo expanded tumor-infiltrating lymphocytes originally isolated from tumor specimens of melanoma patients (Rosenberg, 1988, 1994) adoptive cellular therapy (ACT) is a type of immunotherapy that involves in vitro isolation and expansion of either antigen-specific or specificity-redirected T cells and their incorporation into the body of the patient (Maus et al., 2014; Rosenberg & Restifo, 2015) (Fig. 1.3). ACT-induced immunity has numerous beneficial properties: 1) T cells distinguish between normal and cancerous cells, therefore immune responses will be specific, 2) T cell responses are robust, undergoing clonal proliferation following activation 3) cellular immunity creates memory, which allows maintain immunity responses for many years following initial therapy. In order to elicit durable responses for TIL-based ATC, the presence of effector T cells with anti-tumor activity is necessary, which has not been the case for some types of cancers (Perica et al., 2015). Therefore, new approaches were needed to enhance T cell activity and proliferation for sustained immunity. This led to the development of genetically modified T cells expressing chimeric antigen receptors

(CARs) or novel T-cell receptors (TCRs) and ACT of genetically modified T cells has shown potent and durable clinical results.

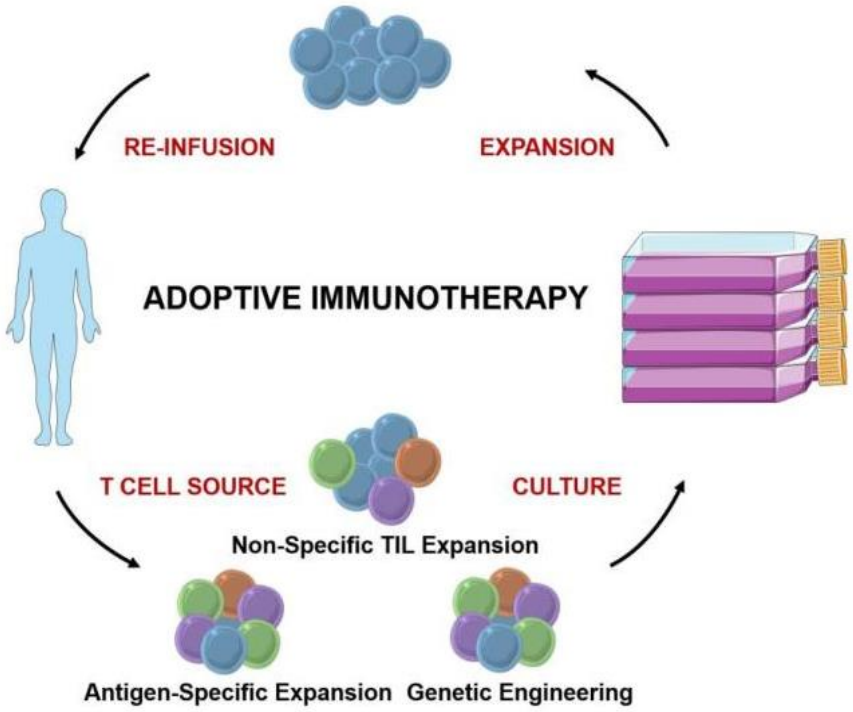

Figure 1.3: Adoptive T-cell immunotherapy. T cells are harvested from either tumors-infiltrating lymphocytes (TILs) or peripheral blood lymphocytes (PBLs). TILs can be expanded non-specifically and PBLs must be generated either through antigen-specific expansions or through genetic engineering. These cells are then reinfused into patients after they have been expanded in vitro. (Karlo Perica et al., 2015).

1.6 Neoantigens

Gene mutations resulting from genetic instability during carcinogenesis occur both in the coding and non-coding region. Changes in amino acid sequences resulting from mutations in coding regions can result in proteins that are not present in normal cells (Nakagawa & Fujita, 2018). These intracellular proteins can be degraded by proteasome into short peptides, which are presented on the cell surface by human leukocyte antigen (HLA) molecules as a peptide-HLA (pHLA) complex (Hewitt, 2003). Peptides bound to HLA molecules can activate the immune system and cause the immune system to attack cancer cells. These altered self-antigens, called neoantigens, are derived from gene mutations and can be recognized by T cells (Tran et al., 2017; Yarchoan et al., 2017). Neoantigens are thus ideal targets for cancer vaccines and T cell-based immunotherapy since they are specific to malignant cells. Neoantigens are divided into shared neoantigens and individual neoantigens (Sahin

& Tureci, 2018; Schumacher & Schreiber, 2015). Shared neoantigens are antigens that are common to cancer patients and are not present in normal genomes. Shared neoantigens that are highly immunogenic have the potential to be applied as broad-spectrum therapeutic cancer vaccines for cancer patients with the same mutated gene (Zhao et al., 2020; Klebanoff & Wolchok, 2018). A personalized neoantigen on the other hand refers to mutated antigens that are unique to most neoantigens and completely differ from patient to patient. Thereby, personalized neoantigen preparation drugs can only be specifically targeted to each patient (Tureci et al., 2018). Tumor antigens can be classified into two major groups based on the origin of the peptide component: tumor-specific antigens (TSAs) and tumor-associated antigens (TAAs). TSAs include mutated self-antigens (neoantigens), specific fusion proteins, and oncogenic viral antigens. TSAs have the potential to be a target for cancer immunotherapy, since they are expressed exclusively by tumor cells, limiting the adverse effects of immune approaches to tumors and mitigating off-target effects (Zhijian & Mitchell, 2021).

1.7 Tumor-associated antigens

Tumor-associated antigens (TAAs) are proteins expressed by unmutated genes. It appears that these antigens are significantly over-expressed by tumor cells but rarely expressed by normal cells (Zamora, 2018). TAAs are subject to central and peripheral immune tolerance, since they are normal host proteins (Yarchoan et al., 2017; Pelletier & Mukhtar, 2020). The majority of TAAs are abnormally overexpressed antigens. Even though targeting TAAs is highly effective, it still results in the death of target-positive normal cells (e.g. anti-CD19 and anti-CD20 antibodies used against B-cell lymphomas) (Aaron et al., 2016).

1.8 Antigen processing and presentation

Protein processing machinery plays a significant role in driving the presentation of TCR epitopes. The proteasome is a major enzyme complex that degrades proteins into short peptide sequences. Degraded cytosolic peptides are transferred to the endoplasmic reticulum (ER) by transporters associated with antigen processing type 1 (TAP1) and TAP2 where the N-terminus can be trimmed by aminopeptidases prior to binding to MHC class I molecules. (Fig. 1.4). Precise knowledge of the rules

governing which protein fragments are ultimately expressed on the cell surface is still warranted, and identification of epitopes is largely an empirical process. In some cases, peptides may be produced, but their affinity for MHC molecules is low. Other peptides may bind to MHC with high affinity, but fail to reach the cell surface due to insufficient processing (Luckey et al., 1998). Thus, many potentially interesting targets are not available as MHC-presented peptides. HLA restriction also selects only a subset of amino acid sequences for presentation, which means the TCR may only be effective for a specific subset of patients (Ataie et al., 2015). Furthermore, since the epitope contains a linear peptide within a MHC molecule, there is also the possibility of cross-activity with other linear peptide sequences that are homologous to the chosen epitope and could be presented on non-target cells.

The presentation of a peptide on a MHC molecule requires adequate intracellular expression of the parent protein, proper proteolytic cleavage, peptide transport into the endoplasmic reticulum (ER) through TAP proteins, and efficient loading of the peptide onto MHC molecules for transport to the cell surface. (Bassani-Sternberg et al., 2015).One of the major obstacles to TCR therapy is down-regulation of MHC class I expression on the tumor cell surface. In some cases, there has been a down-regulation of MHC class I of up to 90% (Cabrera et al., 1996).

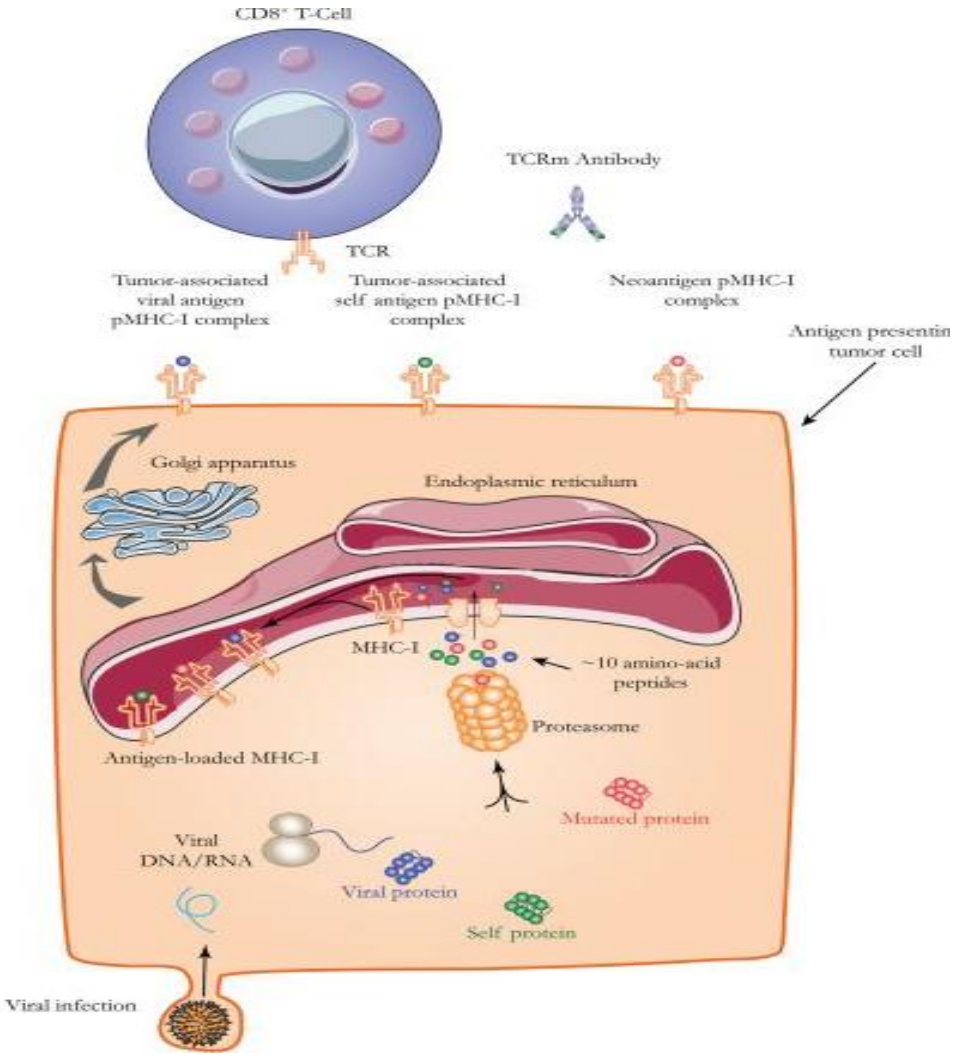

Figure 1.4: Illustration of antigen processing for cell surface presentation. A proteasome processes cytosolic proteins, including foreign proteins from viral infection or phagocytosis. The process generates short peptide sequences that are then transported into the endoplasmic reticulum. There, they bind to MHC class I molecules. The Golgi apparatus transports the pMHC assembly to the cell surface. (Yixiang Xu et al., 2019)

1.9 Neoantigens derived from *KRAS* gene with G12V mutation

To identify potential targets to be exploited in the immunotherapy field, numerous techniques have recently been introduced to reveal repertoires of neoantigens. These techniques include genomic sequencing and algorithm-based predictions, the use of mass spectrometry or targeted detection approaches for profiling the immunopeptidome, as well as indirect assays on T cell reactions (Bassani-Sternberg et al., 2016; Danilova et al., 2018; Wang et al., 2019).

The selection of neoantigens is based on their frequency of mutations and the predicted strength of their binding to HLA alleles. In human cancers, *KRAS* is one of

the most frequently mutated genes, and the mutation G12V is one of the most common mutations in *KRAS*, as well as in *HRAS* and *NRAS* (Andreatta et al., 2016; Maiers et al., 2007). A previous study reported artificial intelligence (AI)-based prediction of HLA-bound peptides derived from this mutation using NetMHC algorithm (Table1.3) (Skora et al., 2015). Peptides bearing the G12V mutation are predicted to bind to HLA-A*0201 and HLA-A*0301, which are the most common alleles of HLA in many human populations. Such computer-based predictions have been demonstrated to be inadequate for clinical use. It is also possible to determine neoantigens by co-culturing tumor cells with autologous T cells followed by tetramer staining or peptide-pulsing assays. As these functional assays are technically challenging and time consuming, they cannot be used in clinical settings (Lu et al., 2014). For the detection of these neoantigens, Mutation Associated Neoantigen Selected Reaction Monitoring (MANA-SRM) has been developed in recent years. This platform has a higher sensitivity than previously published techniques available for this purpose, and no prediction or cell culture is required. All neoantigens evaluated for *KRAS* gene with G12V are presented in the context of HLA class I (Douglass et al., 2021). Neoantigens associated with HLA class I have a length of 8 to 12 amino acids (Sarkizova et al., 2020).

Table 1.3: Neoantigens derived from *KRAS* gene with G12V mutation. NetMHCpan-4.0 algorithm was used for prediction of peptide binding to HLA allele of interest.

Peptide name	Peptide position	Sequence	Predicted HLA-A allele	Affinity (nM)
$KRAS^{G12WT}$	[5-14]	KLVVVGAGGV	HLA-A*0201	506.91*
$KRAS^{G12C}$	[5-14]	KLVVVGA**C**GV	HLA-A*0201	373.60*
$KRAS^{G12D}$	[5-14]	KLVVVGA**D**GV	HLA-A*0201	498.01*
$KRAS^{G12V}$	[5-14]	KLVVVGA**V**GV	HLA-A*0201	300.18*
$KRAS^{G12WT}$	[7-16]	VVVGAGGVGK	HLA-A*0301	396.16
$KRAS^{G12C}$	[7-16]	VVVGA**C**GVGK	HLA-A*0301	375.53
$KRAS^{G12D}$	[7-16]	VVVGA**D**GVGK	HLA-A*0301	938.8

$KRAS^{G12V}$	[7-16]	VVVGAVGVGK	HLA-A*0301	341.99
$KRAS^{G12WT}$	[8-16]	VVGAGGVGK	HLA-A*0301	277.44
$KRAS^{G12C}$	[8-16]	VVGACGVGK	HLA-A*0301	221.43
$KRAS^{G12D}$	[8-16]	VVGADGVGK	HLA-A*0301	1172.08
$KRAS^{G12V}$	[8-16]	VVGAVGVGK	HLA-A*0301	202.62

1.10 Chimeric antigen receptor (CAR)

CAR-T cell therapy has been a great success since its introduction (June et al., 2018). A synthetic CAR redirects immune cells to recognize and eliminate cells expressing specific target antigens. CAR binding to the target antigen on the surface of the cells occurs independent of HLA restriction, which leads to intense activation of immune cells and anti-tumor responses (Sadelain et al., 2013). It also eliminates the problem that tumor cells often down-regulate HLA molecules, rendering the cells invisible to the immune system (Garrido et al., 2016). The US Food and Drug Administration (FDA) approved anti-CD19 CAR-T therapy in 2017 for patients with B cell hematological malignancies (Neelapu, 2017). A CAR consists of a variable antigen-binding region of the antibody linked to the signaling domains of a TCR or other co-stimulatory molecules. By means of genetic engineering, a scFv or, alternatively, the extracellular domain of a natural receptor are combined with a spacer region and internal signaling transduction domains, providing tailored options of CARs for various specific tumors. The first generation of CARs was designed with only an intracellular CD3ζ domain to stimulate T cells (Kuwana et al, 1987); however, these CARs failed in clinical studies due to low proliferation of T cells and cytokine production (Brocker, 2000). Subsequently, the next (2^{nd}.) generation of CARs included the intracellular signaling domain of the co-stimulatory molecules CD28, CTLA-4 or other modulators of T cell activation in order to enhance stimulation and cytotoxic ability of T cells in vivo (Finney et al., 2004; Imai, 2004) (Fig. 1.5). Moreover, more than one co-stimulatory domain can be integrated resulting in a 3^{rd}. generation CAR that contains two signaling moieties in addition to CD3ζ (Fig. 1.5). Upon additional expression of an engineered cytokine receptor or a cytokine under control of an IL-2 responsive NFAT promoter

these redirected T lymphocytes are termed “T cells redirected for antigen-unrestricted cytokine-initiated killing” (TRUCKs) or “4th. generation” CAR T cells (Fig. 1.5). In addition to T lymphocytes, other immune cells such as Natural Killer (NK) cells and macrophages can be modified to express CAR constructs (Liu et al., 2020; Klichinsky et al., 2020).

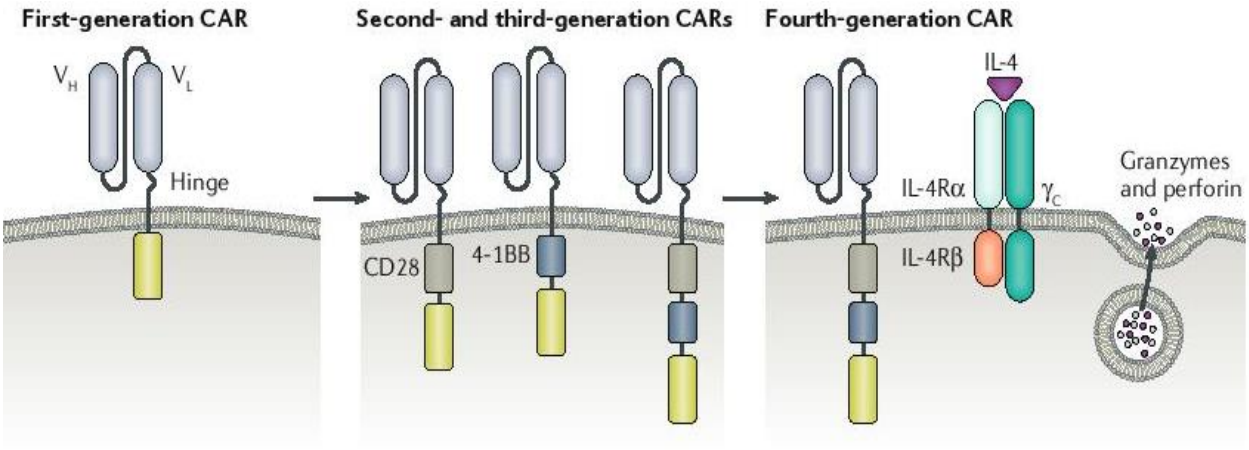

Figure 1.5: Generation of chimeric antigen receptors (CARs). CARs consist of an extracellular single-chain variable fragment of antibody coupled with an intracellular CD3ζ-signaling domain. CARs of the second and third generations contain co-stimulatory domains (CD28 or 4-1BB molecules) that enhance the activation of T cells. In order to overcome the immunosuppression of tumor microenvironment, the fourth generation of armored CARs has been developed. For example, a chemokine cytokine receptor (4αβ) contains of extracellular domain of IL-4Rα linked to IL-2/IL-15Rβ domain, signals to T cell in response to IL4, a most frequent cytokine in tumor microenvironment. (Alex Waldman et al., 2020)

1.11 T-cell receptor mimic CARs and bispecific T-cell engagers

As mentioned above CAR T cell and monoclonal antibody (mAb)-based treatments have demonstrated clinical effectiveness; however, the repertoire of target-antigens is limited to surface antigens, which represent only a small portion of the cancer proteome. These extracellular proteins include e.g. CD19, CD20, CD22, EGFR, B7-H3, and PD1/PDL1 (Kochenderfer et al., 2010; Kreitman et al., 2012; Seaman et al., 2017; Porter et al., 2011). In contrast, the majority of proteins are found intracellularly, including those that are involved in cell proliferation, growth, and death. In a cancer cell, these include overexpressed TAAs, gene products of translocations, oncofetal antigens, and tumor neoantigens such as e.g. mutated tumor suppressors or proteins involved in signaling. Traditional mAbs are not effective against intracellular cancer targets. In addition, as most of these targets are not druggable, small molecules designed for targeted therapy can only inhibit a rather small portion of oncogenic proteins. Hence, developing effective bimolecular tools against these

important and unique intracellular epitopes has recently fueled research in this area of CAR T therapy. Peptides derived from intracellular proteins can be presented on the cell surface by major histocompatibility complex (MHC) class I, also termed to as human leukocyte antigen (HLA) class I, to be recognized by a TCR on an effector T cell (Bassani-Sternberg et al., 2015; Draper et al., 2015; Mizukoshi et al., 2006). One emerging approach is to develop peptide-specific mAbs, also termed TCR-mimic (TCRm) or TCR-like antibodies that recognize epitopes just like a TCR (Wittman et al., 2006; Polakova et al., 2000; Lev et al., 2002; Denkberg et al., 2002). These composite epitopes are composed of a linear peptide sequence bound and presented by a given MHC/HLA molecule. Such epitopes can consist of peptides derived from overexpressed self-antigens, created by many mutations found in cancer cells.

The structure of TCRm antibodies is identical to conventional antibodies. However, whereas conventional antibodies recognize conformational epitopes, TCRm binds to a composite antigen comprised of a variable peptide sequence (typically 9-10 amino acids in length for HLA class I molecules) buried within a given HLA molecule which is largely invariant (Dahan & Reiter, 2012) (Fig. 1.6).

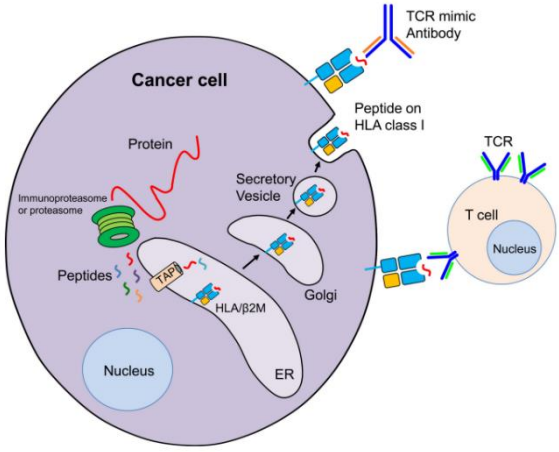

Figure 1.6: TCRm antibodies bind peptide-HLA class I complexes on the cancer cells. Cancer cells can express intracellular proteins, which are degraded by the proteasome into short peptides. Peptides are loaded onto HLA class I molecules and shuttled to the cell surface where they can be recognized by TCR on $CD8^+$ T cells. In order to recognize these intracellular or 'undruggable' proteins, TCRs, which mimic the specificity of TCRs for peptide-HLA class I complexes, can be discovered. (Aaron et al., 2016)

An important difference between a TCRm antibody and natural TCR molecule relates to affinity as TCRm have a $10^3 – 10^5$ fold stronger affinity for target cells and predictable drug-like properties (Stewart-Jones et al., 2009; Poorebrahim et al., 2021). As outlined in the previous section, the effectiveness of CAR therapy against hematological

malignancies has been demonstrated and patients have experienced durable clinical outcomes (Gill & June, 2015; Curran & Brentjens, 2015; Brentjens et al., 2013). However, traditional CARs face the same limitation as traditional mAbs in that they are directed to correctly folded and fully expressed cell surface antigens. TCR-modified T cells, on the other hand, can be directed against an intracellular protein through adaptive transfer. However, this approach is limited by HLA-restriction and thus patient-specific. Moreover, expression of an additional, transgenic, TCR in a T cell that already expresses an endogenous TCR is likely associated with mispairing of TCR chains resulting in a new “off target” specificity that might also cause autoimmunity by cross-activating previously tolerized T cells (Starck et al., 2014). Therefore, TCRm provides new possibilities for cancer treatment as they can be exploited for multiple innovative approaches.

TCRm antibodies can be conjugated with fluorescent reagents to measure the expression levels of peptide-HLA complexes on tumor cells. Using TCRm antibodies directed against MUC1-D6-derived peptide-HLA complexes on the surface of tumor cells, Cohen and colleagues quantified the number of mucin epitopes (MUC1-D6-HLA-A2) on the surface of tumor cells (hundred copies per cell). (Cohen, 2002). The study by Michaeli et al. found that melanoma cell lines express an average of approximately 4000 copies per cell of the complex of HLA-A2 and tyrosinase (369-377) and a few hundred copies per cell of gp100 and MART-1 complexes by using of TCRm antibodies directed against peptide-HLA complexes of tyrosinase, gp100, and MART-1, respectively (Michaeli, 2009). In addition, TCRm antibodies can be exploited to generate a TCR-mimic or TCR-like CAR by simply combining the scFv of TCRm with other components of a CAR already described in section 1.10. Numerous TCR-like antibodies (Fab or scFv) isolated from phage display libraries have been successfully converted to CARs (Ma, 2016). A TCR-like CAR construct can transmit a signal through transmembrane and intracellular domains without competing with endogenous TCR signaling domains. Willemsen and coworkers first introduced this approach in 2001 when a CAR construct was fused with a TCR-mimic antibody targeting the MAGE-A1/HLA-A1 complex. Through amino acid modification, affinity enhancement of TCR-mimics can improve their recognition and interaction with HLA-bound peptides (Willemsen et al., 2001). Once T cells have been transduced with lentiviral or retroviral vectors, the scFv region of the TCR-like CAR can bind to peptide-

HLA complexes on tumor cell surfaces. Multiple signaling pathways can be activated by the intracellular domain of TCR-like CAR to cause T cells to activate, differentiate, and secrete cytokines (Chames, 2000; Lev, 2002). Recently, anti-tumor effects of TCR-mimic antibodies targeting pHLA complexes have been reported in preclinical studies, and many of these components are now in clinical trials. In the past, it has been established that the use of antibody-derived moieties as the antigen recognition domain of CARs has the ability to significantly eradicate cancer cells with down-regulated antigen expression (200 copies/cell) (Watanabe et al., 2015). In this regard, Sadelain and colleagues generated TCR-mimic CAR cells restricted to NY-ESO-$1_{157\text{-}165}$ /HLA-A2. Despite the high affinity of soluble Fab fragments, they found that CAR-T cells expressing extracellular Fab domain demonstrated moderate lysis of NY-ESO-$1_{157\text{-}165}$ /HLA-A2 expressing target cells. The authors hypothesized that this might be due to the strong affinity of the Fab molecules for HLA-A2. By using a rational mutagenesis approach, they were able to lower the binding affinity of Fab to TCR level and, consequently, improved the specificity and efficacy of TCR-mimic CAR-T cells (Maus et al., 2016). Moreover, using a TCRm targeting a gp100 pMHC complex, Zhang and colleagues generated CAR-T cells against melanoma cells. These derived CAR-T cells demonstrated specific cytotoxicity against tumor cells and suppressed melanoma progression in a xenograft model (Zhang et al., 2014). Human TCRm antibodies against AFP$_{158\text{-}166}$ complexed with HLA-A2 were isolated by Liu and colleagues and converted into a CAR format for use in liver cancer treatment. In liver cancer lines and xenograft models, the AFP CAR-T cells showed potent antitumor activity (Liu et al., 2017).

In addition to TCRm based CARs, TCRm mAbs can be applied in the format of bispecific T-cell engagers (BiTEs) to target intracellular proteins by cellular immunotherapy. Thus, TCRm can be fused to scFv recognizing cell surface structures on T - or NK cells that specifically activate these immune cells. Commonly, BiTEs contain anti-CD3 scFv antibodies, which bind to T cells in a non-specific manner thereby positioning T cells in close proximity to a given cancer cell upon binding of the TCRm to the peptide-HLA complex on the surface of tumor cells. Following activation, this T cell will elicit cytotoxic effector functions and additionally release cytokines such as IFN-γ and IL-2, which will attract further immune cells, resulting in tumor cell lysis. (Dao, 2015) (Fig. 1.7). Clinical studies have demonstrated the efficacy of engineering

bispecific mAbs and bispecific T-cell engagers to induce polyclonal T cell cytotoxicity. Both $CD4^+$ and $CD8^+$ T cells are redirected by BiTEs to kill tumor cells in a serial manner, independently of the cells' intrinsic antigen specific recognition mechanisms or their co-stimulatory ligands. However, as TCRm-CD3 BiTEs depend on HLA restriction just as a TCR, peptide-specific TCRm need to be developed for HLA class I alleles that are frequently expressed in humans. In this regard, HLA-A2 and HLA-A3 are the most common alleles found at the HLA-A locus and are thus highly suitable for developing TCRm-anti-CD3 BiTEs (Bradi et al., 2012). There several reports in the literature demonstrate that this is feasible and has already been achieved in the past as for example a WT1 peptide-specific ESK-BiTE, a BiTE construct derived from the ESK1 scFv, was able to bind cancer cells expressing WT1-HLA-A2 and showed potent therapeutic activity in vitro and in vivo against multiple human cancer models by redirecting human T cell cytotoxicity (Dao et al., 2015). Moreover, Hsiue et al. developed a TCRm targeting $p53^{R175H}$ mutation-derived peptide complexed with HLA-A2. Bispecific antibodies derived from this TCRm were effective in activating T cells to kill tumor cells with this mutation (Hsiue et al., 2021). However, in contrast to conventional mAbs recognizing fully surface expressed target structures development of TCRm antibodies might be challenged with the fact the number of given peptide/HLA class complexes presented on the cancer cell surface may be limited, yielding target densities magnitude lower than typical targets for a mAb in clinical use. Despite this potential disadvantage Douglass et al. recently identified a TCRm antibody to target mutant $KRAS^{G12V}$ peptide bound to HLA-A3. Their studies demonstrated that bispecific antibodies derived from this TCRm antibody had potent anti-tumor activity against cancer cells harboring this endogenous mutation despite having low number of the complex on the cell surface (Douglas et al., 2021). Moreover, these data support earlier findings, that TCR-mimic CAR-T cell can distinguish wild-type epitopes from mutation-derived neoepitopes (Parkhurst et al., 2016) and thus may represent a very valuable approach to design CARs that are capable of recognizing tumor neoantigens derived from mutations.

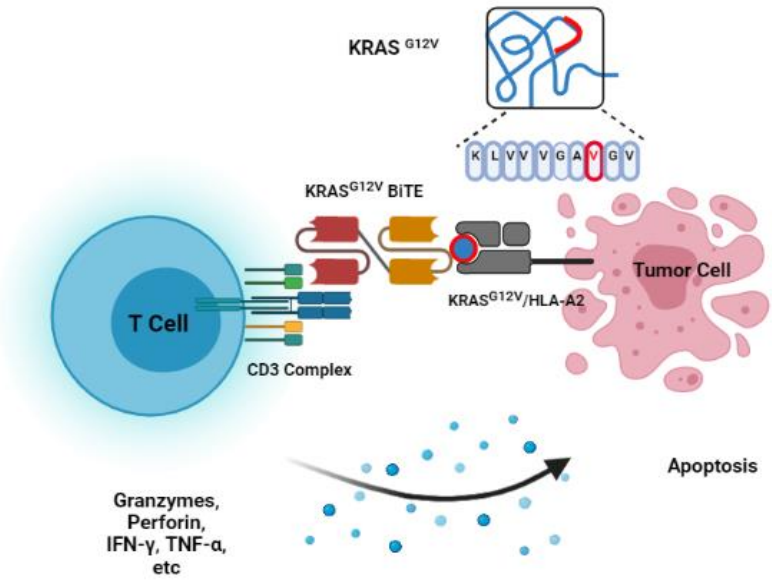

Figure 1.7: KRAS^{G12V}-specific bispecific antibody activates T cells in presence of cells presenting KRAS^{G12V} neoantigens. A diagram illustrating the mechanism of action of a bispecific antibody targeting KRAS^{G12V} peptides bound to HLA-A2. The illustration was created with https://BioRender.com.

1.12 Objectives of the project

Mutation-associated neoantigens (MANAs) are a target of anti-tumor T cells. T cells can recognize HLA-presented neoantigens. Thus, immunogenic agents targeting mutation-derived neoantigens may prove beneficial for treatment of patients harboring particular MANAs. In two recent studies conducted by one research group, single-chain variable fragments (scFvs) that bind mutation-derived neoantigens have been identified. Additionally, they have developed TCR-mimic antibodies targeting KRAS^{G12V} MANAs complexed with HLA class I (Skora et al., 2015; Douglass et al., 2021). Research on TCRm-based CARs and TCRm-derived bispecific antibodies targeting mutant (m) KRAS-derived epitopes complexed with HLA proteins has not yet been reported.

1) Therefore, the aim of this research was to design novel-target CAR and bispecific antibody constructs based on TCR-mimic and generate mKRAS-specific immune cells to destroy tumor cells presenting mutant KRAS neoepitopes, hoping to expand neoantigen-targeted therapies for future mutation-derived neoantigens.

2) To take advantage of these recently identified MANA-specific antibodies, in this work we sought to design novel-target TCRm-based CARs targeting mutant KRAS^{G12V} neoepitopes presented by HLA class I. Furthermore, this study aimed to examine the

functional impact of different KRAS^{G12V}–specific CAR constructs. Thus, two different CARs with different spacer domains should be designed. As previous comparative experiments by other groups showed that the inclusion of the hinge region with different molecule size and biological structures into CAR receptors had a different impact on functional activity of CAR formats, we aimed to explore two KRAS-specific receptors containing human IgG1-CH2-CH3 Fc and Strep-tag II as spacer domains. To characterize biological function of optimized mKRAS-specific receptors and to evaluate the presentation of mKRAS^{G12V} epitopes by tumor cells, expression of the TCR-based CARs in a NFAT inducible reporter T cell line or effector immune cells, e.g. NK-92 and T cells, served as sensitive probes.

3) We aimed to select KRAS^{G12V}/HLA-A*0201 and KRAS^{G12V}/HLA-A*0301 complexes as target. We also planned to generate TCRm-derived bispecific antibodies by genetic engineering technology to study whether mutant KRAS are presented by cognate HLA class I on cancer cells. Afterwards, a comprehensive evaluation of the properties of bispecific antibodies ("scFv-UHT1" and "LH-UCHT1") was necessary, including binding affinity, T-cell engagement using reporter cells, and antitumor activity.

2. Materials

2.1 Instruments and equipment

Table 2.1: Instruments and equipment

Equipment	**Manufacturer**
Autoclave	KGS-Sterilisatoren (Olching, BRD)
Biofuge Fresco Heraeus	ThermoFisher Scientific (Waltham, USA)
CO_2 Incubator (Heracell 150i)	ThermoFisher Scientific (Waltham, USA)
Cell counting chamber (Neubauer)	Sigma-Aldrich (Steinheim, Germany)
Cryofreezing container (5100 Cryo 1 °C)	Nalgene (Neersje, Belgium)
Electrophoresis chamber mini horizontal	neoLab (Heidelberg, Germany)
Flow cytometer (BD FACSCanto II)	BD GmbH (Heidelberg, Germany)
Fluorescence microscope (Evos)	ThermoFisher Scientific (Waltham, USA)
FluostarOmega-Reader	BMG LabTech (Ortenberg, Germany)
Freezer (Herafreez -80 °C)	Heraeus (Hanau, Germany)
Heating block (Thermomixer 5436)	Eppendorf (Hamburg, Germany)
Heraeus Megafuge 16R	ThermoFisher Scientific (Waltham, USA)
iBright gel documentation system	Thermo Fisher (Dreieich, Germany)
Ice machine (UBE 50/35)	Ziegra (Isernhagen, Germany)
Immunospot analyzer	CTL Europe GmbH (Bonn, Germany)
Laminar flow hood (HERAsafe)	Thermo Fisher (Dreieich, Germany)
Magnetic stirrer	Thermo Scientific (Waltham, USA)
Microscope (Axiovert 25)	Carl Zeiss AG (Jena, Germany)
Microtiter Plate-Harvester 96	Tomtec (Hamden, USA)
Microwave	Bosch (Stuttgart, Germany)
Multimode plate reader infinite 200 Pro	TECAN (Switzerland)
Multichannel pipette	Eppendorf (Hamburg, Germany)
Nitrogen cryobank (Espace 331 Gaz)	Air liquid DMC (Marne-la-Vallée, France)
Nitrogen tank	Cryotech (Orthoway, USA)
Pipettes (Research plus)	Eppendorf (Hamburg, Germany)
Pipettor (Pipetboy acut)	Integra Biosciences (Fernwald, Germany)

Precision scale (EW150-3M)	Kern (Balingen-Frommern, Germany)
Refrigerator-Freezer Combo (+4 °C / -20 °C)	Liebherr (Ochsenhausen, Germany)
Shaker / Incubator hood TH30	Edmund Bühler (Hechingen, Germany)
Single-channel pipettes (10 µL, 200 µL, 1000 µL)	Gilson (Middleton,USA)
Sorvall R66 Plus Centrifuge	ThermoFisher Scientific (Waltham, USA)
Spectrophotometer (NanoDrop-1000)	ThermoFisher Scientific (Waltham, USA)
Sterile work bench (Herasafe HS18)	Heraeus (Hanau, Germany)
Thermocycler	MWG-Biotech (BRD)
UV-Transilluminator	ThermoFisher Scientific (Waltham, USA)
Vortex mixer	VWR (Darmstadt, Germany)
Water bath	Memmert (Schwabach, Germany)

2.2 Consumables

Table 2.2: Consumables

Item	**Manufacturer**
Black 96-well flat-bottom plates	Greiner (Frickenhausen, Germany)
Cell culture dish (60 / 145 mm)	Greiner (Frickenhausen, Germany)
Cell culture flask (T25 / T75)	Greiner (Frickenhausen, Germany)
Cell culture plate (6 / 12 / 24 / 48 / 96-well)	Greiner (Frickenhausen, Germany)
Centrifugal filters (Amicon 10 kDa)	Millipore (Eschborn, Germany)
Cryotubes (freezing vials)	Greiner (Frickenhausen, Germany)
Disposable gloves	Semperit (Wien, Östereich)
Disposable scalpel	Feather Safety Razor Co. (Osaka, Japan)
FACS tubes	BD Biosciences (Heidelberg, Germany)
Falcon tubes (15 / 50 mL)	BD Biosciences (Heidelberg, Germany)
Pipette tips (10 / 100 / 1000 µL)	Starlab (Ahrensburg, Germany)
QIAshredder spin columns	Qiagen (Hilden, Germany)
Reaction tubes (0.2 / 0.5 / 1.5 / 2 mL)	Eppendorf (Hamburg, Germany)
Sample bag	PerkinElmer Wallac (Wellesley, USA)

Serological pipettes (2 / 5 / 10 / 25 mL)	Greiner (Frickenhausen, Germany)
Syringe (2 / 5 / 10 mL)	BD (Heidelberg, Germany)
Syringe-Filter (0.45 µm)	VWR (Darmstadt, Germany)

2.3 Chemicals, media, and additives

Table 2.3: Chemicals

Item	**Manufacturer**
α-MEM (Minimum Essential Medium Eagle Alpha Modification)	Gibco BRL (Karlsruhe, Deutschland)
Amino-ethylcabazole (AEC) tablets	BD Biosciences (San Jose, USA)
anti-human CD28 antibody	BioLegend (San Diego, USA)
Agarose (StarPure)	Starlab (Ahrensburg, Germany)
Ampicillin (100 mg/mL)	Sigma Aldrich (Steinheim, Germany)
Bovine serum albumine (BSA)	Sigma-Aldrich (Steinheim, Germany)
Cut smart buffer	New England Biolabs (Hitchin, UK)
Dimethyl sulfoxide (DMSO)	Carl Roth (Karlsruhe, Germany)
DNA ladder (Gene Ruler 1kb Plus)	ThermoFisher Scientific (Waltham, USA)
Dulbecco´s Modified Eagle´s Medium	Gibco BRL (Karlsruhe, Germany)
Ethanol (> 99%)	Carl Roth (Karlsruhe, Germany)
Fetal calf serum (FCS)	Gibco BRL (Karlsruhe, Germany)
Fugene transfection reagent	Promega (Madison, USA)
Gel loading dye blue (6X)	NEB GmbH (Frankfurt, Germany)
GelRed nucleic acid stain	Biotium (Hayward, USA)
Glycerol	Sigma-Aldrich (Steinheim, Germany)
Hexadimethrine bromide (Polybrene)	Sigma-Aldrich (Steinheim, Germany)
Hydrochloric acid (HCl)	Carl Roth (Karlsruhe, Germany)
Hydrogen peroxide (30%, H_2O_2)	Sigma-Aldrich (Steinheim, Germany)
Hygromycin B	AppliChem GmbH (Darmstadt, Germany)
Isopropanol	Carl Roth (Karlsruhe, Germany)
Lysogeny broth (LB)-agar	Sigma-Aldrich (Steinheim, Germany)
LB-medium	Sigma-Aldrich (Steinheim, Germany)

(D-)Luciferin	Thermo Fisher Scientific (Dreieich, Germany)
Methanol	Carl Roth (Karlsruhe, Germany)
Neisser solution	Carl Roth (Karlsruhe, Germany)
Nuclease-Free water	Qiagen (Hilden, Germany)
OKT-3 (InVivoMab anti-human CD3)	BioXCell (Cologne, Germany)
ONE-Glo luciferase system assay	Promega (Madison, USA)
Paraformaldehyde (PFA)	Applichem (Darmstadt, Germany)
Penicillin (10,000 IU/mL)	Sigma-Aldrich (Steinheim, Germany)
Phosphate buffered saline (PBS)	Gibco BRL (Karlsruhe, Germany)
Phytohaemagglutinin (PHA)	Murex Biotech (Kent, UK)
Potassium acetate (KoAc)	Applichem (Darmstadt, Germany)
Puromycin (10 mg/mL)	Sigma-Aldrich (Steinheim, Germany)
Recombinant human IL-2	Novartis (Nürnberg, Germany)
RNase A	ThermoFisher Scientific (Waltham, USA)
Roswell Park Memorial Institute (RPMI) medium 1640 (1X) + Glutamine	Gibco BRL (Karlsruhe, Germany)
Sodium azide	Merck (Darmstadt, Germany)
Sodium hydroxide (NaOH)	Applichem (Darmstadt, Germany)
Sodium lauryl sulfate (SDS)	Carl Roth (Karlsruhe, Germany)
TransIT-LT1	Mirus (Madison, USA)
Tris base	Carl Roth (Karlsruhe, Germany)
Trypan blue (0.4%)	Merck (Darmstadt, Germany)
Trypsin-EDTA (1X)	Pan-Biotech (Aidenbach, Germany)
Tween20	Bio-Rad (München, Germany)
2-Mercaptoethanol (ß-MeOH)	Sigma-Aldrich (Steinheim, Germany)

2.4 Antibodies and tetramers

Table 2.4: Antibodies

Antibody	**Manufacturer**
Anti-human CD3 (APC)	BD Biosciences (Heidelberg, Germany)

Anti-human CD4 (FITC)	BD Biosciences (Heidelberg, Germany)
Anti-human CD8 (PE)	BD Biosciences (Heidelberg, Germany)
Anti-human CD56 (PE)	BD Biosciences (Heidelberg, Germany)
Anti-HA-tag (PE)	BioLegend (San Diego, USA)
Anti-His-tag (PE)	MiltenyiBiotec(BergischGladbach, Germany)
Anti-HLA-A2 (PE)	BioLegend (San Diego, USA)
Anti-HLA-A3 (FITC)	MiltenyiBiotec(BergischGladbach,
Anti-human IgG (PE)	SouthernBiotech (Birmingham, USA)
Anti-mouse IgG (PE)	SouthernBiotech (Birmingham, USA)
Anti-Strep-tag II (Biotin)	GenScript Biotech (Leiden, the Netherlands)
HLA-A*0201-Tetramer (PE)	Tetramer Shop(Kongens Lyngby, Denmark)
Streptavidin (APC)	BioLegend (San Diego, USA)

2.5 Enzymes

Table 2.5: Enzymes and master mixes

Enzyme / Master mix	**Manufacturer**
Ampliqon Taq DNA Polymerase	Ampliqon (Odense, Denmark)
EcoRI	NEB GmbH (Frankfurt, Germany)
PacI	NEB GmbH (Frankfurt, Germany)
Q5 High-Fidelity DNA Polymerase	NEB GmbH (Frankfurt, Germany)
SacII	NEB GmbH (Frankfurt, Germany)
SfiI	NEB GmbH (Frankfurt, Germany)
T4 DNA Ligase	NEB GmbH (Frankfurt, Germany)
XhoI	NEB GmbH (Frankfurt, Germany)

2.6 Kits

Table 2.6: Kits

Item	**Manufacturer**
Anti-human IFN-γ mAb 1-DK-1	MABtech (Nacka Strand, Sweden)

Elite Pu 1600 Standard Vectastain ABC Kit	Vector Laboratories (Burlingame, USA)
Inside Stain Kit	Miltenyi Biotec(Bergisch Gladbach, Germany)
NEBuilder Hifi DNA Assembly Cloning	NEB GmbH (Frankfurt, Germany)
NuecleoBond Xtra plasmid Midiprep	Macherey-Nagel (Düren, Germany)
PCR & Gel Cleanup Kit	QIAGEN (Düsseldorf, Germany)

2.7 Bacteria and cell lines

Table 2.7: Bacteria and cell lines

Abbreviation	**Characteristics**
HEK-293FT	Ideal cell line to generate high-titer lentiviral particles.
HEK-293T	Transfectable derivatives of human embryonic kidney 293 cells (HEK-293) that express a mutated version of the SV40 large T antigen.
CFPAC-1	A cystic fibrosis pancreatic adenoma carcinoma cell line expressing mutant *KRAS* G12V gene.
CHO	Chinese ovary hamster epithelial cell line used in the production of recombinant therapeutic proteins.
NCI-H441	Cell line derived from a patient with papillary lung adenocarcinoma expressing endogenous *KRAS* G12V gene.
Jurkat NFAT-luciferase reporter	This cell line is derived from human T Lymphocyte and stably expresses firefly luciferase reporter gene under the control of NFAT response element.
NK-92	IL-2 dependent Natural killer cell line derived from PBMCs of a patient with non-Hodgkin´s lymphoma.
NK-92 $CD3^+$	Genetically engineered NK-92 to express the CD3 signaling complex.
PBMC	Human peripheral blood mononuclear cells obtained from whole blood samples.
Phoenix-Ampho	Second-generation retrovirus producer cell line derived from HEK-293T cells.
Stbl3	Chemically competent Escherichia coli bacteria derived from the HB101 E. coli strain.
T2	Subclone of the T1 cell line, which expresses only small amounts of HLA-A2 on the cell surface.

2.8 Buffers

Table 2.8: Buffers for agarose gel electrophoresis

TAE-Buffer 50X

Substrate	**Amount**
Tris base	242 g
Glacial acetic acid	57,1 mL
EDTA 0,5 M (pH 8.3)	100 mL
H_2O	filled up to 1 L

Table 2.9: Buffers for DNA isolation via miniprep

Resuspension Buffer

Substrate	**Amount**
Tris (pH 7.4)	50 mM
EDTA	10 mM
RNase A	7 mM

Lysis Buffer

Substrate	**Amount**
Sodium hydroxide (NaOH)	200 mM
SDS	1%

Neutralization Buffer

Substrate	**Amount**
Potassium acetate (KoAC)	3 M (pH 5.5)

Table 2.10: Buffers for flow cytometry

FACS buffer

Substrate	**Amount**
PBS	-
Bovine serum albumin (BSA)	3% (v / v)
Sodium azide	1% (w / v)

Cell fixation buffer

Substrate	Amount
PBS	-
Paraformaldehyde	0,4% (v / v)

Table 2.11: Buffers for ELISpot assay

Acetate buffer

Substrate	Amount
dH_2O	985,3 mL
Sodium acetate	2,88 g
Acetic acid	14,7 mL of 100%

Table 2.12: Buffers for cell culture

Freezing medium for human cell lines

Substrate	Amount
RPMI medium 1640 (1X) + GlutaMAXTM-I	-
Heparin	10 IU/mL
Human albumin	8% (v / v)
DMSO (added prior to use)	10% (v / v)

2.9 Plasmids

Table 2.13: Plasmids

Name	Properties	Resistance
pMX-IRES-Puro	Retroviral transfer vector, Mo-MulV-LTRs, psi packaging signal, IRES, puromycin resistance	Ampicillin, Puromycin
pMX-D10 scFv-hIgG-hCD28TMD-hCD28STD-hCD3z-IRES-Puro	Retroviral transfer vector, Mo-MulV-LTRs, psi packaging signal, D10 scFv binds to $KRAS^{G12V}$ peptide in the context of HLA-A2, hIgG, IRES, puromycin resistance	Ampicillin, Puromycin

pMX-D10 scFv-Strep-tag II-hCD28TMD-hCD28STD-hCD3z-IRES-Puro	Retroviral transfer vector, Mo-MulV-LTRs, psi packaging signal, D10 scFv binds to $KRAS^{G12V}$ peptide in the context of HLA-A2, Strep-tag II, IRES, puromycin resistance	Ampicillin, Puromycin
pMX-D10-7 scFv-UCHT1-IRES-Puro	Retroviral transfer vector, Mo-MulV-LTRs, psi packaging signal, D10-7 scFv binds to $KRAS^{G12V}$ peptide in the context of HLA-A2, IRES, puromycin resistance	Ampicillin, Puromycin
pMX-LH-UCHT1-IRES-Puro	Retroviral transfer vector, Mo-MulV-LTRs, psi packaging signal, LH scFv binds to $KRAS^{G12V}$ peptide in the context of HLA-A3, IRES, puromycin resistance	Ampicillin, Puromycin
pDisplay-HA-tag-D10-7 scFv-Myc-PDGFR-Neo & Kano	Expression vector, CMV promoter, Hemagglutinin A epitope tag, D10-7 scFv binds to $KRAS^{G12V}$ peptide in the context of HLA-A2, Myc tag, PDGFR-TM, Kanamycin resistance gene	Ampicillin, Geneticin (G-418)
PresentER-$KRAS^{G12V}$-IRES-Puro	Retroviral transfer vector, Mo-MulV-LTRs, psi packaging signal, mCherry, IRES, puromycin resistance	Ampicillin, Puromycin
607 pBullet-LK-CEA-IgG-CD28-CD3ζ	Retroviral vector, CMV promoter, psi packaging signal, Lk-BW431-26-scFv-Fc hsCD28-hsCD3ζ, pBR322 promoter, ampicillin resistance	Ampicillin
pSEC-D10-7 scFv-Xencor-Fc-Hygro	Mammalian expression vector, Igκ-chain leader sequence, D10-7 scFv-BGH	Ampicillin, Hygromycin
pcDNA3.4-LHLH-BiTE	Mammalian expression vector, IL-2 leader sequence, LHLH	Ampicillin, Geneticin (G-418)
pCOLT-GALV	GALV envelope gene cloned in expression plasmid pCOLT	Ampicillin

pHIT60	retroviral packaging plasmid providing the gene products gag and pol	Ampicillin

2.10 Primers

Table 2.14: Primers

Name	**Sequence 5′→ 3′**	**Description**
UH360	GCATCGCAGCTTGGATACAC	5’ sequencing primer binding upstream to MCS in pMX vectors
UH361	AAGCGGCTTCGGCCAGTAAC	3’ sequencing primer binding downstream to MSC in pMX vectors
UH565	GCACTCTTGGCCGTATTGGCCCCGCCACCTGTGAGCGGGAAACTTGTGGTAG	5’ primer for NEBulider assembly cloning of *KRAS* G12V fragment into PresentER Plasmid
UH566	CGATCTTTGGCCTGTTTGGCCTTATACGCCAACAGCTCCAACTACCACAAGTTTCC	3’ primer for NEBulider assembly cloning of *KRAS* G12V fragment into PresentER Plasmid
UH567	GCGCAAGATTAACCGAAAGGTG	5’ sequencing primer binding upstream cassette of *KRAS* G12V
UH568	AGATAATTGCTCCTAAAGTAGCCC	3’ sequencing primer binding downstream cassette of *KRAS* G12V
UH569	GCCGGATCTAGCTAGTTAATGCCGGATCTAGCTAGTTAATTAACCA	5’ primer for NEBulider assembly cloning of D10 scFv KRAS^{G12V} fragment
UH572	GCGGCGCGCCGGCCCCCGGATCTCTCGAGGATTAGC	3’ primer for NEBulider assembly cloning of hIgG-hCD28TMD-hCD28STD-hCD3ζ fragment
UH574	GCGGGATCCCCACTACTCACGG	3’ primer for NEBulider assembly cloning of D10 scFv KRAS^{G12V} fragment

UH586	ATAATGGCCCAGCCGGCCATG	5’ primer for D10-7 scFv KRAS^{G12V} cloning into pDisplay vector, SfiI restriction site
UH587	ATCTGCCGCGGCGATGAGACGGTGACCAGGG	3’ primer for D10-7 scFv KRAS^{G12V} cloning into pDisplay vector, SacII restriction site
UH588	GCCGGATCTAGCTAGTTAATTAAATGGAGACA GACACACTCCTG	5’ primer for NEBulider assembly cloning of D10-7 scFv KRAS^{G12V} fragment
UH589	CCTCCGCCCGATGAGACGGTGACCAGG	3’ primer for NEBulider assembly cloning of D10-7 scFv KRAS^{G12V} fragment
UH590	CTCATCGGGCGGAGGTGGGAGT	5’ primer for NEBulider assembly cloning of UCHT1 fragment
UH591	CTCGAGGCCTGCAGGAATTCTTAATGGTGGTG GTGATGGTGAGAG	3’ primer for NEBulider assembly cloning of UCHT1 fragment
UH600	GCGGCCGCACTACTCACGGTCACCAGAGT	3’ primer for NEBulider assembly cloning of D10 scFv KRAS^{G12V} fragment overlapping with Strep-tag II
UH601	GAGTAGTGCGGCCGCATGGAG	5’ primer for NEBulider assembly cloning of Strep-tag II fragment
UH602	ACCCAAAATGCGGCCGCGCT	3’ primer for NEBulider assembly cloning of Strep-tag II fragment
UH603	GGCCGCATTTTGGGTGCTGGTGGT	5’ primer for NEBulider assembly cloning of hCD28TMD-hCD28STD-hCD3ζ fragment

2.11 Size standard

To determine size and quantification of DNA-fragments by agarose gel electrophoresis, either GeneRuler 1 kb DNA Ladder (Thermo Scientific) or GeneRuler 1 kb Plus DNA Ladder (Thermo Scientific), and the Quick-Load Purple 100bp DNA Ladder (NEB) were applied (Fig. 2.1).

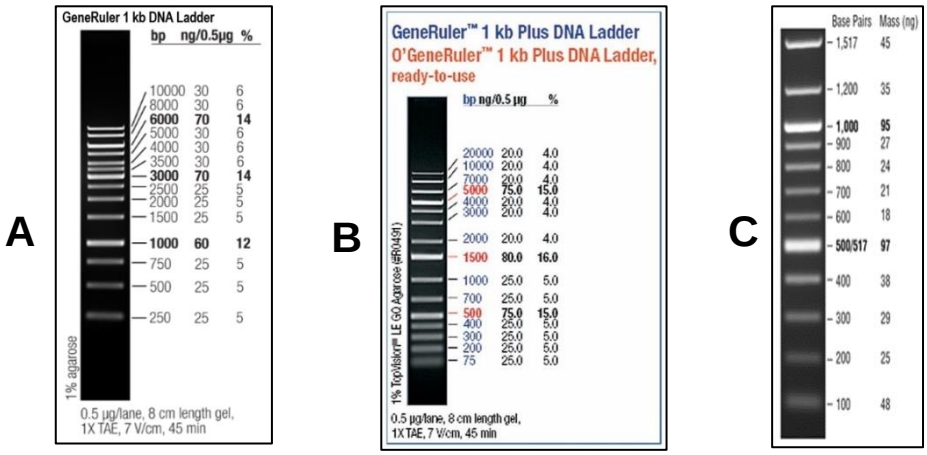

Figure 2.1: Applied DNA ladders for gel electrophoresis. (A) GeneRuler 1 kb DNA ladder (B) GeneRuler 1 kb Plus DNA ladder (C) Quick-Load Purple 100 bp DNA ladder for gel electrophoresis. The banding pattern indicates the length of DNA-fragments in base pairs (source: Thermo Fisher Scientific & NEB webpage).

2.12 Software

Table 2.15: Software

Software	**Company**
BD FACSDiva software version 6.1.3	BD Biosciences (Heidelberg, Germany)
FlowJo software version 10	FlowJo LLC (Oregon, USA)
GraphPad Prism version 9	GraphPad Software, Inc. (La Jolla, USA)
Office 365 Home	Microsoft (Redmond, USA)
SnapGene	GSL Biotech (Chicago, USA)

3. Methods

3.1 Molecular biology methods

3.1.1 Polymerase Chain Reaction

In order to produce multiple copies of DNA sequences the polymerase chain reaction (PCR) method was applied. For amplification and modification of DNA templates required for CAR-based vectors, 100 ng of DNA was mixed with 10 µM of each forward and reverse primers, 12,5 µL of Q5High-Fidality 2X master mix, and nuclease-free water in a total volume of 50 µL. Primer annealing temperatures were calculated according to the following formula to avoid nonspecific priming and PCR was performed with a program which is indicated in the table below.

$$T_A = 2°C \times (A + T) + 4°C \times (G + C) - 2°C$$

A= adenine, T= thymine, G= guanine, C= cytosine

Table 3.1: Thermocycling profile for DNA amplification by Q5 polymerase.

Step	**Temperature**	**Time**	
Initial denaturation	98°C	30 sec	
Denaturation	98°C	10 sec	30 cycles
Annealing	50-72°C	30 sec	
Elongation	72°C	1 min/kb	
Final elongation	72°C	2 min	
Hold	4°C	∞	

3.1.2 Agarose gel electrophoresis

Agarose gel electrophoresis was prepared to separate DNA fragments based on their size. Therefore, 1% agarose was dissolved in an appropriate amount of 1X Tris-acetate-EDTA (TAE) buffer. For the visualization of DNA fragments using UV light, 3 µL of Gel Red nucleic acid stain was mixed with 50 mL of the boiling gel. Afterwards, 10 µL DNA sample was mixed with 2 µL of 6X DNA loading dye, loaded onto the gel and subjected to electrophoresis at 100 V for 50 min together with a GeneRuler 1 kb DNA ladder to determine the length of DNA fragments.

3.1.3 Restriction digestion

Restriction digestion is usually applied to prepare a DNA fragment for subsequent cloning. Thus, different amounts of plasmid or PCR amplified DNA were mixed with 1 µL of appropriate restriction enzymes, 5 µL of corresponding 10X digestion buffer and dH_2O in a total volume of 50 µL and incubated at 37 ℃ for 2 hours to cleave at specific nucleotide sequences.

3.1.4 DNA extraction from an agarose gel

In order to isolate and purify PCR products and digested plasmid vectors from enzymes and other components, DNA fragments were run on an agarose gel. Next, the desired DNA bands were cut out from the gel under UV light and purified using a NucleoSpin Gel kit or PCR clean-up kit according to the manufacturer's instructions. Subsequently, the amount of purified DNA was measured by a spectrophotometer.

3.1.5 Ligation

DNA ligation is a method, which is commonly used to physically joint vector DNA to a gene of interest. Thus, an appropriate amount of a vector DNA was mixed with an insert fragment at a 1:3 molar ratio. The ligation was performed in total volume of 20 µL mixing 1 µL T4 DNA ligase with 2 µL of corresponding 10X ligation buffer and dH_2O. After 2 hours incubation at room temperature, the ligation reaction was used for the transformation of chemically competent bacteria cells.

3.1.6 NEBuilder cloning

For performing cloning with more than one DNA fragment, NEBuilder HiFi DNA Assembly kit (NEB) was applied. In order to ensure that fragments are ligated into a vector DNA with correct order, we considered 15 bp overlapping ends for design of each primer. Therefore, 60 ng linearized vector, the respective amount of each amplified PCR product at a molar ratio of 1:3, and 10 µL of NEBuilder Assembly 2X master mix were mixed. Next, this mixture was filled up with dH_2O to a final volume of 20 µL and placed in a thermocylcer to be incubated at 50 ℃ for 60 min. Finally, the reaction mixture was utilized for the transformation of competent Stbl3 bacteria.

3.1.7 Transformation of competent bacteria

To propagate and amplify plasmids, DNA was transformed into competent bacteria cells. Hence, after thawing of bacteria on ice, 20 µL of the ligation mixture was gently added to 50 µL of competent bacteria and followed by incubation on ice for 20 min. To facilitate transfer of plasmid DNA into the competent cells, the bacteria mixture was heat shocked at 42 ℃ for 90 second in a water bath and quickly placed on ice for 2 min followed by adding 350 µL of LB medium. Transformed bacteria were subjected to a shaking incubator at 190 rpm for 60 m in LB medium without antibiotic. Following centrifugation 100 µL of resuspended transformed bacteria were plated out on a LB-agar plate containing ampicillin 100 µg/mL as selective antibiotic and incubated overnight at 37 ℃.

3.1.8 Colony screening

Colony PCR was conducted to validate successful transformation of cloned vector DNA. Thus, single bacteria colonies were picked from LB-agar plates and inoculated in 3 mL of LB- medium containing 100 µg/mL ampicillin. After 5 hours incubation at 37 ℃, 3 µL of the bacteria suspension was mixed with 10 µM of respective forward and reverse primers, and 12,5 µL of Taq Optimix Clear 2X master mix and finally filled up to an end volume of 25 µL with dH_2O. The PCR program was defined as indicated in the table 3.2 below.

Table 3.2: Thermocycling program for colony PCR

Step	**Temperature**	**Time**	
Initial denaturation	95°C	5 min	
Denaturation	95°C	30 sec	30 Cycles
Annealing	50-68°C	40 sec	
Extension	68°C	1 min/kb	
Final extension	68°C	5 min	
Hold	4°C	∞	

3.1.9 Plasmid DNA isolation

After individual transformed bacteria colonies were proven to contain correct cloned vector DNA via colony PCR, larger amounts of plasmid DNA were prepared by inoculating, 2 mL of the bacteria colony suspension in 100 mL LB-liquid medium supplemented with 100 µg/mL ampicillin. Hereafter, bacterial culture was incubated in a shaking incubator overnight at 37 ℃. Isolation of plasmid DNA from bacteria was performed according to the instructions of Macherey-Nagel NucleoBond Xtra Midi kit.

3.1.10 DNA sequencing

For validation of cloned constructs, purified plasmid DNA was sent for sequencing. Thus, 1 µg of isolated plasmid DNA was mixed with 3 µL of corresponding sequencing primers (10 µM) and shipped to “StarSeq” in Mainz. All sequences of scFvs used in this study are listed in Table S1 in the appendix section.

3.1.11 Preparation of bacteria stocks

Approved plasmid DNA was stored by freezing respective bacteria suspension in glycerol stocks. Therefore, 150 µL of molecular grade glycerol was mixed with 850 µL of bacteria culture in a cryotube and immediately frozen in liquid nitrogen. Thereafter, samples were stored at -80 ℃.

3.2 Cellular Methods

3.2.1 Thawing of cells

Frozen cryotubes were placed into a pre-heated water bath at 37℃. As soon as thawed cells were mixed with 1 ml of culture medium, transferred in 10 ml medium to remove DMSO and centrifuged at 1500 rpm for 5 min. The cell pellet was resuspended in fresh pre-warmed culture medium and cells were cultured at 5% CO_2, 37°C.

3.2.2 Media and cell culture

All cell lines were kept in an incubator with 5% CO_2 at 37℃. Adherent cell lines, including Phoenix-Ampho, NCI-H441, and CFPAC-1 cells were cultured in Dulbecco’s Modified Eagles Medium (DMEM) containing 10% fetal bovine serum (FBS) and 1% penicillin/streptomycin (P/S). On the contrary, adherent growing CHO cells were

maintained in RPMI-1640 medium containing 10% FBS plus 1% P/S. and passaged every 3-4 days when confluency exceeded more that 80%. Therefore, cell culture supernatant was aspirated, cells rinsed with PBS and afterwards treated with 2 mL pre-warmed Trypsin-EDTA for 5 min. Detached cells were harvested, centrifuged, and cell pellet was resuspended in a fresh cell culture.

Suspension cells, including Jurkat-NFAT-Luciferase reporter cells, and T2 cell lines were maintained in RPMI-1640 medium supplement with 10% FBS and 1% P/S. PBMCs were isolated from human primary blood cells and also cultured using RPMI-1640 completed with 10% FBS and 1% P/S. In order to maintain these cell lines in the culture, they were weekly either polyclonally or antigen-specifically re-stimulated. NK-92 cell lines were cultured in Minimum Essential Medium Eagle Alpha Modification (α-MEM) containing 20% FBS, 1% P/S, 0,2 mM Inositol, 0,1 mM β-mercaptoethanol, and 0,02 mM folic acid. The culture medium was replaced with fresh medium every 2-3 days plus addition of 200 IU/mL IL-2.

3.2.3 Cell Counting

To determine viability, resuspended cells were stained with Trypan blue dye, which stains dead but viable live cells. For this purpose, an appropriate ratio of cells was diluted in Trypan blue dye and then a volume of the mixture was transferred into a Fuchs-Rosenthal counting chamber to be counted using a light microscope. For calculation of cell number, the following formula was applied.

$$\text{number of counted cells} \times \text{dilution factor} \times \text{chamber factor } (0.5 \times 10000) = \text{cells / ml}$$

3.2.4 Cryopreservation of cells

To store cells for a long period of time, cells were harvested, counted, and centrifuged at 1500 rpm for 5 min. Furthermore, cell pellet was resuspended in an appropriate amount of freezing medium containing 10% DMSO, immediately aliquoted and kept at -80 ℃. After 24 – 36 hours frozen cryotubes were transferred into a liquid nitrogen tank at -190 ℃.

3.2.5 Generation of retroviral particles by transfection of Phoenix-Ampho cells

For production of retroviral particles containing supernatants, Phoenix-Ampho cells were transfected with a transfer plasmid encoding a gene of interest, packaging vector pHIT60, and envelope vector pCOLT-GALV (Fig. 3.1). Two days prior to transfection, amount of Phoenix-Ampho cells were plated in a 10 cm cell culture petri dish. On the day of transfection, an appropriate amount of FuGENE reagent was diluted into RPMI medium and incubated for 5 min at room temperature. Depending on the volume of FuGENE reagent/ DNA, 10 µg of transfer plasmid vector, together with 5 µg of each helper plasmids were mixed in transfection mixture and incubated for 15 min to allow a formation of a FuGENE/DNA mixture. After that, this transfection mixture was distributed dropwise on Phoenix-Ampho cells. Next day, cell culture medium was replaced with 8 mL of fresh RPMI medium. On the day of transduction, supernatant containing viral particles was harvested, passed through a 0,45 µm syringe filter and subsequently applied for transduction of target cells.

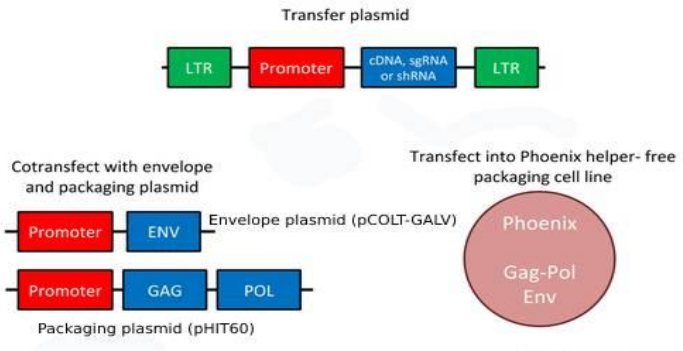

Figure 3.1: Schematic of retroviral packaging system. (Source: https://www.addgene.org/guides/retrovirus/).

3.2.6 Generation of lentiviral particles using transfection of HEK-293FT cells

This procedure was performed similarly to retrovirus production system described in section 3.2.5. However, instead of the components described the envelope, packaging, and transfer plasmids for production of lentivirus particles consisted of pMD2.G, psPAX2, and pLenti-Fluc-GFP respectively (Fig. 3.2).

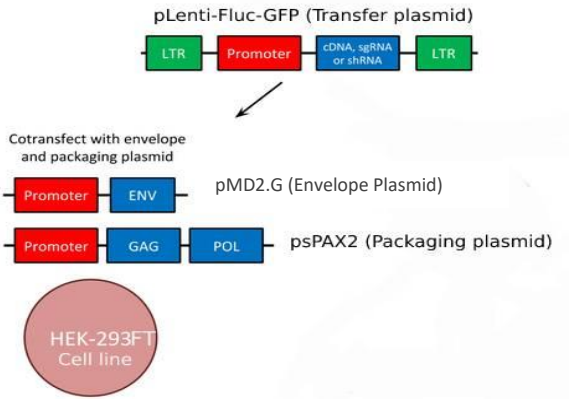

Figure 3.2: Overview of lentiviral plasmid system. (Source: https://www.addgene.org/guides/).

These three plasmids were mixed with TransIT-LT1 transfection reagent, and then cotransfected into HEK-293FT cell line. Quantities required for the transfection protocol are listed below (Table 3.3).

Table 3.3: Composition of reaction mixture for transfection of HEK-293FT cells

Component	**Amount**
RPMI-1640	270 µL
TransIT-LT1	20 µL
Envelop vector (pMD2.G)	300 ng
Packaging vector (psPAX-2)	1,8 µg
Transfer vector (pLenti-Fluc-GFP)	3 µg

3.2.7 Transient Expression of single-chain Fv in HEK-293T cells

One day prior to transfection, HEK-293T cells were seeded in 10 cm cell culture petri dishes at a density of 0.1×10^6 cells/mL. Transfection was performed using an appropriate amount of FuGENE reagent and 10 µg of expression vector encoding scFv. Three days after transfection, cells were harvested for analyzing of target gene expression.

3.2.8 Transduction of PBLs

To evaluate expression of TCR-mimic CARs on the surface of human T cells, peripheral blood lymphocyte cells were transduced using retroviral particles

supernatant through the spin-infection method. For expansion of T cells, PBMCs were stimulated with 1 µg/mL anti-CD3, 0,5 mg/mL anti-CD28 antibodies, and by addition of 600 IU/mL human IL-2. Three days after transduction, stimulated PBMCs were harvested, centrifuged, and resuspended in an appropriate amount of cells in 1 mL of viral supernatant containing 10 µg/mL polybrene. Thereafter, plate was centrifuged with 2000 rpm without brake for 90 min at 32℃. Afterwards, the culture plate was transferred into an incubator at 37℃. Finally, transduced T cells were selected using puromycin with a final concentration of 1,5 µg/mL.

3.2.9 Transduction of CHO cells

For transduction of CHO cells, an appropriate amount of cells was resuspended in 1 mL of fresh viral supernatant by addition of 10 µg/mL polybrene. For efficient transduction, the spin-infection method was applied through centrifugation at 2000 rpm without brake for 90 min at 32℃. To select for transduced CHO cells 15 µg/mL puromycin was utilized.

3.2.10 Transduction of Jurkat-NFAT reporter cells

Jurkat-NFAT reporter stable cell line was established by transduction using a pTA-NFAT-luciferase reporter vector (kindly gifted by Dr. Christian Klein from the Roche Innovation Center Zurich, Switzerland) followed by hygromycin (200 µg/mL) selection. The hygromycin resistant cells were subsequently applied for the second transduction with plasmid vectors encoding TCRm CAR receptors and followed by second selection utilizing puromycin (1 µg/mL). Transduction procedure was carried out based on the same protocol described in section 3.2.9.

3.2.11 Cell staining for flow cytometry

3.2.11.1 Staining of extracellular antigens

To assess expression of particular extracellular antigens, $0{,}5 \times 10^6$ cells were washed with flow cytometry staining buffer (FACS buffer) and pelleted by centrifugation at 1500 rpm for 5 min. Afterwards, the recommended amount of fluorochrome-conjugated antibody was added and incubated for 15 min at room temperature in the dark. To remove of unbound antibodies, cells were washed by addition of FACS buffer. Finally, cells were resuspended in 100 µL of FACS fixation buffer.

3.2.11.2 Staining of TCRm CAR receptors using HLA-A*0201-Tetramer

To detect and quantify transduced TCRm CAR- T cells that are specific for the mutant $KRAS^{G12V}$ neoepitope, a tetramer assay was utilized. For this purpose, 5 µL of HLA-A*0201 tetramer was loaded with 100 µM peptide and incubated on ice for 30 min in the dark. After washing amount of cells with FACS buffer, loaded -tetramer was mixed gently with cells and incubated for 15 min at 37℃ in the incubator. Afterwards, cells were washed twice with an appropriate volume of FACS buffer followed by centrifugation at 1500 rpm for 5 min. Samples were analyzed by flow cytometry after resuspension in 100 µL FACS fixation buffer.

3.2.11.3 Staining of intracellular antigens

For assessment of intracellular target antigens, recommended amount of cells were washed, pelleted by centrifugation and resuspended in 500 µL of inside fix buffer (inside stain kit). After incubation at room temperature for 20 min in the dark, cells were centrifuged and supernatant was aspirated carefully. For the permeabilization of cells, 500 µL perm inside buffer (inside stain kit) was pipetted into cells and centrifuged at 1500 rpm for 5 min. Next, supernatant was discarded and a recommended amount of fluorochrome-conjugated antibody was mixed with cells followed by incubation at room temperature in the dark for at least 20 min. Subsequently, cells were washed twice with 500 µL perm inside buffer and finally resuspended in a suitable amount of FACS fixation buffer for analysis.

3.2.11.4 Staining of mutant $KRAS^{G12V}$ neoantigen using bispecific antibody

For the detection of $KRAS^{G12V}$ pHLA-A2 complexes on the surface of target cell, bispecific antibody staining assay was performed by incubation 0, 5×10^6 cells or peptide-pulsed T2 cells in 500 µL of concentrated supernatant containing recombinant antibody on ice for 1 hour, followed by one wash in FACS buffer. Afterwards, a recommended amount of respective fluorochrome-conjugated secondary antibody (either anti-His-tag or anti-HA-tag) was mixed with cells, washed, subsequently resuspended in 100 µL fix buffer.

3.2.11.5 Staining of peptide pulsed T2 cells

For the staining of peptide pulsed T2, $0{,}5 \times 10^6$ cells were washed once with PBS and RPMI-1640 without FBS followed by incubation of cells in serum-free RPMI-1640 medium containing 50 µg/mL peptide and 10 µg/mL human β2 microglobulin for 18 hours at 37℃. Pulsed T2 cells were then washed once in FACS buffer and stained with 5 µL of anti-HLA-A2 antibody in 100 µL of FACS buffer followed by washing. Stained cells were fixed in 100 µL of fixation buffer before analyzing by flow cytometry.

3.2.12 IFN-γ Enzyme-linked immunosorbent spot assay

This assay allows detect antigen-specific T cells secreting effector molecules such as e.g. cytokines and chemokines. In this assay, membranes of a MultiScreen HTS plate were activated using 20 µL of 35% ethanol. After washing with PBS, wells are coated with a recommended amount of capture antibody. Thereafter, plates were incubated overnight at 4℃. The next day, after washing wells with PBS, they were blocked using RPMI-1640 and then incubated in an incubator for at least 1 hour. Afterwards, an appropriate amount of effector cells was co-cultured with target cells in a final volume of 200 µL medium. After an incubation of 24 hours, each well was washed with PBS containing 0,05% Tween followed by addition of detection antibody, which had been diluted in PBS supplemented with 0,5% BSA. After 2 hours incubation at 37 ℃, wells were washed and followed by pipetting of ABC solution according to the manufacturer's instructions. ABC solution was incubated with membranes in the dark at room temperature for one hour. In order to visualize spots on the membrane, AEC substrate was applied. Finally, spots were analyzed utilizing an Immunospot reader.

3.2.13 Generation of luciferase-expressing target cells

NCI-H441 and CFPAC-1 cell lines were purchased from ATCC. The T2 cell line was a kind gift from Dr. H. Echchannaoui (III. Dept. of Medicine, University Medical Center Mainz). Stable lentiviral transduction of cells was performed using pLenti-Fluc-GFP encoding firefly luciferase (kindly provided by Dr. C. Wölfel, III. Dept. of Medicine, University Medical Center Mainz). To produce lentiviral supernatant the protocol described in section 3.2.6 was used.

3.2.14 Bioluminescence-based cytotoxicity assay

To measure cytotoxicity activity of effector cells against a given target cell, a bioluminescence (BLI)-based cytotoxicity approach was utilized. For this purpose, luciferase expressing cells were seeded in a black 96-well flat-bottom plate at a concentration of 3×10^5 cells/mL in duplicates, followed by addition of D-Luciferin, and measured with an ELISA-reader. Before occurrence of any cell death and to ensure equal distribution of target cell among wells, BLI baseline was established. Thereafter, effector cells were added at various ratios and incubated at 37℃ for 24 hours. BLI was measured using an ELISA-reader for 10 seconds as relative luminescence units (RLU). Target cells without effector cells were used to measure spontaneous death RLU. Cells were treated with 1% paraformaldehyde (PFA) to determine maximal killing. Subsequently, percentage of lysis was calculated with the following equation:

$$\% \text{ specific lysis} = 100 \times \left(\frac{\text{spontaneous death RLU} - \text{test RLU}}{\text{spontaneous death RLU} - \text{maximal killing RLU}}\right)$$

3.2.15 TCR-mimic CAR-J reporter assay

In order to identify and facilitate optimization of TCR-mimic CAR receptors for their specificity profile, a CAR-J reporter assay was applied. The Jurkat-NFAT reporter cell line was established to express luciferase under the control of a cassette of NFAT response elements. Subsequently, TCRm-based CAR receptors were transduced into Jurkat reporter cells (as described in section 3.2.10). For this procedure, TCRm CAR-expressing Jurkat reporter cells and peptide-pulsed T2 cells were co-cultured in a black 96-well flat-bottom plate in technical duplicates at various effector to target cell (E:T) ratios in a total volume of 200 µL medium. After 24 hours co-incubation at 37℃, cells were harvested, pelleted by centrifugation, and supernatant was aspirated. Afterwards, cells were resuspended in 100 µL of ONE-Glo luciferase assay and after 30 min luminescence was read using Tecan microplate reader.

3.2.16 TCR-mimic bispecific T-cell engager assay

In order to measure bispecific antibody potency, a reporter-based T cell activation assay using Jurkat cell line expressing stably luciferase reporter gene driven by the promoter of NF-κB response-elements was applied. For this purpose, Jurkat-NFAT reporter cells were mixed with target cells at various ratios. TCRm bispecific antibodies

was diluted in the medium and added to cell mixture. After 24 hours incubation at 37℃, cells were pelleted by centrifugation, and NFAT-dependent luciferase reporter gene was quantified by adding ONE-Glo luciferase assay solution and was read out by a laminator reader (Fig. 3.3).

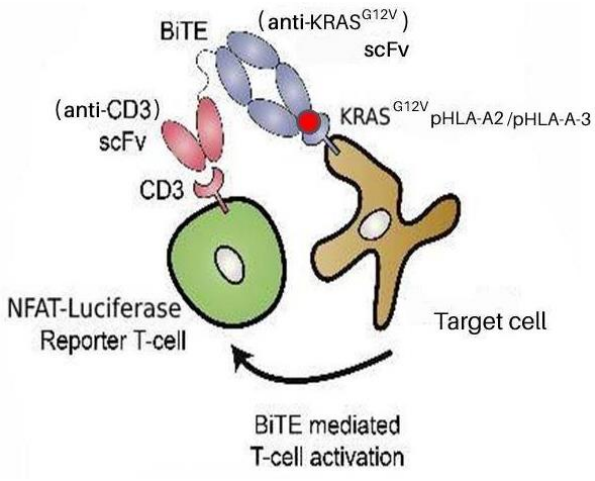

Figure 3.3: Schematic of TCR-mimic bispecific T-cell engager assay using NFAT reporter-based T cell activation. Reporter cells were combined with target cells in the presence or absence of bispecific antibody. NFAT-dependent reporter gene was used to quantify T cell activation following overnight incubation. ''Created with BioRender.com.''

4. Results

4.1 Experimental strategy

To target KRAS mutated ($KRAS^{G12V}$) peptides in the context of HLA-A*0201 and HLA-A*0301 complexes using TCRmimic (TCRm) - based bispecific antibodies, we obtained peptide-specific antibody derived single chain variable fragments (scFv) recognizing $KRAS^{G12V}$in the context of HLA-A*0201 scFv and HLA-A*0301. These scFv, termed “D10” for $KRAS^{G12V}$ pHLA-A*0201 and “LHVH” for $KRAS^{G12V}$ pHLA-A*0301 were cloned into the expression vector pDisplay containing a HA-tag to be transiently expressed in the HEK-293T cell line. Transduced HEK293T cells were then used to examine specific binding of the scFv to the desired pHLA complex in a HLA-A*0201-Tetramer staining assay.

For the purpose of generating TCRm CAR-expressing effector cells that target KRAS-derived peptide-HLA complexes, two TCRm CAR constructs that differ in the hinge region (also referred to as the spacer domain) were developed. Therefore, the sequence of the $KRAS^{G12V}$ -specific scFv“D10” and other CAR fragments were amplified by PCR and subsequently cloned into the retroviral transfer vector pMXs-IRES-Puro via NEBuilder (see M&M section). Finally, the sequences of the two generated retroviral vectors encoding pMXs-scFv D10-hIgG-hCD28TMD-hCD28STD-hCD3ζ and pMXs-D10-Strep-tag II-hCD28TMD-hCD28STD-hCD3ζ (hereafter referred to as hIgG CAR and Strep-tag II CAR, respectively) were verified by Sanger sequencing.

To first verify the signaling capacity of each TCRm CAR construct, the CAR-J reporter assay using the Jurkat-NFAT-Luciferase (JNL) cell line was utilized. For this purpose, retroviral particles were generated by transfecting Phoenix-Ampho cells with i) transfer vector encoding a TCRm CAR, ii) packaging vector pHIT-60 encoding gag and pol, and the vector pCOLT-GALV coding for the viral envelope of gibbon ape leukemia virus. Afterwards, supernatant containing viral particles was harvested from cell culture and used to transduce the JNL cell line. Subsequently, CD3-mediated signaling of both TCRm CARs resulting in activation of NFAT-driven luciferase activity was determined using a NFAT-Luciferase reporter system. Next, successfully tested TCRm CAR constructs were applied to express the CARs in NK-92 cells and peripheral blood lymphocytes (PBLs), which had been stimulated and expanded from

peripheral blood mononuclear cells (PBMCs) prior to retroviral CAR gene transfer. Following flow cytometry-based expression analysis, cytotoxic activity of CAR redirected immune cells was measured in vitro by IFN-γ ELISpot and bioluminescence-based killing assays.

Moreover, recombinant scFvs were utilized to generate bispecific antibodies to be applied as bispecific T cell engager (BiTE). For this procedure, the sequence of $KRAS^{G12V}$ specific scFv was fused to an anti-CD3 scFv (named according to the clone UCHT1) and a short His-tag sequence coding for 6 histidines in a retroviral transfer vector. Then, CHO cells were stably transduced with these constructs to produce recombinant bispecific antibodies in the culture supernatant of established CHO producer lines. Selective binding to HLA-A*0201 was assessed using T2 cells pulsed with $KRAS^{G12V}$, and $KRAS^{G12WT}$ peptides, respectively. Thus, KRAS peptide loaded T2 cells were stained with recombinant antibodies derived from supernatants of CHO cell culture and detected by FACS analysis. Additionally, to target KRAS endogenously presented on HLA-A*0201, we applied endogenous *KRAS* G12V-harboring cancer cells and an overexpression model using PresentER-driven KRAS minigene in T2 cell and subsequently analyzed for binding of the bispecific antibodies by flow cytometry. We tested the potential function of recombinant antibodies using Jurkat reporter cells and in vitro killing assays. In the following section, the above listed experiments are described in detail.

4.2 Identification of specific (anti-$KRAS^{G12V}$) scFv

Prior to generating full-length TCRm CARs or BiTEs, we first verified the specificity of the scFvD10 obtained as sequence from Biocat® ,Thus, the D10 was cloned into the expression vector, pDisplay (a gift from Dr. M. Peipp) (Fig. 4.1). The plasmid map can be found in supplementary figure S1. Transient transfection of pDisplay-scFv D10 into HEK-293T cells was performed to assess the specificity of the scFv against the target antigen $KRAS^{G12V}$ /HLA-A2 complex. Later on, expression of D10 was determined by anti-HA-tag antibody using flow cytometry. We found that most HEK-293T cells expressed the scFv on their surface with a high-level transfection efficiency (Fig. 4.2). In the next step of experiments, specificity of binding characteristics of D10 to the desired target epitope was measured by HLA-A*0201-Tetramer using FACS analysis. As expected, flow cytometry analysis revealed that the

scFv did not interact with a KRAS^{G12WT} - HLA-A*0201 tetramer, whereas it bound to KRAS^{G12V} complexed with tetramer. While 25% of all cells loaded with KRAS^{G12V} peptide could be stained with KRAS^{G12V} - HLA-A*0201 tetramer, no cells loaded with KRAS^{WT} and stained with KRAS^{G12WT} - HLA-A*0201 tetramer could be detected by FACS analysis, indicating the ability of this scFv to distinguish between mutant versus wild-type peptide (Fig. 4.3).

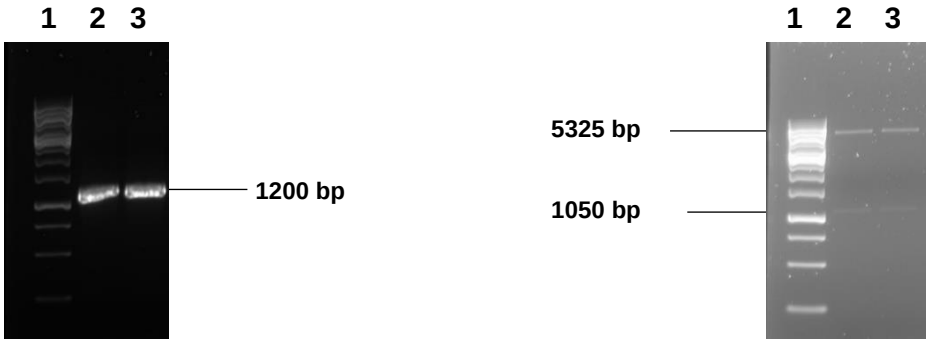

Figure 4.1: Colony PCR and restriction digestion of cloned pDisplay-(anti-KRAS^{G12V}) scFv vectors. The scFv sequence was cloned into pDisplay using T4 DNA ligase, followed by transformation of Stbl3 bacteria. The colony PCR test with two selected transformed bacteria shows a band size of 1200 bp (lanes 2, 3) (left), and cloned vectors digested with EcoRV and XhoI restriction enzymes.

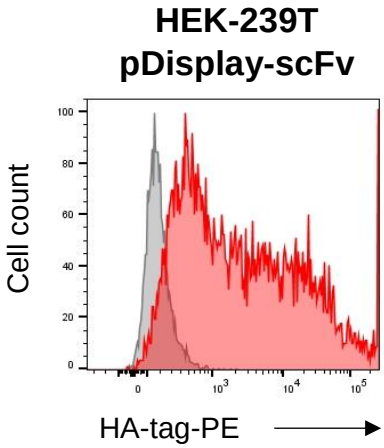

Figure 4.2: Flow cytometry analysis of the surface expression of scFv on HEK-293T cells. The red histogram depicts staining of transfected cells with anti-HA-tag antibody, whereas the gray histogram represents transfected cells incubated with an irrelevant antibody as an isotype control. HA-tag, hemagglutinin-tag; scFv, single-chain variable fragment.

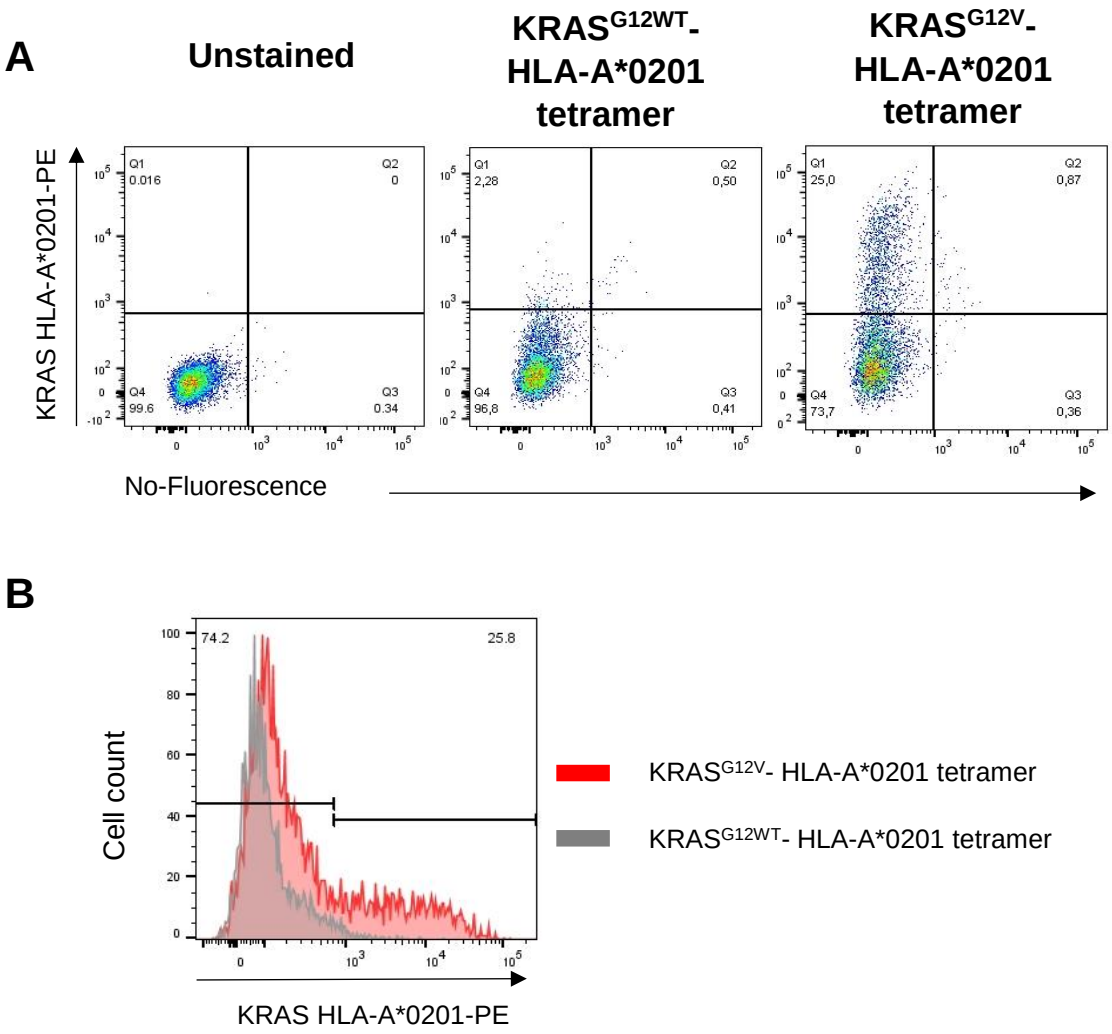

Figure 4.3: Analysis of the specificity function of (anti-KRAS^{G12V}) scFv on HEK-293T cells by flow cytometry. (A) HEK-293T cells transfected with the pDisplay-scFv vector were stained with the KRAS^{G12V} - HLA-A*0201 tetramer to assess the specificity of the (anti-KRAS^{G12V}) scFv. Unstained cells and cells were incubated with only KRAS^{G12WT}- HLA-A*0201 tetramer used as controls. (B) Flow cytometry data shown in (A) are displayed in histogram diagram. The red histogram shows the staining of scFv-expressing HEK-293T cells with the KRAS^{G12V} - HLA-A*0201 tetramer, while the gray histogram demonstrates the staining of transfected HEK-293T cells with the KRAS^{G12WT} - HLA-A*0201 tetramer. KRAS^{G12V}, mutated KRAS peptide; KRAS^{G12WT}, wild-type KRAS peptide; HLA, human leukocyte antigen

4.3 Generation of TCRm CAR transfer vectors

To clone two KRAS^{G12V}-specific CARs with different spacers, different fragments of the CAR structure were amplified by PCR using specific primers designed for NEBuilder cloning (Fig. 4.4). The first CAR containing a hIgG hinge region was created by amplifying the scFv sequence from the already existing retroviral vector “pMXs-scFv D10-mFc-mCD4TMD-mCD28STD-mCD3ζ-IRES-Puro”, while the sequence of the hIgG-hCD28TMD-hCD28STD-hCD3ζ fragment was amplified from the plasmid # 607 “pBullet_IgK-scFVCEA-hIgG-hCD28TMD-hCD28STD-hCD3ζ” obtained as a

courtesy from Prof. Dr. Abken (Leibniz Inst. for Interventional Immunology, University of Regensburg). The second CAR construct containing a Strep-tag II sequence as hinge region was generated in a similar approach; however, the Strep-tag II sequence was obtained from a pMSG-OVA 3rd. generation CAR plasmid (kindly provided by PD Dr. Bockamp, Inst. for Transl. Immunol., UMM) (Appendix, Fig. S2, S3).

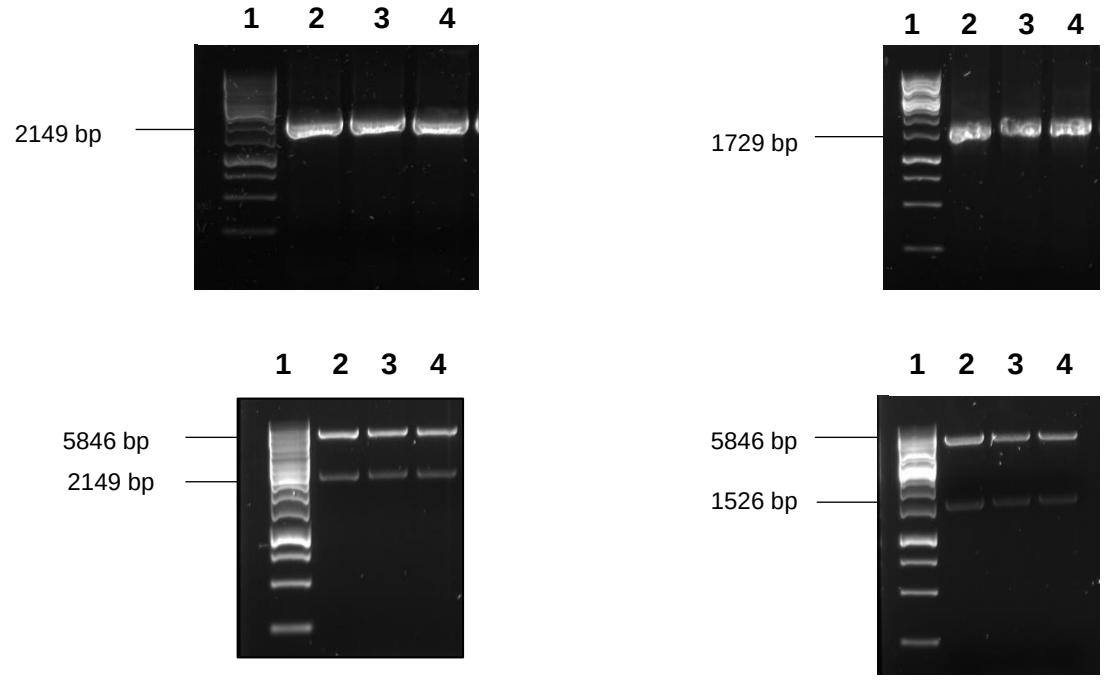

Figure 4.4: Colony PCR and restriction digestion analysis of generated TCRm CAR transfer vectors. Representative electrophoresis image of the PCR products and restriction enzyme analysis of the TCRm CAR encoding vectors. A retroviral backbone pMXs-IRES-Puro was digested with PacI and XhoI restriction enzymes. NEBuilder cloning was used to assemble TCRm CARs fragments and the digested pMXs backbone vector. After transformation into E. coli K12 strain Stable III, individual colonies were identified by colony PCR. The PCR bands for pMXs-scFv D10-hIgG-hCD28TMD-hCDSTD28-hCD3ζ (lanes 2, 3, 4) (left top) and pMXs-scFv D10-Strep-tag II-hCD28TMD-hCDSTD28-hCD3ζ (lanes 2, 3, 4) (right top). A preparative digestion of expanded "midi-prep" pMXs-scFv D10-hIgG-hCD28TMD-hCDSTD28-hCD3ζ yielded two distinct bands at 2149 bp and 5846 bp (lane 2, 3, 4) (left bottom), while pMXs-scFv D10-Strep-tag II-hCD28TMD-hCDSTD28-hCD3ζ produced two fragments with expected bands at 1526 bp and 5846bp (lane 2, 3, 4) (right bottom). GeneRuler 1 kb was loaded on the gel (lane 1) to estimate DNA size. One of three biological experiments is depicted in this image.

4.4 Production of retroviral particles and evaluation of transfection efficiency

Retroviral gene transfer into immune cells was performed using retroviral particles generated in the Phoenix-Ampho cell system (Swift et al., 2001). For the production of amphotropic retrovirus particles, these cells have been transduced with the sequences encoding packaging (gag-pol) proteins and the GALV envelope (env) to generate pseudoptyped virus. Nevertheless, phoenix lines are not capable of packaging encoded cDNA in viral particles due to the lack of the packaging signaling ψ sequence.

Therefore, in order to obtain high titer of viral particles, phoenix cells were not only transfected with the transfer vector containing the CAR sequence but also co-transfected with exogenous helper plasmids such as pHIT60, and pCOLT-GALV.

After 48 hours, transfection efficiency was analyzed for expression of the CARs in HEK-293T cells using flow cytometry. Moreover, the supernatant of the cell culture containing the viral particles was harvested to be used for the transduction of immune cells. In an analogous experiment, we also examined the expression of TCRm CARs on the surface of phoenix cells two days after transfection. Interestingly, we observed that CARs with hIgG- or Strep-tag II-HD show similar levels of surface expression even on Phoenix Ampho cells (Fig. 4.5).

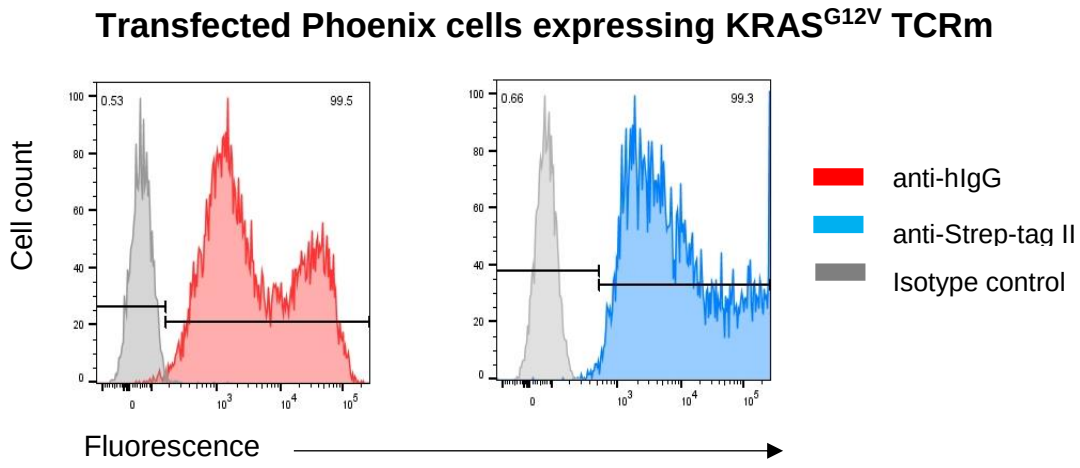

Figure 4.5: Flow cytometry analysis of KRAS TCRm expression on Phoenix-Ampho cells 48 hours after transfection. Phoenix cells that were transfected with the hIgG CAR vector were stained with anti-hIgG-PE mAb (filled red areas). Phoenix lines that were transfected with Strep-tag II CAR were stained with anti-Strep-tag II-Biotin mAb followed by streptavidin (SA)-APC(filled blue area). The isotype control (filled gray area) was obtained from transfected Phoenix cells that were stained with irrelevant antibodies. CAR, chimeric antigen receptor.

4.5 Expression efficiency of TCRm CARs on the surface of transduced cells

In view of the fact that spacer domains (also known as hinge regions) influence the expression and function of CARs on the surface of cells, we first transduced human T cells with our two KRAS^{G12V} TCRm CAR constructs. Peripheral blood lymphocytes (PBLs) were enriched from cultured peripheral blood mononuclear cells (PBMCs) by stimulation with anti-CD3 and anti-CD28 mAbs plus 100 u/mL human IL-2 for 48 – 72 hours prior to transduction. Afterwards, PBLs were transduced with supernatant cells containing retrovirus particles via spin infection. Transduction efficiency was

determined one week post-transduction using flow cytometry. The Figure 4.6 (A) depicts FACS results of transduced T cells for both KRAS^{G12V} TCRm CAR constructs one week after transduction. Co-expression of KRAS TCRm CAR and CD3 was investigated to exclude high proportion of other transduced immune cells including NK and B cells, as they do not express TCR-related CD3 molecules on their surface cells. FACS analysis of T cells transduced with two different TCRm CAR constructs demonstrated no significant differences in the level of KRAS TCRm CAR expression and transduction efficiency one week after transduction (35.0% KRAS^{G12V} hIgG CAR vs 35.6% KRAS^{G12V} Strep-tag II CAR of PBMC cells). Based on this result we assumed that TCRm CAR-expressing T cells should recognize mutated KRAS^{G12V}/HLA-A2 complexes on the surface of tumor cells resulting in proliferation. Therefore, KRAS^{G12V} peptide-pulsed and irradiated (10.000 Gray) T2 cells were co-cultured with CAR T cells at an effector (E) / target (T) ratio of 5:1. After three times antigen-specific stimulation using peptide-pulsed T2 cells, FACS analysis was conducted. As shown in the Figure 4.6 both KRAS hIgG CAR- and KRAS Strep-tag II CAR-T cells recognized KRAS^{G12V} peptide and expanded at least 2-fold to approximately 80% of KRAS-specific effectors (compare Fig. 4.6 (A) & (B)). Flow cytometry analysis with antibodies against hinge regions of TCRm CARs also revealed that, even three weeks after antigen-specific stimulation, there was no significant difference in the amount of CARs on the surface of transduced T cells. We did not see any comparable difference in TCRm CAR expression on human T cells (79.6% D10-hIgG CAR vs 79.5% D10-Strep-tag II CAR) (Fig 4.6 (C)). Next, in a side-by-side comparison study, we measured expression levels of two KRAS^{G12V} TCRm CARs on the surface of Jurkat reporter cells in order to determine if the hinge region of the CAR can affect expression levels. Hence, retroviral culture supernatant containing viral particles was filtered and utilized for transduction of JNL cells. Transduced Jurkat cells were expanded in the presence of puromycin to be selected for CAR expressing cells starting on day six after spin infection. Expression level of TCRm CARs was determined using corresponding fluorochrome-labeled mAbs against the hIgG and Strep-tag II hinge domains by flow cytometry analysis. Flow cytometric analysis of the histograms revealed that there was no apparent difference in the expression rate of TCRm CARs on the surface of Jurkat reporter cells six days following transduction (Fig. 4.7).

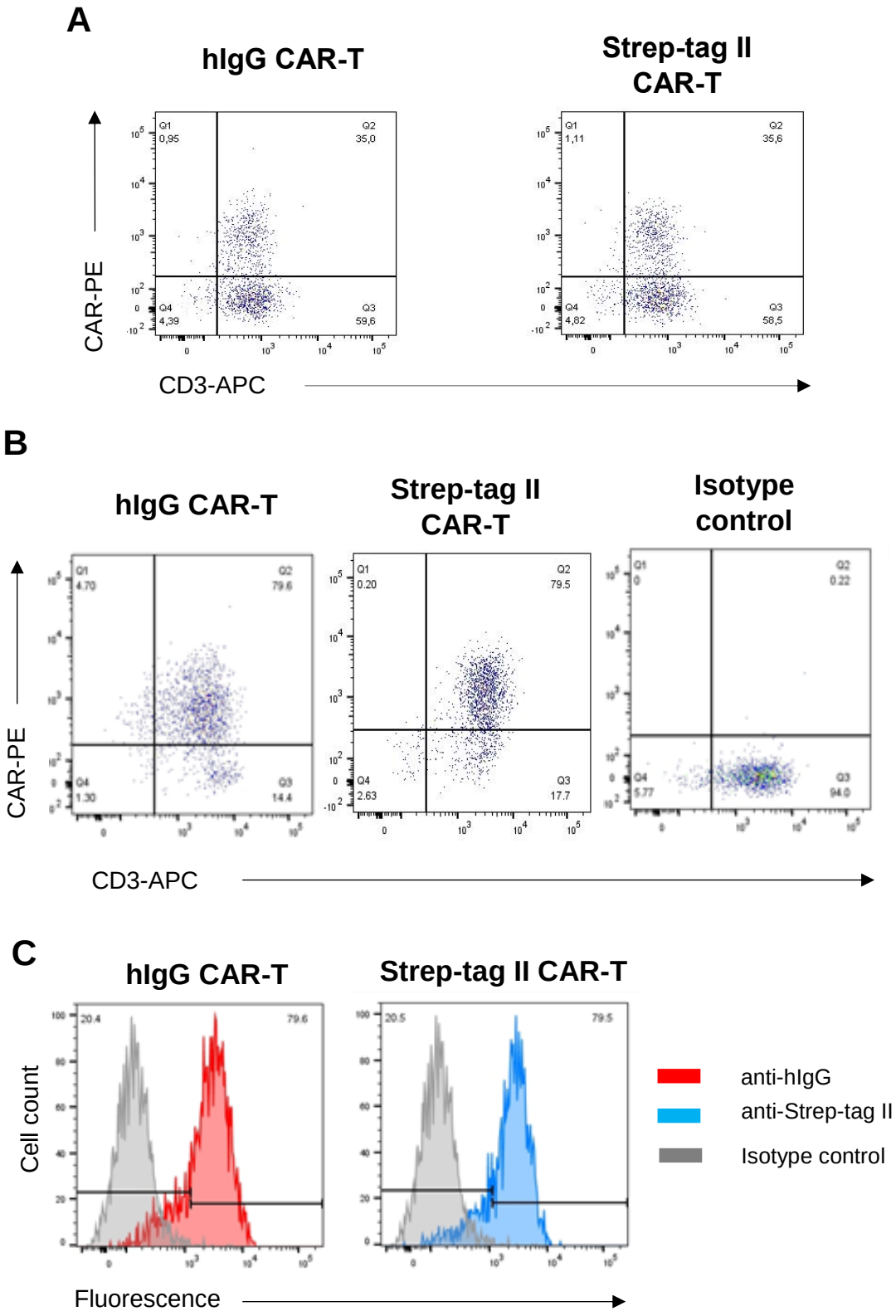

Figure 4.6: TCRm CARs expression on reprogrammed T cells. (**A**) Representative flow cytometry analysis of TCRm CARs and CD3 expression on T cells one-week after transduction. (**B**) A representative flow cytometry analysis of TCRm CARs and CD3 expression by in vitro expanded reprogrammed T cells co-cultured with peptide-pulsed T2 target cells after three weeks. Expression of TCRm CARs and CD3 were analyzed by flow cytometry with mutated $KRAS^{G12V}$ peptide-loaded HLA-A*0201-tetramer and anti-CD3 mAb as indicated. $KRAS^{G12WT}$ loaded- HLA-A*0201 tetramer was

served as an isotype control for staining of TCRm CAR-modified T cells. (**C**) A representative histogram of flow cytometric analysis of hIgG CAR-T and Strep-tag II CAR-T cells, which were stained with anti-hIgG and Strep-tag II mAbs for TCRm CARs expression as shown in (B). The red histogram shows hIgG-CAR-T cells, which were stained with anti-hIgG-PE antibody and the blue histogram, represents Strep-tag II CAR-T cells, which were stained with anti-Strep-tag II mAb followed by (SA)-APC. Gray histograms display transduced CAR-T cells were stained with irrelevant antibodies as an isotype control. CAR-T, chimeric antigen receptor-T cell.

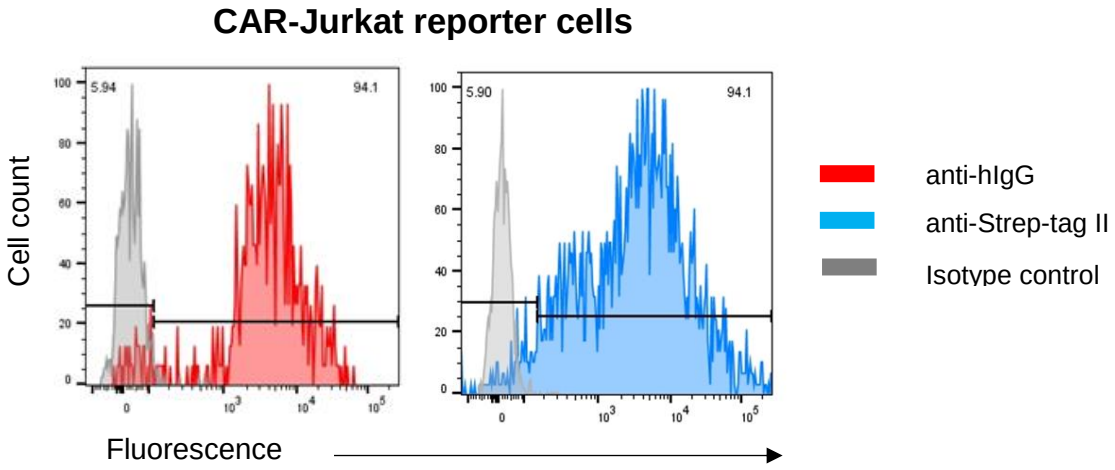

Figure 4.7: Flow cytometric analysis of the surface expression of TCRm CARs on Jurkat reporter cells. The red histogram indicates the staining of the transduced hIgG CAR-J cells with antibodies against the human IgG hinge region. The blue histogram represents Strep-tag II CAR-J cells were stained with the anti-Strep-tag II-Biotin followed by SA-APC. The gray histograms illustrate transduced cells stained with irrelevant antibodies in order to serve as an isotype control. CAR, chimeric antigen receptor.

4.6 Signaling analysis of TCRm CARs

NFAT responsive luciferase reporter Jurkat cell lines (JNL cells) are derived from wild type Jurkat and express a firefly luciferase reporter gene under the control of NFAT response elements. A number of studies have already shown that T cell activation induces the transcription factor nuclear factor of activated T-cells (NFAT) via stimulation of TCR and results in an anti-tumor response. Therefore, the induction of NFAT correlates strongly with the activation of TCR molecules (Marangoni et al., 2013; Maguire et al., 2013). Interestingly, signaling mechanisms and transcription factor networks found in primary T cells are highly conserved in Jurkat cells. Using this knowledge, we hypothesized that activation of JNL cells through CAR signaling pathways would correlate with stimulation of CAR redirected primary T cells.

In this line JNL cells expressing the $KRAS^{G12V}$ hIgG CAR were activated either with anti-CD3 plus anti-CD28 or anti-hIgG mAbs. This should result in either a TCR-activation signal mediated by the endogenous TCR expressed in JNL cells or a

CAR-mediated signal induced by agonistic binding of anti-hIgG mAb to the hIgG spacer. As depicted in the Figure 4.8 (A) KRAS hIgG CAR-JNL cells elicited a strong luciferase signal 24 hours post stimulation when compared to non-stimulated CAR-JNL cells used as negative control. Next, hIgG CAR-expressing reporter cells were assessed for signaling induced upon binding of KRAS peptide loaded HLA-A*0201-tetramer. Again, specific luciferase signal could be detected which was significantly stronger as compared to CAR-JNL cells stimulated with the $KRAS^{G12WT}$ peptide-loaded HLA-A*0201-tetramer control (Fig. 4.8. (B)). In the next set of experiments, we sought to determine activation of NFAT in CAR-JNL cells by stimulation with T2 KRAS presentER cells expressing $KRAS^{G12V}$/HLA-A*0201 complexes on the cell surface. Therefore, co-culture experiments with $KRAS^{G12WT}$ peptide-pulsed T2 and T2 expressing PresentER-$KRAS^{G12V}$ minigene stimulator cells and CAR-JNL was performed. We observed that $KRAS^{G12V}$ pulsed T2 cells induced a high level of luciferase signal in CAR-JNL cells, whereas no signal was detected with $KRAS^{G12WT}$ peptide-pulsed T2 stimulator cells. Additionally, no CAR-JNL activation was observed with T2 presentER-$KRAS^{G12V}$ stimulator cells after 24 hours of co-culture (Fig 4.8 (C)).

Similar experiments conducted with KRAS CAR Strep-tag II-JNL cells revealed the same results supporting the data described above and supporting the notion that apparently the $KRAS^{G12V}$ peptide was not presented by the T2 presentER cells (Fig 4.8 (D)). Interestingly, co-culture with $KRAS^{G12V}$ pulsed T2 cell and Strep-tag II CAR JNL cells for 24 hours resulted in a higher luciferase signal than observed for hIgG CAR JNL cells although both TCRm CAR constructs clearly induced NFAT-Luciferase activity in JNL cells.

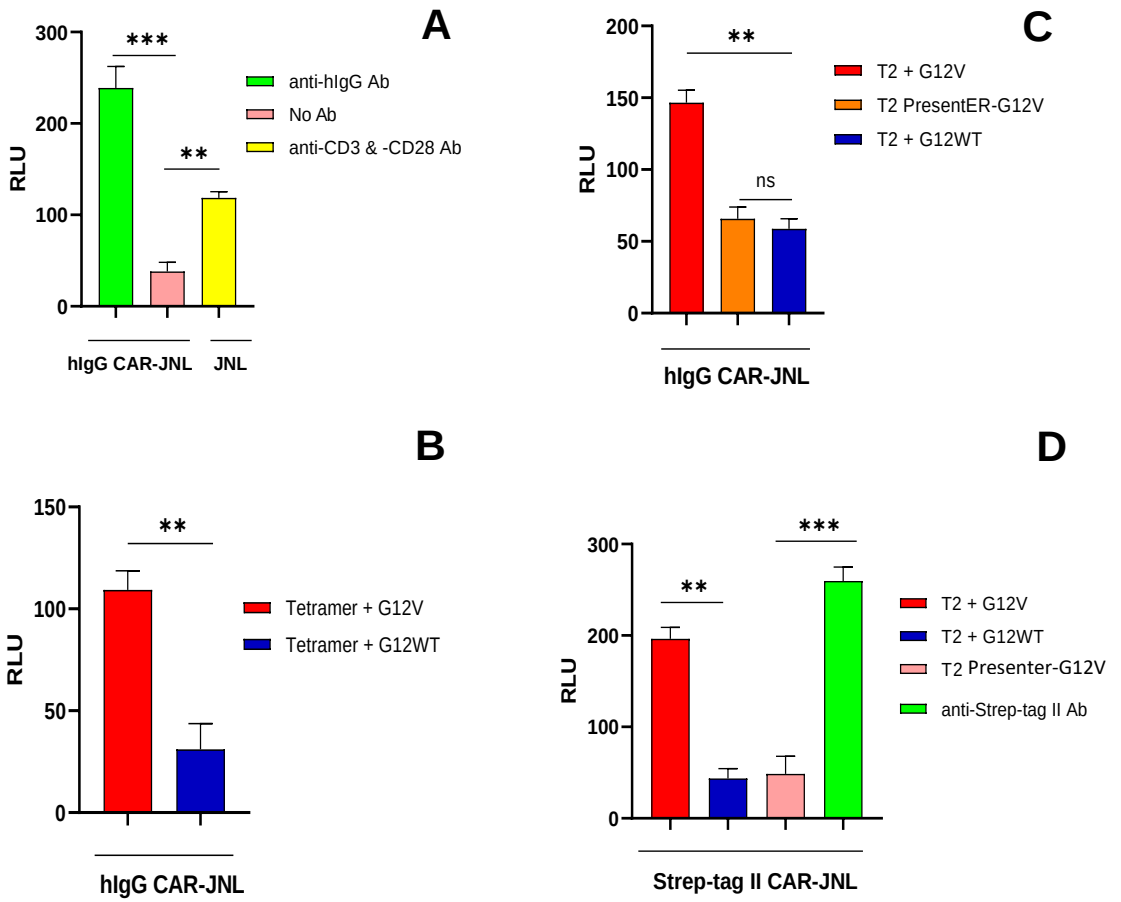

Figure 4.8: Identification of TCRm CAR signaling using CAR-J reporter cells. Luciferase signal is followed by NFAT activation of hIgG CAR-J reporter cells after stimulation with (**A**) either anti-CD3 and anti-CD28 mAbs (2 µg/mL) or anti-hIgG mAb (2 µg/mL) against the hIgG hinge region within TCRm CAR or (**B**) loaded HLA-A*0201-Tetramer (1 µg/mL) with KRAS peptides (200 µM). (**C**) Luciferase signal is assessed when hIgG CAR reporter cells are combined with peptide-pulsed T2 cells or T2 cells expressing PresentER-KRAS^{G12V} minigene. (**D**) NFAT-mediated activation of Strep-tag II CAR-J reporter cells is detected upon combination with peptide-pulsed T2 target cells or in the presence of 2 µg/mL of antibodies targeting Strep-tag II hinge region. The expression of luciferase signal was evaluated 24 hours after co-incubation at an E/T ratio of 1:1 at 37°C. Data indicate mean values ± SD of three technical replicates and are representative of two independent experiments which were analyzed by two-tailed unpaired Student's t-test. ** P<0.01, *** P<0.001. ns: P>0.05. mAb, monoclonal antibody; CAR-JNL, chimeric antigen receptor-Jurkat NFAT-Luciferse reporter cell; E/T, effector to target ratio; G12V, mutated KRAS peptide; G12WT, wild-type KRAS peptide; ns, non statistical significance; RLU, relative luminescnece unit.

4.7 Functional activity of TCRm CAR-modified T cells

An important feature of activated T cells is the production of pro-inflammatory cytokines, such as IFN-γ. This cytokine plays an important role in anti-tumor immunity and high level of IFN-γ production correlates with an effective immune response (Schroder et al., 2004). To evaluate specificity of TCRm CAR constructs and anti-tumor response of TCRm CAR-reprogrammed T cells against tumor cells in vitro,

IFN-γ was measured using ELISpot assay. Thereby, hIgG CAR- or Strep-tag II CAR -modified T cells were co-cultured with different sets of cell lines at an E: T ratio of 5:1 for 24 hours. As the figures 4.9 (A) and (B) display, Strep-tag II CAR-expressing T cells secreted high level of IFN-γ cytokine upon exposure to $KRAS^{G12V}$ peptide-pulsed T2 cells as compared to T2 cells pulsed with $KRAS^{G12WT}$ peptide and this difference was significant after 24 hours co-incubation. Meanwhile, co-culture with Strep-tag II CAR-redirected T cells and different targets (T2-PresentER-$KRAS^{G12V}$ minigene, NCI-H441, and CFPAC-1 tumor cells) revealed no significant difference when compared to $KRAS^{G12WT}$ peptide-pulsed T2 cells (negative control). Similarly, hIgG CAR–expressing T cells elicited the same difference in IFN-γ release when exposed to each of the indicated target cells. Moreover, hIgG CAR-modified T cells released less cytokine than CAR-containing Strep-tag II redirected-T cells when exposed to mutant KRAS pulsed T2 cells, indicating that the anti-KRAS response of Strep-tag II CAR T cells was more effective.

As the lytic activity of T lymphocyte cells is not entirely influenced by cytokine production, cytolytic activity was assessed using a bioluminescence-based killing assay (Varadarajan et al., 2011). A Firefly luciferase reporter based assay was performed to assess TCRm CAR-T cell cytotoxicity co-incubated with exogenous KRAS peptide-pulsed T2 target cells, since previous assays showed that mutant KRAS peptide-pulsed cells induced IFN-γ release in activated KRAS CAR-T cells (see Fig 4.9 (A) & (B)). Therefore, Peptide-pulsed T2 cells were co-cultured with TCRm CAR-T cells at different E: T ratios for 12 hours. As shown in the Figures 4.9 (C) and (D), Strep-tag II CAR-T cells mediated stronger anti-tumor activity than hIgG CAR-T cells against mutant KRAS peptide-pulsed T2 cells. Lytic activity of $KRAS^{G12V}$ pulsed T2 cells mediated by Strep-tag II CAR-T cells was approximately 40% at an E: T ratio of 1:1, and cytotoxicity increased up to 60% at an E: T ratio of 20:1. In contrast, hIgG CAR-T cells elicited about 20% cytotoxicity lysis at an E: T ratio of 1:1 against $KRAS^{G12V}$ pulsed T2 cells and this lysis reached > 40% at the highest E: T ratio of 20:1. In addition, we observed less than 20% lysis in T2 cells pulsed with $KRAS^{G12WT}$ (as a negative control) at all ratios after 12 hours co-culture. Taken together, these data demonstrate that both types of KRAS CAR redirected T cells elicited potent IFN- γ release and cytolytic activity upon recognition of $KRAS^{G12V}$ peptide. Moreover, the KRAS Strep-tag II CAR appeared to be more potent.

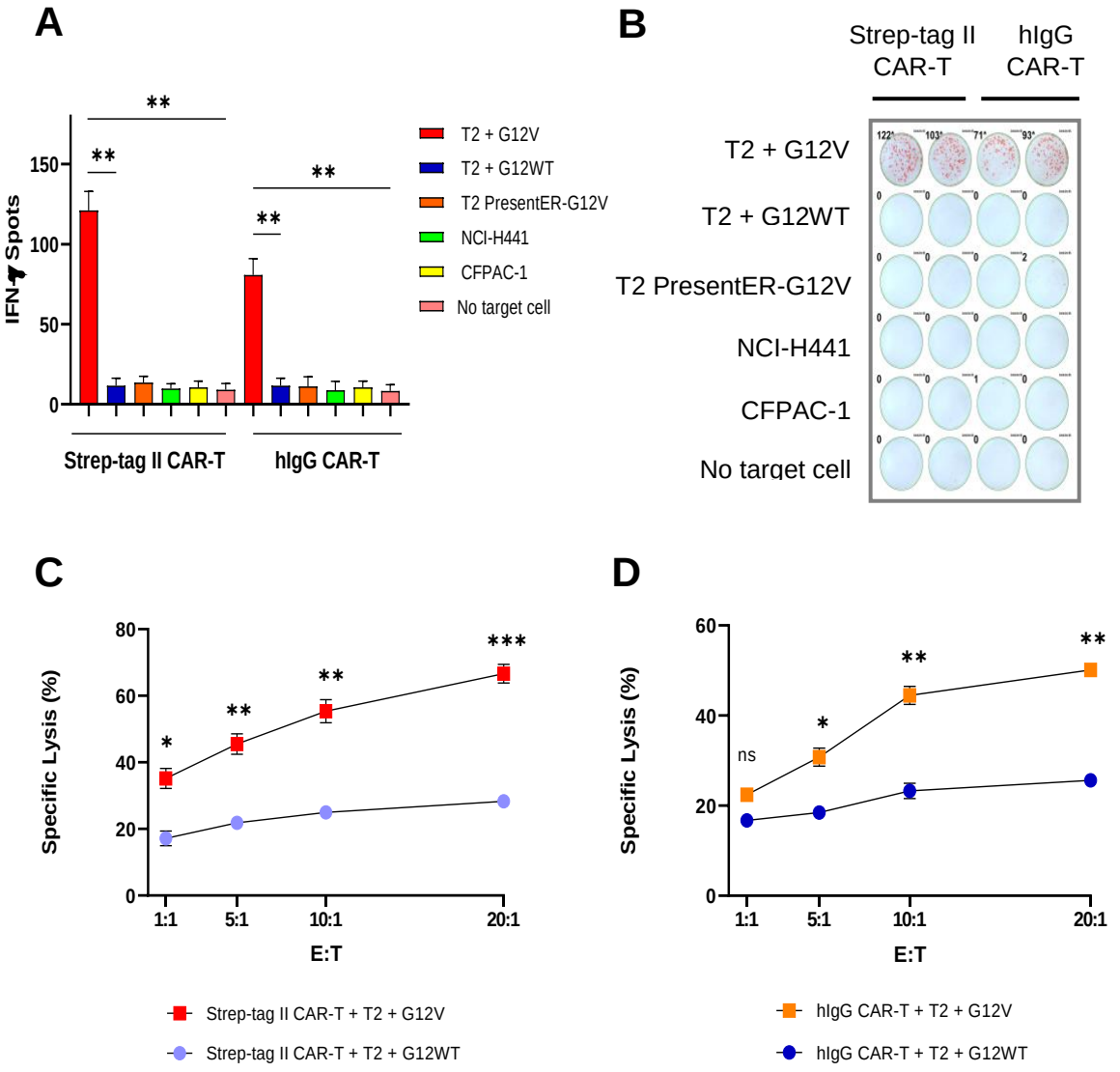

Figure 4.9: TCR-mimic CAR-T cell-mediated activation in response to target cells. (**A**) Measurement of IFN-γ released by TCRm CAR-T cells co-cultured with target cells. IFN-γ release was assayed after combination of 1×10^5 hIgG CAR- or Strep-tag II CAR-engineered T cells with 2×10^4 target cells (E:T = 5:1) for 24 hours. Data are presented as mean values with standard deviation of two individual ELISpots (mean values ± SD) and representaive of three independent experiments. Data were analyzed by two-tailed unpaired Student's t-test. ** indicates $P < 0.01$. (**B**) Representative image of IFN-γ spots appeared on the ELISpot membrane and IFN-γ spot numbers were determined with the use of image analyser equipped with software. This image represents one of three biological experiments. (**C**) (**D**) Cytotoxicity of TCRm CAR-T cells exposed to T2 cells pulsed with exogenous KRAS peptides. Target cells were pulsed with indicated peptides and then co-cultured with Strep-tag II CAR-T cells or hIgG CAR-T cells at various E: T ratios for 12 hours. TCRm CAR-T cell cytotoxicity was evaluated by firefly luciferase reporter system assay. Data indicate mean values ± SD of three technical replicates and are representative of two independent experiments. Data were analyzed by two-tailed unpaired Student's t-test. *P<0.05, **P<0.01, ***P<0.001. ns: p>0.05. CAR-T, chimeric antigen receptor-T cell; E:T, effector to target ratio; G12V, mutated KRAS peptide; G12WT, wild-type KRAS peptide; ns, not significant.

4.8 Generation and functional activity of TCRm CAR-equipped NK-92 cells

The expression of tumor-specific CARs in NK-92 cells facilitates selective and efficient killing of tumor cells expressing respective target antigens (Uharek et al., 2002; Müller et al., 2008). Therefore, having demonstrated specificity of TCRm CAR-modified T cells, we sought to additionally evaluate anti-tumor ability of NK-92 cells with a TCRm CAR containing hIgG spacer region. NK-92 cells were retrovirally transduced and subsequently expanded and enriched for transduced cells over two weeks. Cell surface expression of the KRAS CAR molecule was confirmed by flow cytometry and revealed that approximately 72.8 % of transduced cells were CAR-positive when compared to parental NK-92 cells (Fig 4.10 (A) & (B)). Once NK-92 cells were enriched for CAR expression, transduced cells were tested for their ability to recognize $KRAS^{G12V}$ neoantigen.

As an initial readout of CAR-positive NK-92 activation, we assayed for IFN-γ release. Therefore, T2 cells were pulsed with mutant or wild type KRAS peptide, co-cultured with CAR-redirected NK-92 cells, and assayed for IFN-γ secretion using ELISpot assay. As depicted in the figures 4.10 (C) and (D), KRAS CAR NK-92 cells exerted some nonspecific reactivity upon stimulation with $KRAS^{G12WT}$ peptide-pulsed T2 cells. Similarly, CAR NK-92 cells secreted small amounts of IFN-γ upon exposure to T2 PresentER-$KRAS^{G12V}$ cells when compared to T2 pulsed G12WT cells. In contrast, when TCRm CAR-reprogrammed NK-92 cells were co-cultured with T2 cells pulsed with $KRAS^{G12V}$, CAR NK-92 effector cells released threefold more IFN-γ cytokine as compared to the control.

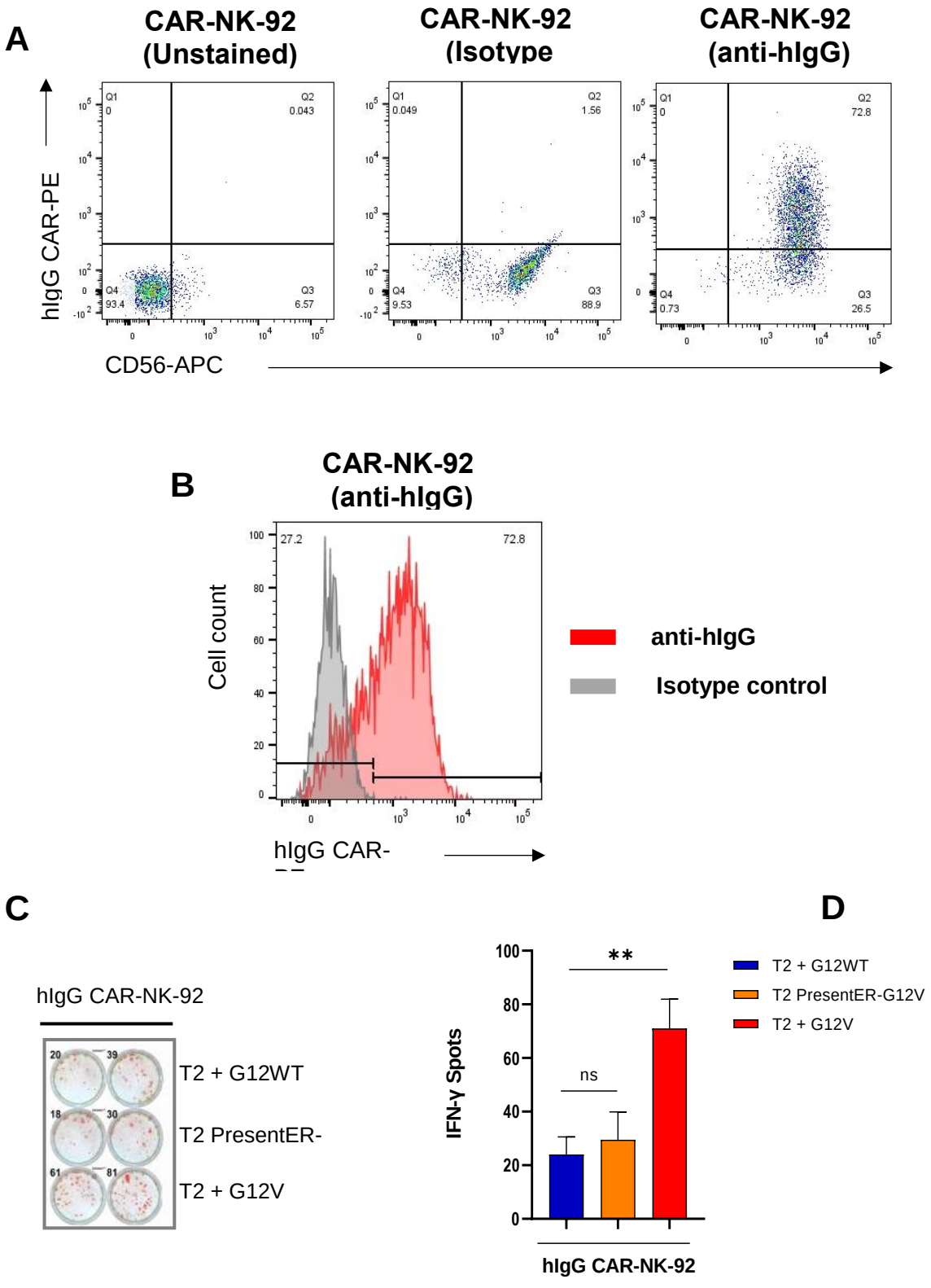

Figure 4.10: Flow cytometry analysis of TCRm CAR-modified NK-92 cells and functional activity of TCRm CAR-equipped effector cells. (**A**) Transduced cells were stained with anti-CD56 mAb and followed by anti-hIgG mAb before flow cytometric analysis. Controls included unstained cells and cells incubated with an irrelevant mAb of the same isotope. (**B**) The red histogram depicts the staining of TCRm CAR-expressing NK-92 cells with anti-hIgG antibody and the gray histogram depicts the staining

of transduced cells with the appropriate antibody as an isotype control. (**C**) Representative image of IFN-γ spots appeared on the ELISpot membrane and spot numbers were evaluated with an image analyzer equipped with a software. One representative image out of three biologiccal experiments is represented. (**D**) Results of the IFN-γ ELISpot assay after 1× 10^5 hIgG CAR-modified NK-92 effector cells were incubated with 2× 10^4 target cells (E: T= 5:1) for 24 hours . Data indicate mean values ± SD of two technical replicates and are representative of three independent experiments. Data were anlayzed by two-tailed unpaired Student's t-test. ** indicates P< 0.01, and ns denotes p>0.05. CAR-NK-92, chimeric antigen receptor-NK-92 cell; E:T, effector to target ratio; G12V, mutated KRAS peptide; G12WT, wild-type KRAS peptide; mAb, monoclonal antibody; ns, not significant.

4.9 Construction of a BiTE targeting KRAS^{G12V} pHLA-A2 molecules

To generate a BiTE capable of redirecting T cells onto tumors harboring KRAS^{G12V} pHLA-A2 on the surface, the previous scFv D10-7 fragment was fused to an anti-CD3 scFv (hereafter referred to as UCHT1) (provided by Dr. Bert Vogelstein, Dept. of Pathology, Johns Hopkins University School of Medicine) with a long linker (Fig. 4.11).

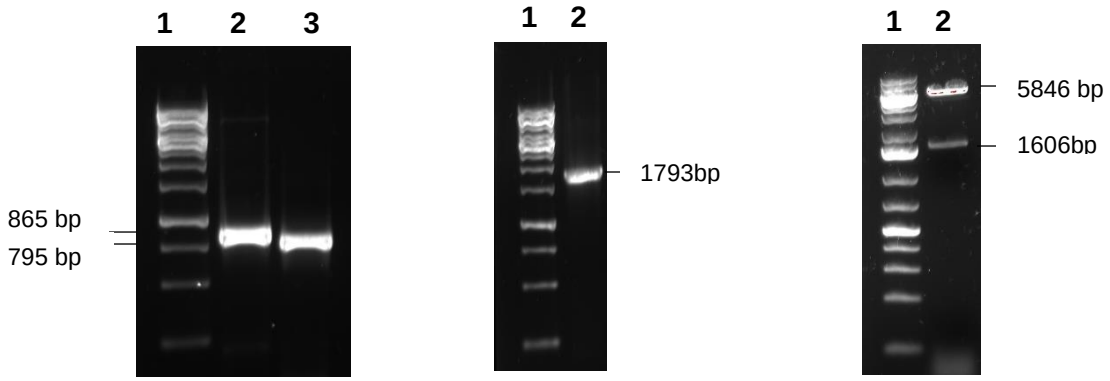

Figure 4.11: Molecular process of scFv D10-7 -UCHT1 bispecific antibody. Representative electrophoresis image of the PCR products and restriction enzyme analysis of the scFv-UCHT1 encoding vector. PCR amplification of scFv and UCHT1 fragments showed bands at 865 and 795 bp, respectively (left). After transformation of E coli K12 strain Stable III with cloned vectors, individual colonies were identified by colony PCR. A successful cloning revealed an insertion fragment of 1793 bp (middle). EcoRI and PacI restriction digestion of the cloned vector revealed estimated bands at 5846 bp and 1606 bp for the insert fragment and backbone vector, respectively (right). GeneRuler 1 kb was loaded on the gel (lane 1) to estimate DNA size. This image illustrates one of three biological experiments.

For the production of bispecific antibody, CHO producer cells were stably transduced with transfer vector encoding scFv D10-7-UCHT1 (Appendix, Fig. S5) by retroviral particles, (the retrovirus system procedure was discussed in M&M section). Finally, transduction efficiency was determined by intracellular staining using anti-HA-tag antibody (Fig. 4.12).

Results of intracellular staining were confirmed by flow cytometry, which showed that over 90% of transduced cells produced bispecific antibodies with a high level of antibody production when compared to non-transduced cells.

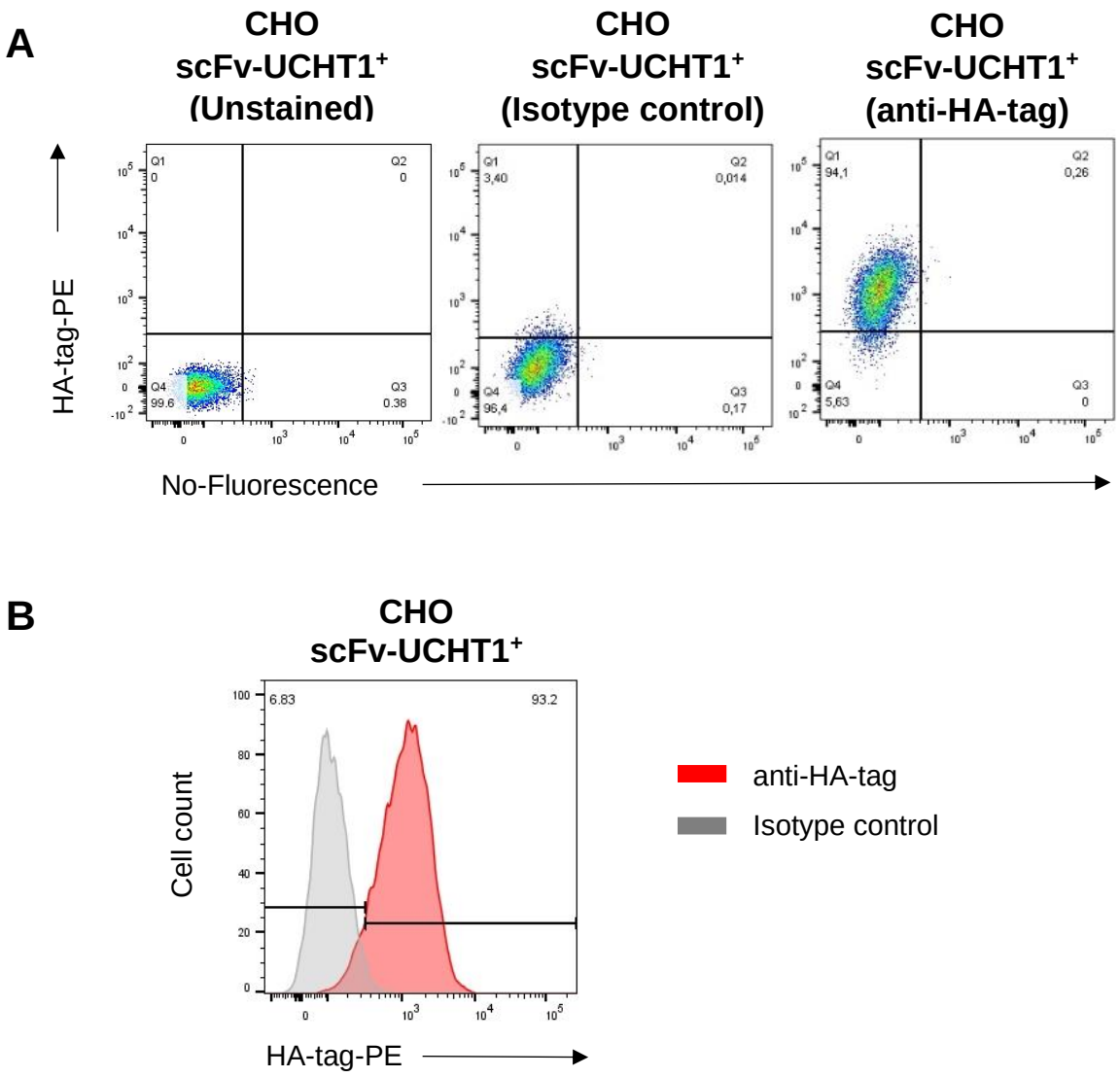

Figure 4.12: Flow cytometric analysis of scFv-UCHT1 expression in CHO cells. (**A**) Intracellular staining of scFv-UCHT1-expressing CHO cells with an anti-HA-tag antibody. Unstained cells and cells were only incubated with the antibody of the same isotype served as controls. (**B**) Flow cytometry data shown in (A) are presented as a histogram. The red histogram indicates transduced CHO cells stained with anti-HA-tag antibodies, whereas the gray histogram represents transduced cells stained with an irrelevant antibody as an isotype control. CHO, chinese hamster ovary cells; HA-tag, hemagglutinin-tag.

4.10 Exploring T2 cells expressing PresentER-encoded KRAS^{G12V} pHLA-A2

To produce precise KRAS^{G12V} neoantigens associated with HLA-A2 on the surface of cells, we have developed a minigene-based method (PresentER). This technique can be used to specifically identify TCRm antibodies, and TCRm CAR-expressing T cells targeting this mutant peptide as a ligand. Cells deficient in transporter associated with antigen presentation (TAP), including the human cell line T2 and mouse cell line RMA/S, are naturally unable to process endogenous peptides derived from mutant genes and present them on the cell surface as pHLA complexes. However, PresentER minigene enables the transport of KRAS^{G12V} peptide directly to the endoplasmic reticulum with the use of a signal sequence. (Fig. 4.13). Thus, PresentER-driven peptides can be generated from full-length protein sequences without the need to go through endogenous protein processing steps. (Bacik et al., 1994).

For this procedure, we designed two DNA oligomers encoding KRAS^{G12V} peptide with SfiI cassette and then PCR products were subcloned into a PresentER retroviral backbone (kindly provided by PD Dr. Bockamp, Inst. for Transl. Immunol., UMM) (Fig. 4.13 (A)). The PresentER plasmid map can be found in supplemental information figure S5. Successful cloning was proved by DNA Sanger sequencing. As sequencing result depicted in the figure 4.13 (B), in comparison to reference DNA sequence which can be translated to a 10-mer wild-type peptide (KLVVVGAGGV), sequence of PresentER-KRAS^{G12V} encodes a 10-mer peptide (KLVVVGAVGV), in which Valine residue (V) at position 8 represents one G12V mutation. Subsequently T2 cells were stably transduced with retrovirus-containing supernatant via spin infection and finally transduced cells were enriched using puromycin selection. (Fig. 4.14). To confirm that PresentER-driven antigens can be processed and presented on the surface of TAP-deficient cells, we also generated mouse TAP-deficient RMA/S cells expressing PresentER-SIINFEKL peptide (Fig. 4.14). Flow cytometry results of binding 25-D1.16 antibody to mouse H-2Kb/SIINFEKL was evident in comparison to cells without antigen minigene expression, suggesting that PresentER system allows epitope display in cells lacking in endogenous presentation of HLA-associated peptides (Fig. 4.15).

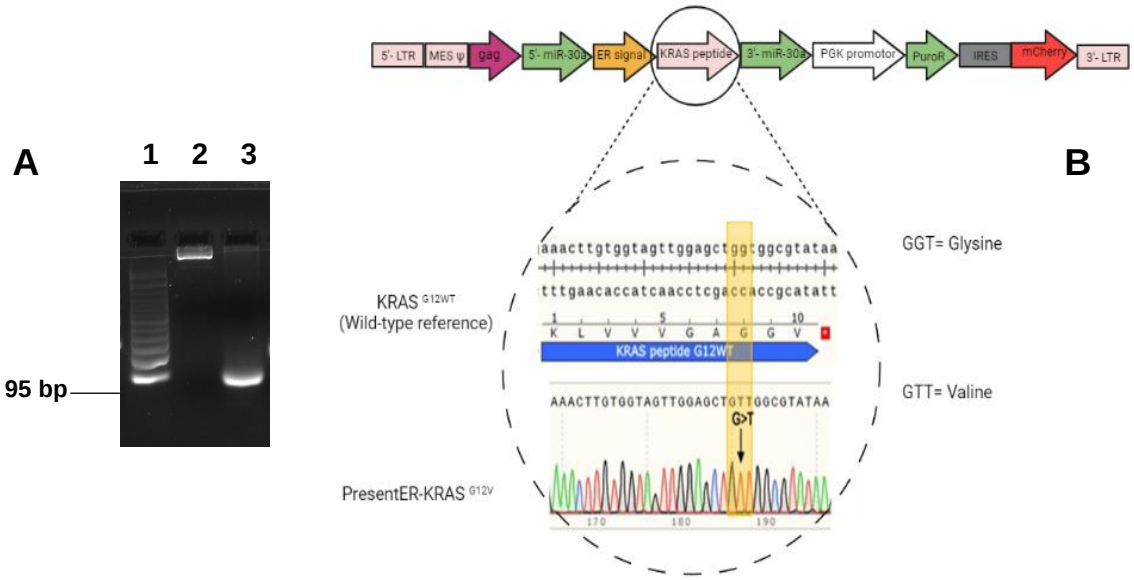

Figure 4.13: Design and characterization of PresentER-KRAS^{G12V} minigene. (**A**) Representative image of colony PCR was performed for the newly generated plasmid DNA encodes PresentER-KRAS^{G12V}. The PCR product shows an expected band of 95 bp (lane 3). Quick-Load purple 100 bp DNA ladder was loaded on the gel lane 1 to estimate DNA size. The lane 2 was negative control. This image illustrates one of three biological experiments. (**B**) Representative sequence result of PresentER vector, which encodes a 10mer-peptide KRAS^{G12V} compared to reference sequence.

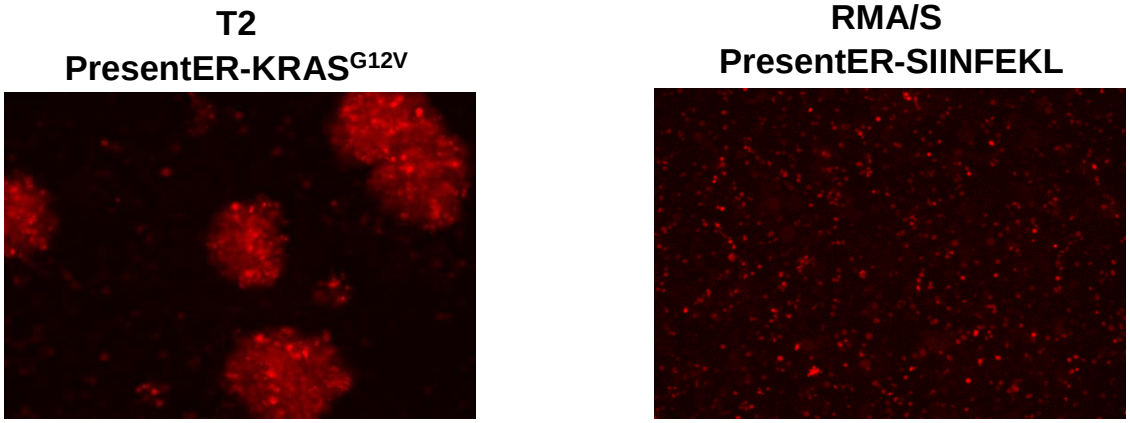

Figure 4.14: Analysis of mCherry expression in cells transduced with PresentER-minigenes. T2 cells expressing PresentER-KRAS^{G12V} (mCherry) and RMA/S cells expressing PresentER-SIINFEKL (mCherry) were visualized with a Texas-Red filter under a fluorescence microscope.

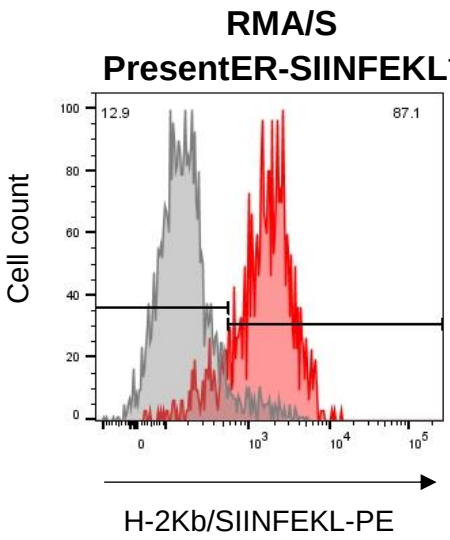

Figure 4.15: Flow cytometry analysis of RMA/S cells expressing the PresentER-SIINFEKL minigene. The red filled area illustrates the staining of transduced RMA/S cells with anti-H2Kb/SIINFEKL antibody and the gray filled area represents the staining of transduced cells with an irrelevant antibody as an isotype control.

4.11 HLA stabilization assay and recognition of HLA-A2-restricted $KRAS^{G12V}$ neoantigens on cancer cells

In this study, we chose to use the $KRAS^{G12V}$ peptide as a target epitope and predicted that it was capable of binding to HLA-A2 molecules using the NetMHCpan-4.0 algorithm (Table 1.3). We also demonstrated the binding ability of mutant peptide $KRAS^{G12V}$ using the T2 binding assay. T2 cells are derived from lymphoma cell lines; however, they can only present exogenous peptides since they carry a deletion in gene encoding TAP1 and TAP2 transporters, which are responsible for presenting endogenous peptides (Salter et al., 1985). T2 cells naturally express a low amount of HLA-A2 molecules on their surface cells; these molecules, however, can be stabilized by the addition of HLA-A2-binding peptides and can be detected by antibodies that are capable of targeting the HLA-binding peptides (Luft, 2001). To investigate the binding ability of KRAS peptides to the HLA-A*0201 molecule, we pulsed T2 cells with $KRAS^{G12V}$ (KLVVVGAVGV), $KRAS^{G12WT}$ (KLVVVGAGGV). Peptide-pulsed T2 cells were stained with anti-HLA-A2 mAb, and staining analysis were quantified by flow cytometry. Our observation showed both $KRAS^{G12V}$ and wild type $KRAS^{G12WT}$ peptides induced an increase in cell surface HLA-A2 stabilization compared to background (T2 cell without peptide). This induced up-regulation of HLA-A2 proteins indicates the

binding affinity of both mutant and WT peptides to HLA-A2 molecules as predicted (Fig. 4.16).

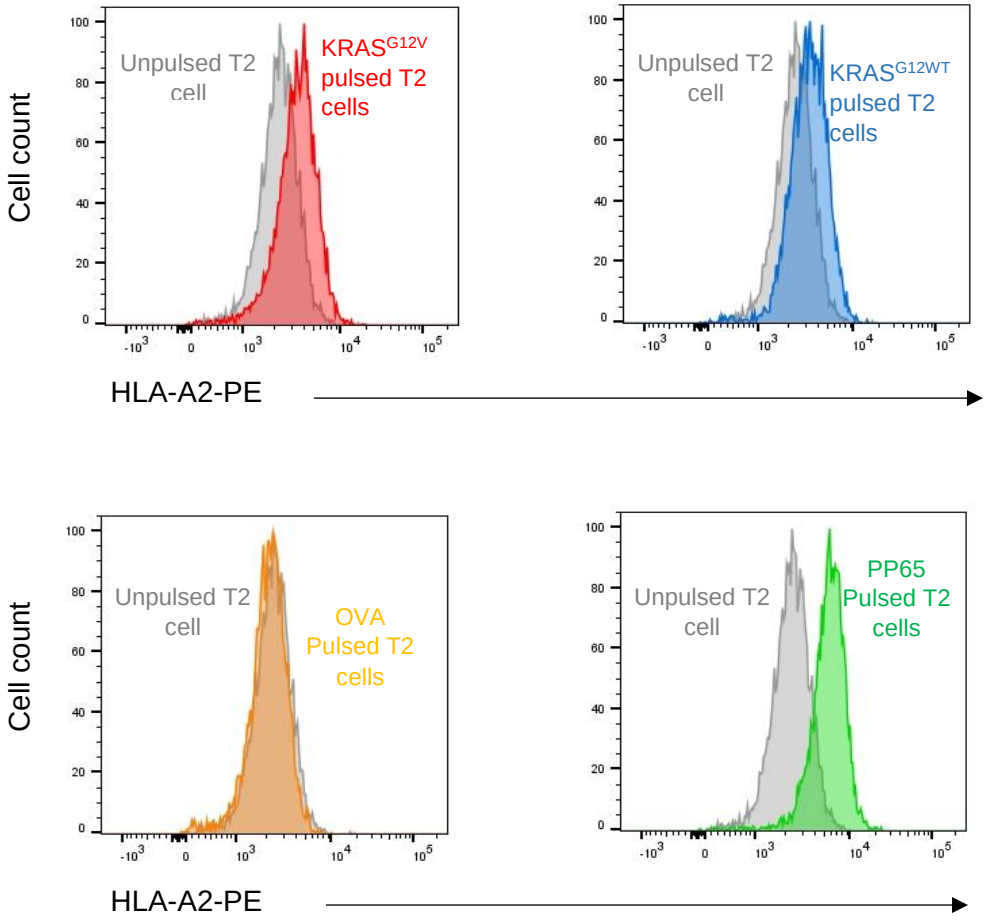

Figure 4.16: HLA stabilization test using T2 cells. An analysis of the levels of HLA-A2 on the surface of T2 cells by flow cytometry. The red histogram displays cells pulsed with KRAS^{G12V}, while the blue histogram represents wild-type KRAS peptide-pulsed cells. A negative control peptide, OVA peptide (SIINFEKL), and a positive control peptide, PP65 peptide, are displayed as orange and green histograms, respectively. The gray histogram demonstrates cells without peptides. HLA, human leukocyte antigen; KRAS^{G12V}, mutant KRAS peptide; KRAS^{G12WT}, wild-type KRAS peptide; OVA, ovalbumin peptide; pp65, 65 kDa phosphoprotein of human cytomegalovirus.

In the following step, we investigated whether the scFv D10-7-UHCT1BiTE could recognize KRAS^{G12V} pHLA-A2 complexes on the surface of cells. Thus, peptide-pulsed T2 cells were stained with scFv D10-7-UCHT1 followed by Flow cytometry analysis of KRAS^{G12V} peptide-pulsed T2 cells incubated with scFv D10-7-UCHT1 confirmed that BiTE bound to KRAS^{G12V} peptide-pulsed T2 cells, whereas no binding to KRAS^{G12WT} peptide-pulsed T2 cells was observed (Fig. 4.17 (A)). Our flow cytometry analysis of the expression of HLA alleles in tumor cells demonstrated that

both NCI-H441 (lung adenocarcinoma) and CFPAC-1 (pancreatic ductal adenocarcinoma) cells express HLA-A2 molecules on the surface of the cells (see Fig. 4.19). In our next step, we tested scFv D10-7-UCHT1 for its ability to recognize KRAS^{G12V} pHLA-A2 complexes, formed through natural antigen processing, on *KRAS* G12 mutated cells, including the tumor cell lines NCI-H441 and CFPAC-1. Our study demonstrated that scFv D10-7-UCHT1 failed to recognize KRAS^{G12V} pHLA-A2 derived from the endogenously mutated *KRAS* gene (Fig. 4.17 (C) & (D)). In support of this result we could also not stain PresentER G12V-expressing T2 cells with scFv-UCHT1, again demonstrating that the BiTE was not able to bind to cells expressing PresentER-encoded KRAS^{G12V} (Fig. 4.17 (B)).

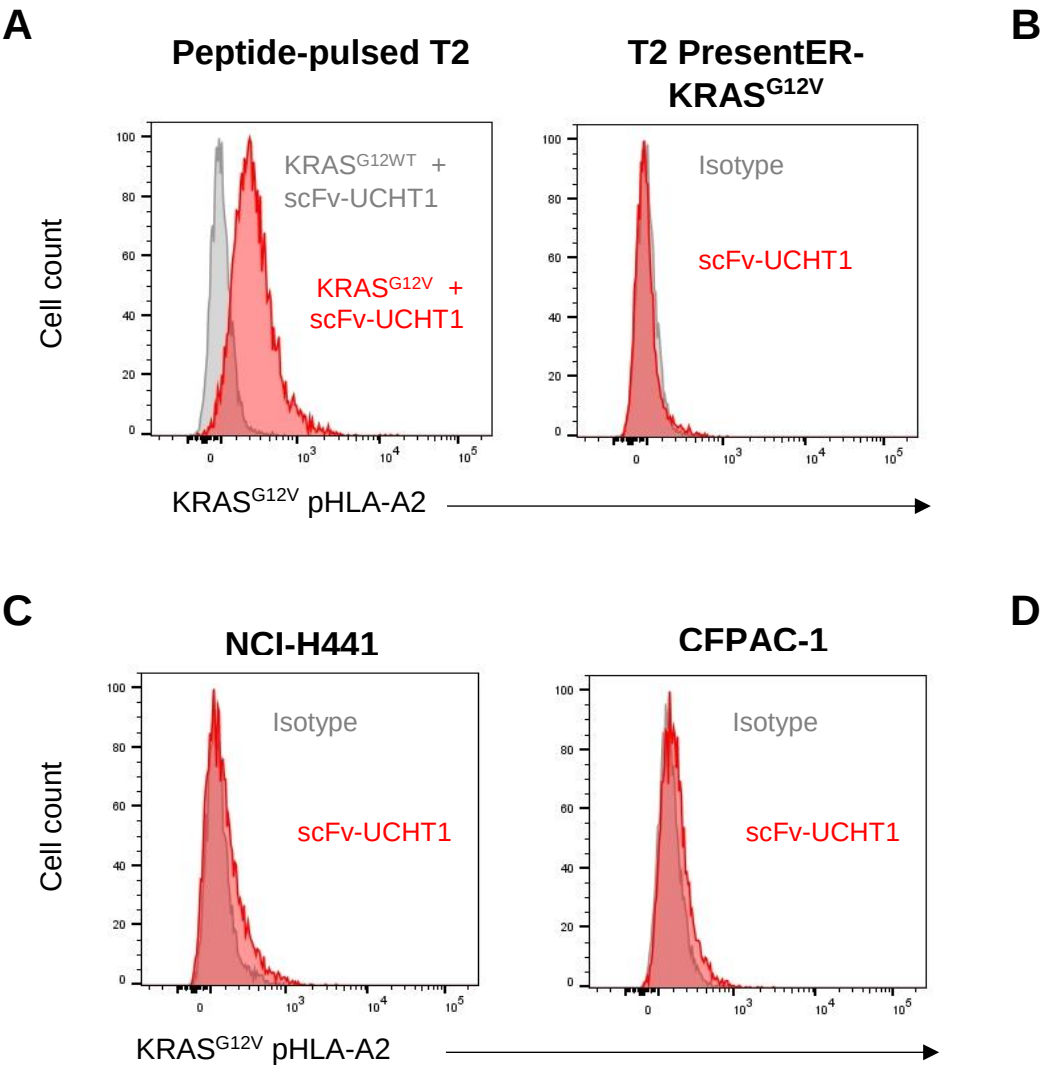

Figure 4.17: Recognition of HLA-A2-resticted KRAS^{G12V} neoantigens on cells by scFv D10-7-UCHT1. (**A-D**) The binding of scFv D10-7-UCHT1 to HLA-A2-bound KRAS^{G12V} peptide was investigated by flow cytometry on the surface of peptide-pulsed T2 cells as well as endogenous *KRAS* G12V gene-containing cancer cells (red filled areas). Ten µg/mL of BiTE was incubated with 5 × 10^5 cells. The cells that were only incubated with irrelevant antibodies (gray filled areas) were used as isotype controls.

$KRAS^{G12WT}$ peptide-pulsed T2 cells were incubated with only scFv D10-7-UCHT1 to serve as controls (gray filled areas) in experiments that cells were pulsed with peptides. $KRAS^{G12V}$, mutant KRAS peptide; $KRAS^{G12WT}$, wild-type KRAS peptide; pHLA, peptide-HLA (human leukocyte antigen). Effect of scFv D10-7-UCHT1 antibody on the lytic activity of T cells

4.12 Effect of scFv D10-7-UCHT1 antibody on the lytic activity of T cells

In order to show that scFv D10-7-UCHT1 bispecific antibody is capable of inducing T cells to react against target cells harboring mutant KRAS pHLA-A2, IFN-γ ELISpot assay was performed. For this experiment, we included peptide-pulsed T2 cells and T2 cells expressing PresentER-$KRAS^{G12V}$ minigene. We co-cultured T cells with target cells in the presence of scFv D10-7-UCHT1 bispecific antibody. Our findings showed that this bispecific antibody caused a high release of IFN-γ from T cells when co-cultured with G12V peptide-pulsed T2 cells. In contrast, low levels of IFN-γ was observed when T cells were exposed to G12WT peptide-pulsed T2 cells in the presence of bispecific antibody. Moreover, this difference in the amount of cytokine secretion was comparable. We also found that low IFN-γ spots were observed after co-culture of T cells with T2 cells expressing PresentER-$KRAS^{G12V}$ antigen in the presence of bispecific antibody. This amount of IFN-γ was negligible in comparison with wild-type KRAS peptide-pulsed T2 target cells combined with T cells in the presence of scFv D10-7-UCHT1 antibody (Fig. 4.18 (A) & (B)). This minimal difference in the amount of cytokine secreted from T cells is likely in response to the non-specific reaction of T cells to other exposed antigens on the surface of target cells.

To confirm that scFv D10-7-UCHT1 is able to exhibit cytotoxicity activity in co-cultures with T cells and G12V-expressing target cells, bioluminescence-based killing assay was performed. For this assay, T cells were co-cultured with luciferase-expressing peptide-pulsed T2 (Fig. 4.23 (E)) target cells in the medium containing scFv D10-7-UCHT1 bispecific antibody. In one experiment, various ratios of effector to target cells (E: T) from 1:1 to 20:1 were prepared. Our results revealed that T cells lysed G12V peptide-pulsed T2 cells considerably greater than G12WT peptide-pulsed T2 cells in all ratios and this difference is highly obvious at 20:1 ratio effector to target cells after 18 hours co-incubation. As we expected, wild-type peptide-pulsed target cells did not trigger T cell activation with antibody, even at a ratio of 20:1 effector to target cells (Fig. 4.18 (C)). In an autologous experiment, time-dependent specific cytotoxicity killing of bispecific antibody was measured. This experiment was done at different certain time points with a ratio of 5:1 effector to target cells. As shown the figure below,

specific lysis of mutant peptide pulsed T2 cells increased from about 30% after 18 hours co-incubation with T cells to over 55% on day two, despite percentage of viable wild-type peptide pulsed T2 cells was over 80% during this period of time (Fig. 4.18 (D)). These data indicate that when T cells were exposed to $KRAS^{G12V}$ peptide-pulsed T2 target cells, scFv D10-7-UCHT1 mediated cell death in a time-dependent manner and target-dependent fashion.

To further confirm the capacity of this BiTE to indice CD3-mediated signaling , we used an engineered Jurkat T cell that expresses luciferase under the control of NFAT response elements. This system can be used to assess whether target cells are being killed by human T cells through the expression of NFAT-dependent luciferase. Therefore, reporter cells were co-cultured with corresponding peptide-pulsed T2 cells at the ratio of 1:1 in medium containing bispecific antibodies. The luciferase signal was measured using a luminescence reader after 24 hours. Our results showed a low background luciferase signal in the presence of only T cells with bispecific antibody scFv D10-7-UCHT1. The addition of $KRAS^{G12V}$ peptide-pulsed T2 cells to an effector cell system with soluble BiTE significantly enhanced luciferase expression in effector cells, whereas T2 cells pulsed with wild-type peptide caused no appreciable increase in luciferase signal, representing specific interaction of scFv to $KRAS^{G12V}$ peptide loaded onto the cell surface of target cells. These data also indicated that in the presence of target cells pulsed with the mutant peptide, scFv D10-7-UCHT1 interacts with $KRAS^{G12V}$ pHLAs on target cells (via anti-$KRAS^{G12V}$ scFv) and T cells (through anti-CD3 scFv) to stimulate Jurkat NFAT-dependent luciferase cells. A similar experiment was performed whether scFv D10-7-UCHT can activate reporter cells through mutant peptide-HLAs formed from endogenously processed mutated *KRAS*. In line with previous data, the results showed no difference in luciferase expression between T2 cells containing PresentER-G12V and the corresponding control cells (Fig. 4.18 (E)). As T cell activation in the reporter-gene-assay is dependent on binding of scFv D10-7 to any $KRAS^{G12V}$ pHLA-A2 complex on the surface of PresentER expressing cells in addition to CD3, this suggested, that no BiTE mediated T cell activation occurred as no endougenously processed $KRAS^{G12V}$ was presented by HLA-A2.

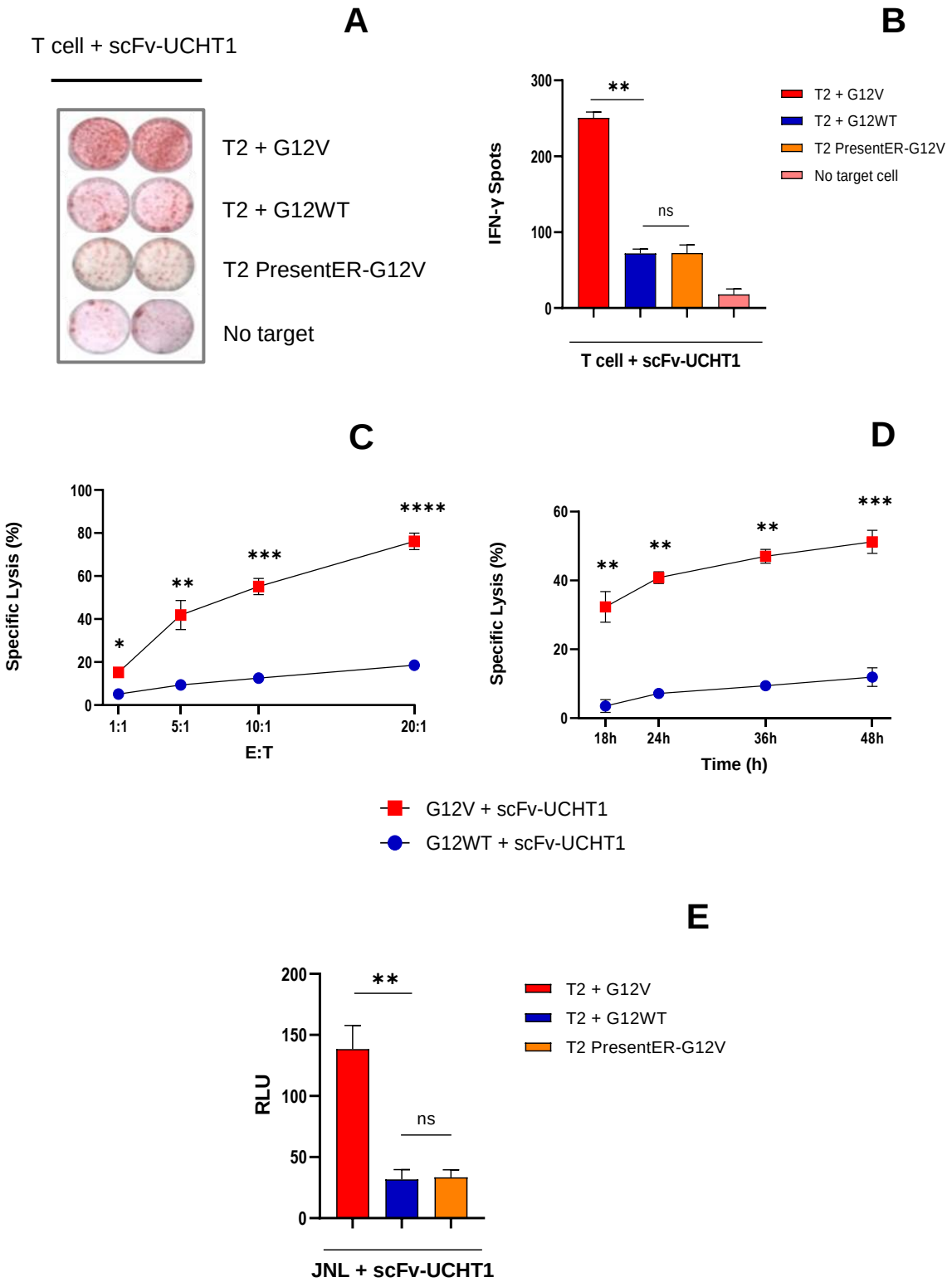

Figure 4.18: Analysis of scFv D10-7-UCHT-mediated T cell activation upon stimulation with T2 PresentER G12V . (**A**) One representative image of IFN-γ spots appearing on the ELISpot membrane and calculation of spot numbers using an image analyser is shown. (**B**) To conduct an ELISpot assay 1×10^5 T cells were co-cultured with 2×10^4 target cells (E: T = 5:1) in the presence of 1 µg/mL of scFv D10-7-UCHT1 for 24 hours. Data indicate mean values ± SD of two technical replicates and are representative of three independent experiments. Data were anlayzed by two-tailed unpaired Student's t-test. ** indicates P< 0.01, and ns denotes P>0.05. (**C)** Cytotoxic activity of T cells against KRAS

peptide-pulsed T2 cells in the presence of bispecific antibody (red squares) or the absence of recombinant scFv D10-7-UCHT1 (blue circles) was calculated by bioluminescence-based killing assay after different ratios of effector to target cells for 24 hours. (**D**) Cytotoxicity data for T cells in the presence of scFv D10-7-UCHT1 (red squares) or the absence of BiTE (blue circles) after co-culture with peptide-pulsed T2 cells for various incubation times at an E/T ratio of 5:1. Specific lysis data indicate mean values ± SD of three technical replicates and are representative of two independent experiments. Data were analyzed by two-tailed unpaired Student's t-test. *P<0.05, **P<0.01, ***P<0.001, ****P<0.0001. ns: p>0.05. (**E**) The effect of scFv D10-7-UCHT1 on activation of Jurkat reporter cells exposed to target cells, including peptide-pulsed T2 and PresentER-G12V expressing cells was determined by BiTE assay after co-incubation at an E/T ratio of 1:1 for 24 hours in the presence of 1 µg/mL of BiTE. Data indicate mean values ± SD of three technical replicates and are representative of two independent experiments. Data were analyzed by two-tailed unpaired Student's-t test. ** indicates P<0.01, and ns denotes P>0.05. E:T, effector to target ratio; JNL, Jurkat NFAT-Luciferse reporter cell; G12V, mutated KRAS peptide; G12WT, wild-type KRAS peptide; ns, not significant; RLU, relative luminescnece unit; scFv-UCHT1, recombinant bispecific antibody.

4.13 Expression analysis of HLA-A*0201 and HLA-A*0301 on cancer cells

Considering that HLA-A*0201 and HLA-A*0301 (hereinafter referred to as A2 and A3) are the most commonly found HLA alleles in the human population (Maiers et al., 2007), we focused our efforts on developing either BITE or TCRm CAR-reprogrammed T cells targeting mutant $KRAS^{G12V}$ peptide bound to these two HLA alleles. Therefore, we chose the cell lines NCI-H441 (lung adenocarcinoma) and CFPAC-1 (pancreatic ductal adenocarcinoma) representing tumor cells with appropriate haplotype and stained both targets with anti-HLA-A2 and anti-HLA-A3 antibodies to confirm expression of HLA alleles. As depicted in the Figure 4.19, both NCI-H441 and CFPAC1 cells expressed HLA-A2 and HLA-A3; although, expression of HLA-A2 and HLA-A3 on the surface of CFPAC-1 cells was slightly higher than on representing tumor cells with appropriate haplotype and NCI-H441 cells.

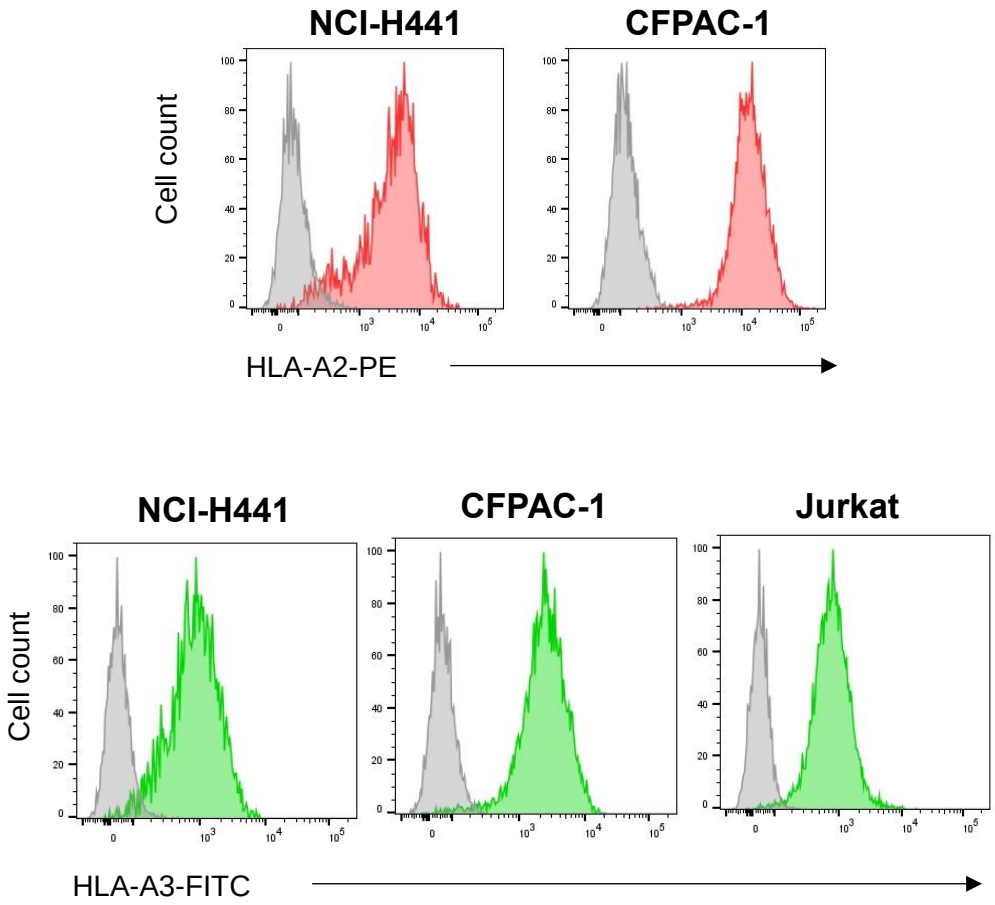

Figure 4.19: Analysis of HLA-A2 and HLA-A3 expression on cancer cells by flow cytometry. The red filled area is a representation of cells stained with anti-HLA-A2-PE mAb (top), whereas the green filled area represents cells stained with anti-HLA-A3-FITC mAb (bottom). An isotype control with an irrelevant mAb is shown in the gray filled area.

4.14 Development of a BiTE targeting mutant KRAS^{G12V} pHLA-A3

As shown above, we aimed to target the KRAS^{G12V} peptide restricted by HLA-A*0201 and thus developed TCRm CAR-T cells and a BiTE recognizing the KRAS^{G12V} 10-mer (KLVVVGAVGV) bound to HLA-A2. However, they could not recognize the endogenous KRAS^{G12V} peptide presented by HLA-A2. Therefore, we attempted to develop a BiTE that could detect KRAS^{G12V} –pHLA-A3 complex (Fig. 4.20). The plasmid map can be found in supplemental information Figure S6. On the other hand, NCI-H441 (lung adenocarcinoma) and CFPAC-1 (pancreatic ductal adenocarcinoma) are two cancer cell lines that express both HLA-A3 and *KRAS* G12V mutations (Scholtalbers et al., 2015). Jacqueline Douglass et al. found that these two cell lines present a low amount of KRAS^{G12V} (VVVGAVGVGK) restricted by HLA-A3. Due to this

fact, we focused our efforts on the mutant peptide-HLA-A3 complex presented on the surface of these two cell lines.

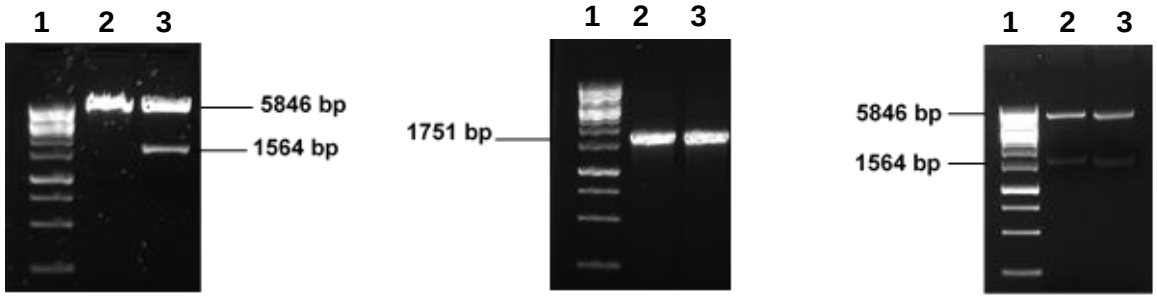

Figure 4.20: Design and cloning of LH-UCHT1 bispecific antibody for KRAS^{G12V} pHLA-A3. Representative electrophoresis image of the PCR products and restriction enzyme analysis of the scFv LH-UCHT1 encoding vector. LH-BiTE already cloned into pcDNA3.4 (lane 3) and pMXs-IRES-Puro (lane 2) vector were digested with PacI and EcoRI restriction enzymes, and the products were 1564 and 5846 base pairs in size (left panel). Individual colonies were identified by colony PCR after bacteria were transformed with cloned vectors. The results of successful cloning revealed an insertion fragment with an estimated band of 1751 base pairs (middle panel). The PacI and EcoRI restriction digestions of the cloned vector yielded fragments of 1564 and 5846 base pairs, respectively (right panel). GeneRuler 1 kb was loaded on the gel (lane 1) to estimate DNA size. The image shown represents one of three biological repeats.

The CHO cells were subsequently transduced with viral particles to produce KRAS^{G12V} scFv LH-UHCT1 BiTE. Transduced CHO cells were stained with anti-His-tag mAb to be analyzed by flow cytometry. We observed that, In comparison to control cells, more than 91% of transduced cells expressed recombinant protein after intracellular staining (Fig. 4.21).

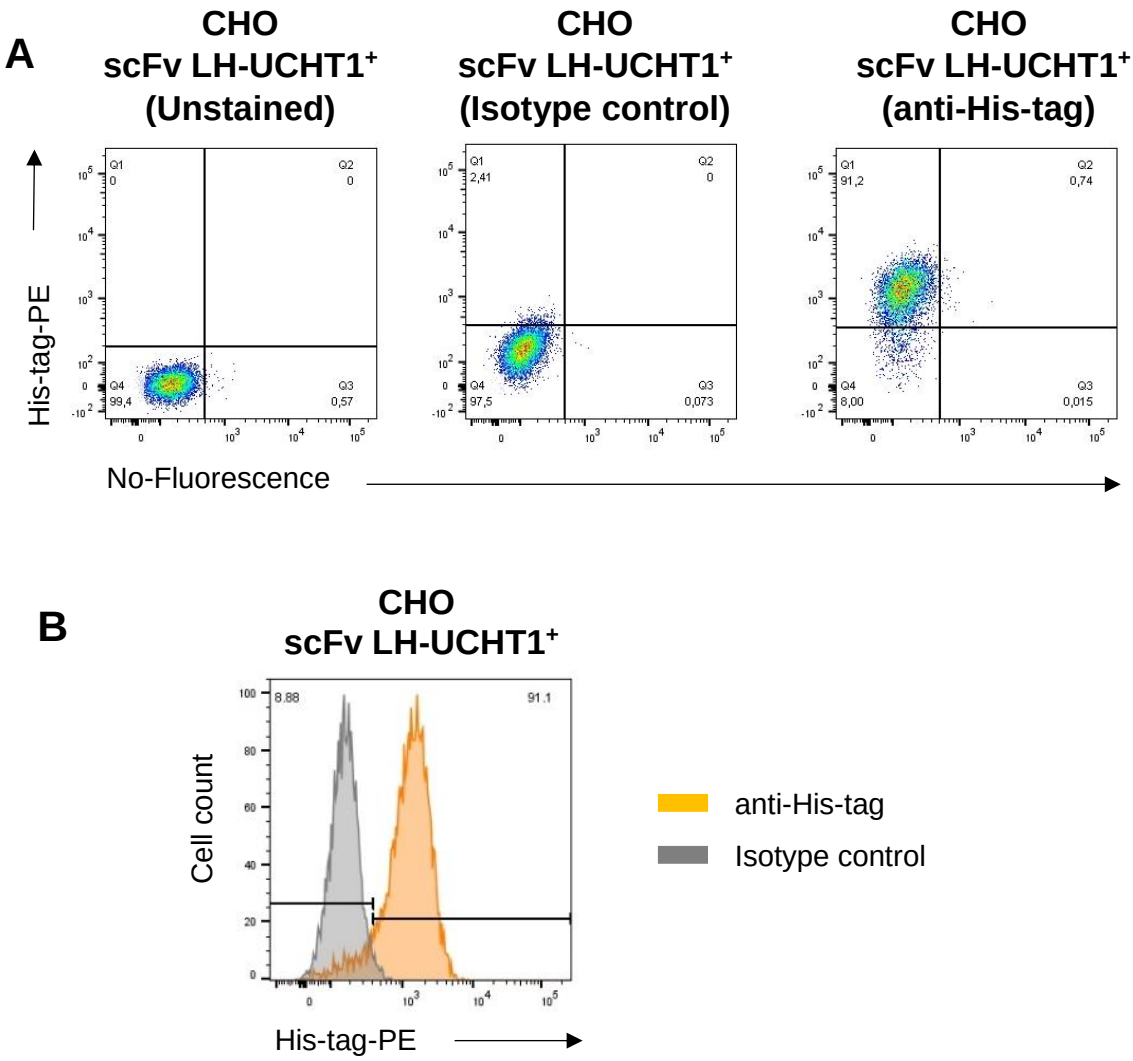

Figure 4.21: Flow cytometric analysis of scFv LH-UCHT1 expression in CHO cells. (**A**) Intracellular staining of scFv LH-UCHT1-expressing CHO cells with an anti-His-tag mAb. Unstained cells and cells were only incubated with the antibody of the same isotype served as controls. (**B**) The flow cytometry data from (A) are presented as a histogram. The orange colored histogram indicates transduced CHO cells stained with anti-His-tag mAb, whereas the gray histogram represents transduced cells stained with an irrelevant mAb as an isotype control. CHO, chinese hamster ovary cells; His-tag, polyhistidine-tag. Effect of LH-UCHT1 antibody on the functional activity of T cells

4.15 Effect of LH-UCHT1 antibody on the functional activity of T cells

In order to assess the ability of scFv LH-UCHT1 to activate T cells in response to target cells expressing HLA-A3-restricted $KRAS^{G12V}$, an IFN-γ ELISpot assay was carried out. T cells were co-cultured with NCHI-H441 and CFPAC-1 cells in the presence or absence of scFV LH-UCHT1. In contrast to controls, T cells released a significant amount of IFN-γ in response to target cells as shown in the Figure 4.22. The amount

of released cytokine was slightly higher in response to NCI-H441 cells than to CFPAC-1 cells. Moreover, scFv LH-UCHT1 appeared not to induce non-specific T cell activation in the absence of KRAS^{G12V} peptide.

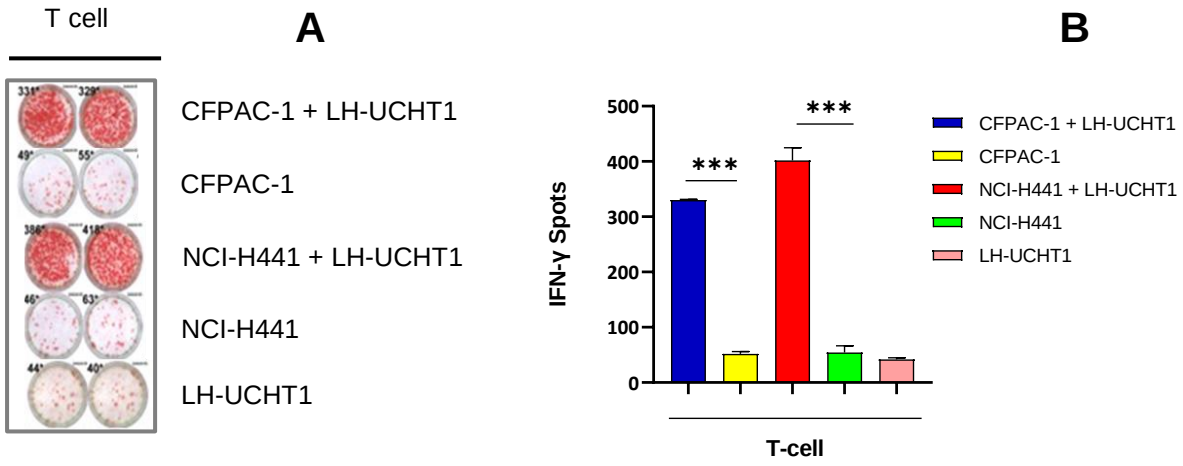

Figure 4.22: Analysis of T cell activation induced by LH-UCHT1 bispecific antibody in response to target cells bearing *KRAS* G12V mutation and HLA-A3. (**A**) A representative IFN-γ ELISpot assay is shown, and spot numbers were calculated using an image analyzer. (**B**) Result of an ELISpot assay after 1×10^5 T cells were co-cultured with 2×10^4 target cells (E: T = 5:1) in the presence of 1 µg/mL of scFv LH-UCHT1 for 24 hours. Data indicate mean values ± SD of two technical replicates and are representative of three independent experiments performed. Data were analyzed by two-tailed unpaired Student's t-test. ** indicates P< 0.001. scFV LH-UCHT1, recombinant BiTE.

In the next set of experiment, we assessed whether T cells are capable of killing cells harboring endogenous mutant KRAS^{G12V} peptide-HLA-A3 complexes with scFv LH-UCHT1 BiTE. Bioluminescence-based killing assay was performed with lentivirally transduced NCI-H441 and CFPAC-1 target cells expressing luciferase. (Fig. 4.23 (E)). Our luciferase-based cytotoxicity results showed that LH-UCHT1 elicited T cell cytotoxicity when exposed to NCI-H441 and CFPAC-1 harboring endogenous mutated *KRAS* G12V gene in a ratio effector / target and time-dependent manner (Fig. 4.23 (A)-(D)). In contrast, only about 10% of target cells were killed in the absence of BiTE following exposure of T cells to NCI-H441 or CFPAC-1 target cells.

To further investigate the ability of scFv LH-UCHT1 to kill target cell expressing mutant KRAS^{G12V} peptide on HLA-A3 molecules, a photometrical-based killing assay was performed. In this crystal violet staining T cells induced very high cytotoxicity at an E/T ratio of 5:1 and still strong reactivity at an E/T ratio of 1:1 upon co-culture with CFPAC-1 or NCI-H441 target cells (Fig. 4-24 (A) – (D)) whereas no significant reactivity could be observed in the controls (Fig. 4.24 (A) – (D)). Moreover, LH-UHCT1

induced higher T cell cytolytic activity in NCI-H441 than CFPAC-1 target cells at ratio of E: T (5:1) (Fig. 4.24 (A) – (B)), indicating that more KRAS^{G12V} pHLA-A3 complexes were expressed by NCI-H441 target cells. Taken together, these results supported our data depicted in Fig. 4.23.

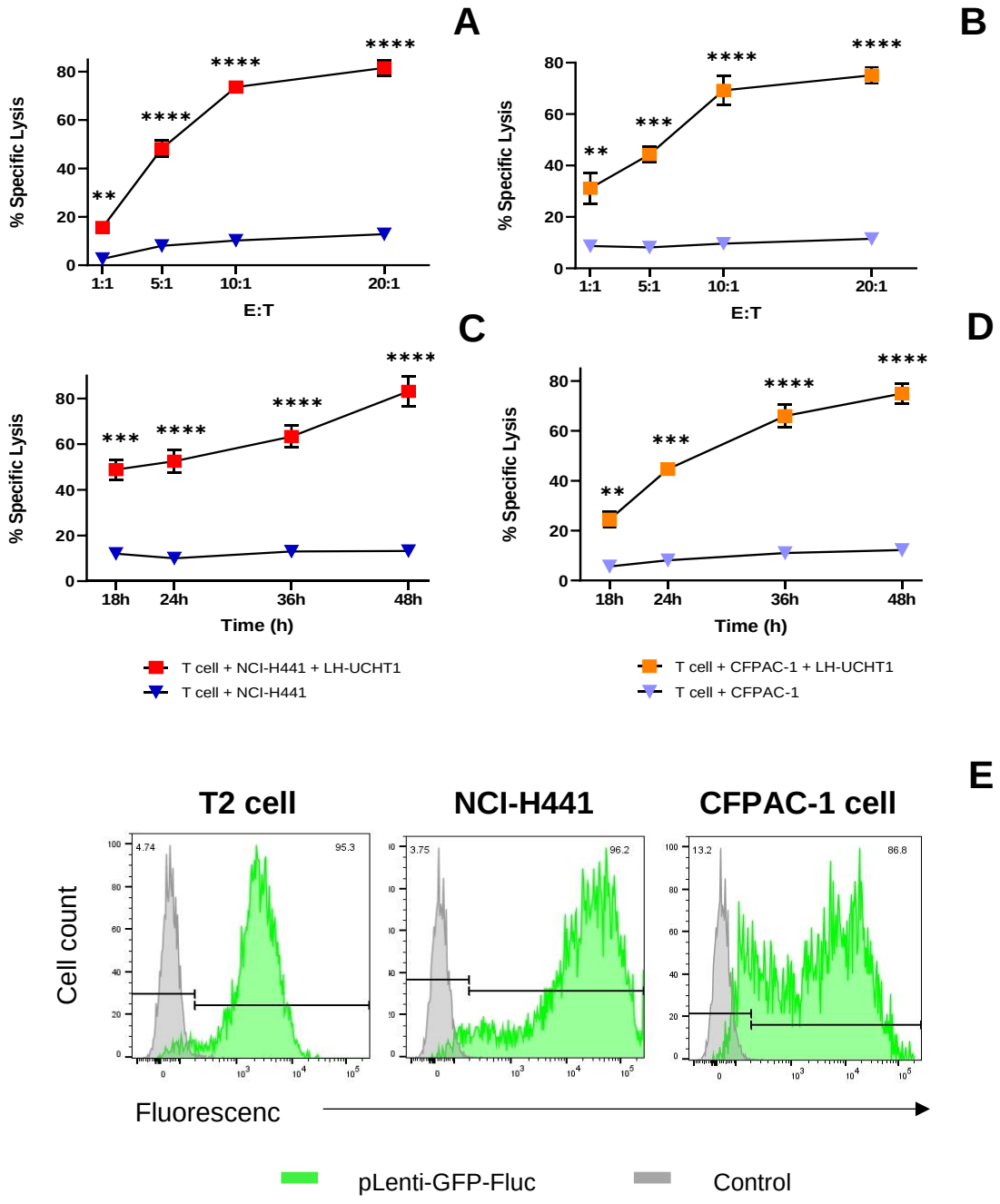

Figure 4.23: Cytotoxicity activity of T cells against NCI-H441 and CFPAC-1 target cells in response to LH-UCHT1 bispecific antibody via bioluminescence assay. (**A, B**) Cytotoxic activity of T cells against NCI-H441 and CFPAC-1 target cells in the presence or the absence of recombinant LH-UCHT1 antibody after different ratios of effector to target cells for 24 hours. (**C, D**) Cytotoxicity data for T cells in the presence or the absence of LH-UCHT1 bispecific antibody after combination with target cells for various incubation times at an E/T ratio of 5:1. Specific lysis data indicate mean values ± SD of three technical replicates and are representative of two independent experiments. Data were

analyzed by two-tailed unpaired Student's t-test. **P<0.01, ***P<0.001, ****P<0.0001. (E) Transduction of T2, NCI-H441, and CFPAC-1 cells with vector encoding luciferase fused to GFP. The gray histogram indicates non-transduced cells (control) and the green histogram shows luciferase-GFP expressing cells. E: T, effector to target ratio; Fluc, firefly luciferase; GFP, green fluorescent protein; LH-UCHT1, recombinant BiTE.

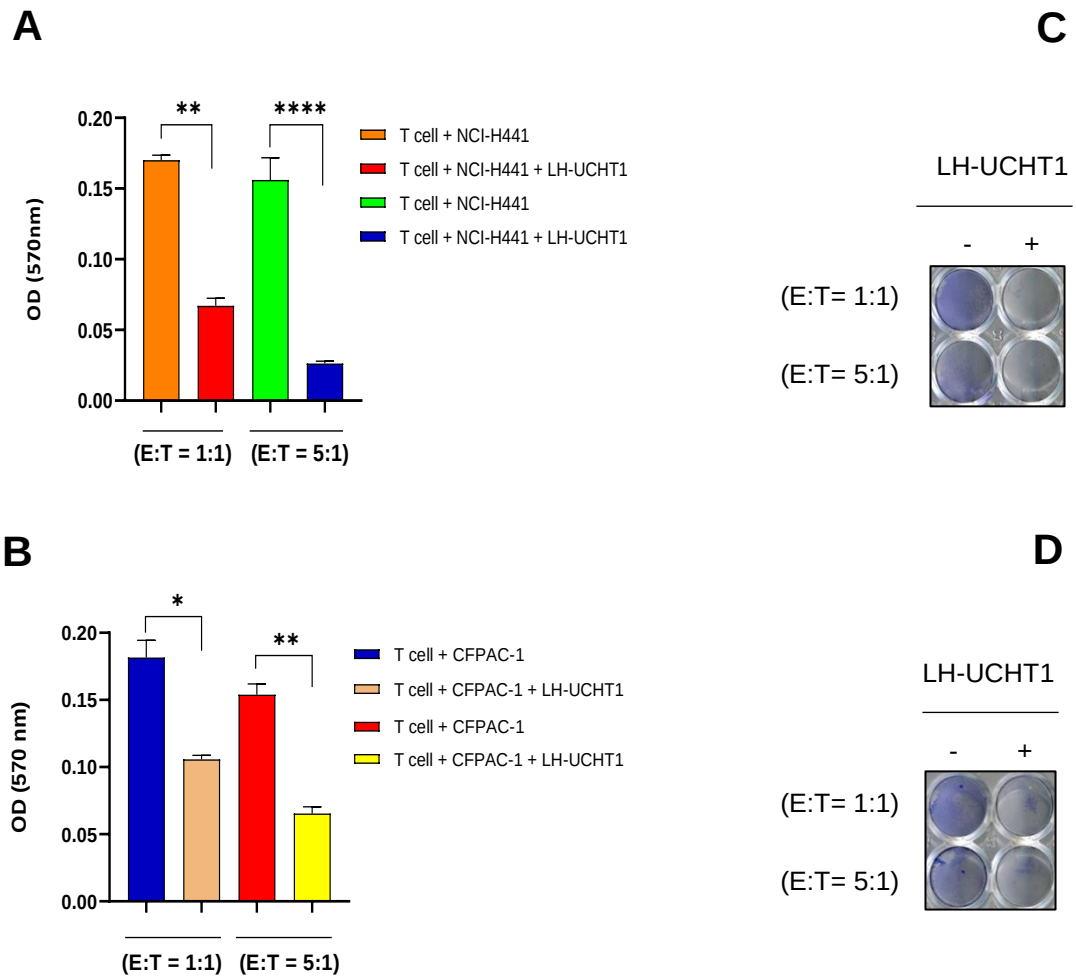

Figure 4.24: Cytotoxicity activity of T cells through LH-UCHT1 bispecific antibody in co-cultures with NCI-H441 or CFPAC-1 cells using crystal violet staining assay. (**A, B**) T cells were co-cultured with NCI-H441 or CFPAC-1 target cells at indicated effector to target ratios (E: T= 1:1 and 5:1) in the presence or the absence of LH-UCHT1 for 48 hours. Data indicate mean ± SD of two technical replicates and are representative of three independent experiments, analyzed by two-tailed unpaired Student's t-test. *P<0.05, **P<0.01, ****P<0.0001. (**C, D**) Representative images of a crystal violet staining assay showing cytolytic activity of LH-UCHT1 bispecific antibody in co-cultures of T cells with NCI-H441 or CFPAC-1 cells with indicated effector to target cell ratios. One representative image out of three biological experiments is shown. E: T, effector to target ratio; LH-UCHT1, recombinant BiTE; OD, Optical Density.

To further evaluate whether , LH-UCHT1 can recognize only KRAS^{G12V} pHLA-A3 complexes on the cell surface and does not show any l cross activity to other HLA-A3-bound peptides, Jurkat NFAT-dependent luciferase cells were combined with KRAS^{G12V}-expressing target cells at different E/T ratios for 24 hours. The Figures 4.25

(A) and (B) illustrate that Jurkat T cells were activated by either NCI-H441 or CFPAC-1 in the presence of the LH-UHCT1; but no activation was observed in the absence of BiTE. As we tested effector to target cell ratios from 1:1 to 10:1 we again observed highest activation of Jurkat cells at a 10:1 E/T ratio, demonstrated by a low RLI as the reduction of luciferase activity corresponds with the amount of killed target cells and hence absence of luciferase activity (Fig. 4.25). Therefore, the cytolytic activity seen in our assays could clearly be associated with a CD3-mediated T cell activation induced by the LH-UHCT1 BiTE.

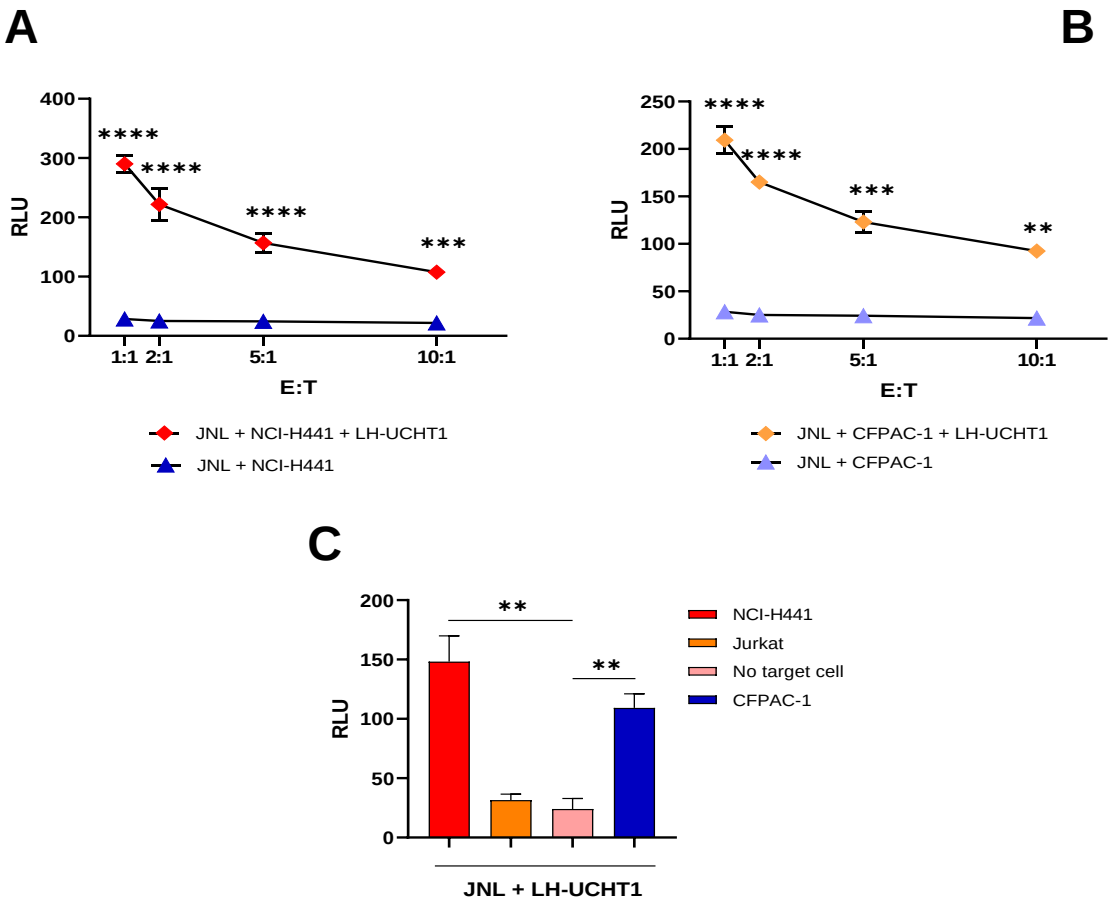

Figure 4.25: Analysis of LH-UCHT1-mediated activation of Jurkat reporter cells exposed to target cells with KRAS^{G12V} mutation and HLA-A3. (**A, B**) Jurkat reporter cells were combined with or without LH-UCHT BiTE and NCI-H441 or CFPAC-1 cells at indicated ratios of effector to target cells (E: T) for 24 hours. Data show mean ± SD of three technical replicates and are representative of two independent experiments. Data were analyzed by two-tailed unpaired Student's-t test. **P<0.01, ***P<0.001, ****P<0.0001. (**C**) 1× 10^5 Jurkat reporter cells co-cultured with 1× 10^5 target cells (E: T=1:1) in the presence of LH-UCHT1. The cells were incubated for 24 hours and assayed for the expression of luciferase. Data represent the mean ± SD of three technical replicates and are representative of two independent experiments, analyzed by two-tailed unpaired Student's-t test. ** indicates P<0.01. E: T, effector to target ratio; JNL, Jurkat NFAT-Luciferase reporter cell; RLU, relative luminescence unit; LH-UCHT1, recombinant BiTE.

4.16 Effect of LH-UCHT1 on lytic activity of TCR/CD3-positive NK-92 cells

To assess whether BiTE facilitates anti-tumor ability of NK-92 cells against target cells harboring $KRAS^{G12V}$ neoantigens in the context of HLA-A3, we generated TCR/CD3-expressing NK-92 cells. In comparison to wild-type NK-92 cells ($CD56^+$ $CD3^-$), modified NK-92 cells displayed 94% expression of CD3 molecule on their surface following stable TCR αβ expression as demonstrated by flow cytometry analysis (Fig. 4.26).

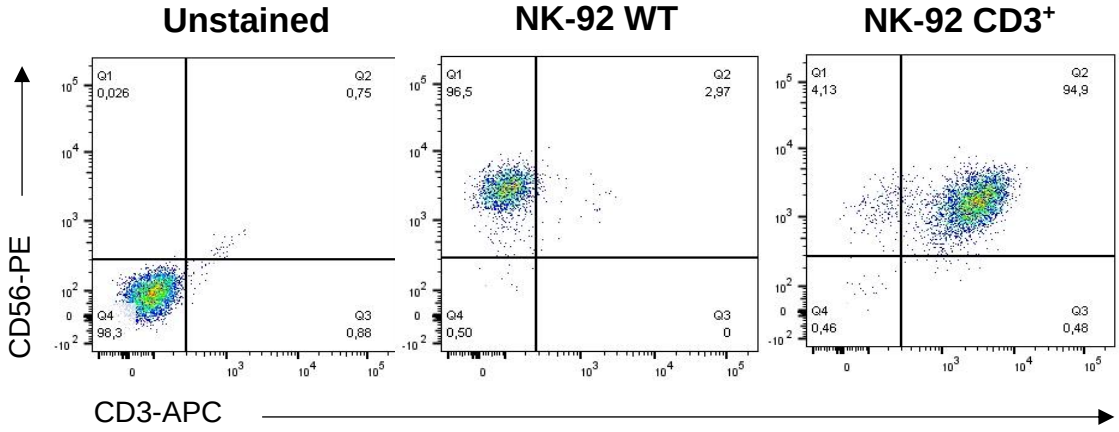

Figure 4.26: Flow cytometry analysis of CD3-positive NK-92 cells. NK-92 cells were stained with anti-CD56 antibody and followed by anti-CD3 antibody before analysis by flow cytometry. Controls included unstained cells and wild-type NK-92 cells as an isotype control. NK-92 WT; wild-type NK-92.

Our ELISpot analysis showed that LH-UCHT1 induced IFN-γ cytokine release from $CD56^+$ $CD3^+$ NK-92 cells upon co-culture with either NCI-H441 or CFPAC-1 target cells and amounts of cytokine secretion from CD3-expressing NK-92 cells were remarkably higher in the presence of BiTE as compared to cultures performed without BiTE. As anticipated, BiTE did also not activate wild-type NK-92 cells in the presence of either NCI-H441 or CFPAC-1. (Fig 4.27 (A) & (B)).

To further study whether LH-UCHT1 would trigger cytotoxic activity of CD3-positive NK-92 cells in the presence of NCI-H441, we performed bioluminescence-based killing cell assays. Effector cells were co-cultured with target cells at a ratio of E: T (5:1) in medium containing BiTE for up to 48 hours. As shown in Figure 4.27 (C) we observed that LH-UCHT1 lysed 50% of NCI-H441 target cells in the presence of $CD56^+$ $CD3^+$ after 48 hours co-incubation. In contrast, only about 10% of non-specific lysis by NK-92 ($CD56^+$ $CD3^+$) was observed (Fig. 4.27 (C)).

In summary, these results demonstrated that in addition to T cells a KRAS^{G12V} – CD3 BiTE can also be used to induce cytotoxicity mediated by genetically engineered NK cells expressing a full CD3 complex.

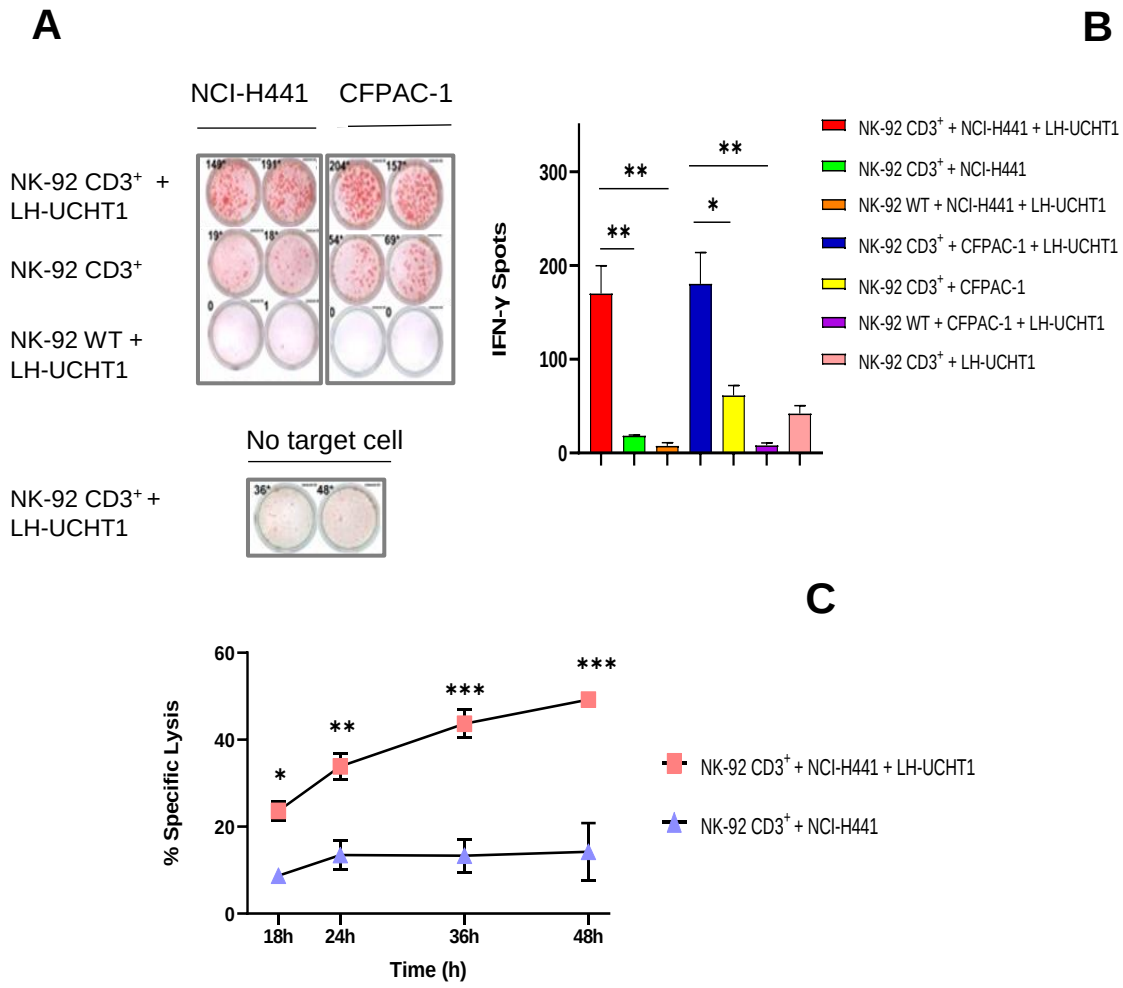

Figure 4.27: Analysis of LH-UCHT1-mediated CD3⁺ NK-92 cell activation in response to NCI-H441 and CFPAC-1 cells. (**A**) A representative image of IFN-γ ELISpot spots is shown and spot numbers were calculated using an image analyzer. (**B**) Results of an ELISpot assay after 1×10^5 NK-92 (CD56⁺ TCR⁺CD3⁺) cells were co-cultured with 2×10^4 target cells (E: T = 5:1) in the presence of 1 µg/mL of scFv LH-UCHT1 for 24 hours. Data indicate mean values ± SD of two technical replicates and are representative of three independent experiments performed. Data were analyzed by two-tailed unpaired Student's t-test. *P< 0.05, ** P< 0.01. (**C**) Cytotoxicity data for CD3-positive NK-92 effector cells in the presence of scFv LH-UCHT1 (pink squares) or the absence of BiTE (blue triangles) after co-culture of NCI-H441 target cells for various incubation times at an E/T ratio of 5:1. Specific lysis data indicate mean values ± SD of three technical replicates and are representative of two independent experiments performed. Data were analyzed by two-tailed unpaired Student's t-test. *P<0.05, **P<0.01, ***P<0.001. E: T, effector to target ratio; scFv LH-UCHT1, recombinant BiTE.

5. Discussion

5.1 Rationale of immunotherapy-based approach targeting KRAS neoantigen

Immunotherapy based on T cell engaging bispecific antibodies (BiTEs) and chimeric antigen receptors (CAR) -T cells has proven to be very effective as 2$^{nd.}$ or 3$^{rd.}$ line therapy for patients with relapse or progressing disease. However, the antigen binding structure of both BiTEs and CARs, which consist of scFvs derived from mAbs, do not provide good access to the vast repertoire of processed tumor neoantigens elicited by the mutation and presented as neo-peptide antigens complexed to HLA molecules on the cell surface. Thus, the development of immunotherapeutic, which can recognize a tumor neo-peptide/HLA complex like a TCR but do not depend on TCR engineered T cells, represents a very attractive approach to improve immunotherapy.

These peptide/HLA complexes can be targeted by antibodies known as TCR-mimic (TCRm) or TCR-like mAbs (Chang et al., 2016). Mutated KRAS^{G12V} is an excellent target for cancer immunotherapy as it occurs specifically and highly frequent in malignant cells. A major challenge in treating cancer patients with TCRm Abs is that tumor cells often downregulate HLA class I expression. Consequently, abundance of pHLA complex is generally low (Douglass et al., 2021; Hsiue et al., 2021; Wang et al., 2019). However, a recent study showed that TCRm mAbs had potent anti-tumor activity to kill cancer cells with KRAS^{G12V} HLA complexes despite having a low number of complexes on the cell surface (Douglass et al., 2021). Since HLA-A*0201 and HLA-A*0301 represent frequently expressed HLA alleles in the Caucasian population thus making them highly suitable candidates for the development of TCRm mAbs (Maiers et al., 2007). The development of a TCR-mimic antibody targeting p53^{R175H} mutation was recently reported in a study (Hsiue et al., 2021). Moreover, TCRm mAbs can also be exploited to engineer potent anti-tumor CAR-T cells e.g. against AFP $_{(158-166)}$ complexed with HLA-A*0201 in the context of liver cancer as shown by Liu and colleagues (Liu et al., 2017).

Consequently, since the *KRAS* G12V mutation is highly prevalent in lung and pancreatic cancer cells, and mutated peptide is predicted to bind to HLA-A*0201 and HLA-A*0301 we developed KRAS^{G12V} specific CAR T cells and BiTEs, respectively, and evaluated the anti-tumor response efficacy in vitro in a proof of concept study.

5.2 Influence of various spacer domain on expression of TCRm CARs

In line with previous experimental evidence that spacer domains influence the expression of CARs on the surface of cells, we evaluated the different spacers used with respect to function of CAR constructs.

After retroviral transduction, our FACS analysis showed that TCRm CARs with hIgG- and Strep-tag II-spacers demonstrate equal levels of surface expression (day 6). Hence, although the hIgG spacer domain is larger than the Strep-tag II hinge region at the molecular level, the expression ability or transduction efficiency of both TCRm CAR constructs were approximately the same when analyzed by flow cytometry, indicating that modification of spacer domains do not affect the expression of TCRm CARs in human T cells. A polyclonal stimulation of transduced T cells, followed by antigen-specific stimulation with inactivated antigen-bearing target cells, was used to enhance the number of TCRm CAR-bearing T cells. We used T2 cells as artificial presenting cells, which are unable to present endogenous pHLA complexes to T cells due to deletions in the MHC class I-encoded genes for transporters involved in antigen presentation. After three times of re-stimulation with mutant KRAS peptide-pulsed T2 cells, the percentage of TCRm CAR-expressing T cells with either the hIgG or the Strep-tag II spacer domain increased significantly, probably due to repetitive antigen-specific re-stimulation. Our findings also indicated that this enrichment of TCRm CAR-positive T cells was comparably achieved through the activation of both hIgG-containing CAR as well as a Strep-tag II-incorporating CAR. Although the fluorescent signal intensity was slightly higher for the Strep-tag II CAR in our first experiment than for the hIgG-based CAR, the percentage of T cells expressing both CARs did not present a marked difference. This comparable intensity of signal may be a consequence of different staining methods applied to detect CARs. Our experience with MHC-Tetramer staining demonstrated that the binding affinity of the tetramer for target antigens was lower than that of fluorochrome-labeled antibodies used for conventional flow cytometry staining. We therefore analyzed these indicated CARs using fluorochrome-conjugated monoclonal antibodies against spacer domains, including anti-Strep-tag II and anti-hIgG antibodies. Subsequent flow cytometry analysis revealed that, even three weeks after antigen-specific stimulation, there was no significant difference in the amount of CARs on the surface of transduced T cells. We did not see any comparable difference in TCRm CAR expression on human T cells

since two TCRm CARs share a CD28-derived transmembrane domain. These results led us to the conclusion that the amount of TCRm CAR varying in hinge regions is independent of the hinge region of CAR.

In a side-by-side comparison study, we confirmed our previous study result by staining TCRm CARs on the surface of Jurak reporter cells. Our flow cytometry histograms demonstrated no obvious difference in the expression rate of TCRm CARs on the surface of Jurkat reporter cells six days post-transduction, strongly suggesting that the hinge region has no effect on the amount of TCRm CARs. In an analogous experiment, we also examined the expression of TCRm CARs on the surface of phoenix cells two days after transfection. Interestingly, we found that differences in hinge regions did not alter the expression level of TCRm CARs on the surface of the cells, confirming that CARs with hIgG- or Strep-tag II-HD show similar levels of surface expression even on Phoenix Ampho cells.

Despite one recent study reporting that different transmembrane domains (TMDs) may affect CAR expression levels as well as its cellular localization Fujiwara and his colleagues observed that the modification of hinge and transmembrane domains do not have any impact on CAR mRNA transcription from the gene (Fujiwara et al., 2020). Their observations also revealed that replacement of the hinge region of CARs did not significantly alter the expression level of CARs on the surface of mouse T cells, but HD/TMD-modified CARs had higher levels of expression six days after retroviral infection compared to their control counterparts. These researchers also found that CAR expression efficiency to the cell membrane and topology of CAR expression on T cells are influenced by both hinge region structure and transmembrane structure through glycosylation and disulfide bonds. Additionally, the stability of CAR expression on the membrane is primarily controlled by the transmembrane domain and not the hinge region (Fujiwara et al., 2020).

5.3 Anti-tumor response of CAR-T cells exposed to target tumor cells

Following evaluation of CAR expression on the surface of transduced T cells, we examined the function of TCRm CAR-mediated T cell activation through in vitro analysis of IFN-γ secretion and cytotoxic activity of TCRm CAR-expressing T cells. An important feature of activated T cells is the production of pro-inflammatory cytokines,

such as IFN-γ. This cytokine plays an important role in anti-tumor immunity, anti-pathogen immunity, and immune regulation. IFN-γ is produced primarily by natural killer cells, natural killer T cells, and Th1 $CD4^+$ and $CD8^+$ effector T cells. A high level of IFN-γ production correlates with an effective immune response (Schroder et al., 2004).

Our ELISpot results indicated that target cells presenting exogenous peptides bound to HLA-A2 were recognized by two both types of CAR-redirected T cells. However, we observed that activation of Strep-tag II CAR T cells was more potent than that of T cells expressing a hIgG CAR in response to exogenous $KRAS^{G12V}$ peptide-HLA-A2 complexes. The difference in IFN-γ production may be explained by different hinge regions incorporated into the structures of the two CARs. These results indicated that TCRm CAR with Strep-tag II have a higher signaling input efficiency associated with antigen binding than TCRm CAR with hIgG-HD. Similarly, Fujiwara and his colleagues demonstrated that the amount of signal input required for CAR antigen binding is highly correlated to CAR expression levels, and this is due to the contribution of the transmembrane domain. Furthermore, hinge region structure may have a direct influence on CAR signaling threshold (Fujiwara et al., 2020).

In contrast to these data, we could not observe any IFN-γ spots when either hIgG- or Strep-tag II-CAR T cells were combined with parental cells (NCI-H441, CFPAC-1) and T2 cells modified with PresentER-$KRAS^{G12V}$ minigene, indicating that irrespectively of the spacer both TCRm CARs could not recognize $KRAS^{G12V}$ pHLA-A2 neoantigens formed by endogenous presenting on the surface of indicated target cells. Therefore, parental target cells did not induce activation of redirected CAR-T cells. Even the T2 cells transduced with plasmids encoding mutant *KRAS* gene were incapable of eliciting a response by TCRm CAR-reprogrammed T cells. These observations led us to the conclusion that TCRm CARs could not recognize mutant $KRAS^{G12V}$ pHLA-A2 molecules derived from endogenously expressed KRAS protein.

In addition to cytokine production, cytolytic activity was assessed using a bioluminescence-based killing assay (Varadarajan et al., 2011). The cytotoxic assay results obtained were consistent with those obtained with ELISpot, confirming the antigen-specific response of TCRm CAR-expressing T cells targeting cells harboring exogenous mutant $KRAS^{G12V}$ peptide loaded onto HLA-A2 molecules. In contrast to

T2 cells expressing KRAS^{WT} peptide as control, both hIgG CAR- and Strep-tag II CAR-T cells exhibited cytotoxic activity upon exposure to mutant peptide-pulsed T2 cells confirming a specific reactivity. Increasing specific lysis was correlated with increased effector: target ratios, indicating that CAR reprogrammed T cells showed target-dependent lysis. Similar to IFN-γ results, hIgG CAR-T cells demonstrated a lower cytotoxic ability as compared to Strep-tag II CAR-T cells targeting mutant peptide-pulsed T2 cells, and this difference in lysis potency was especially evident at the highest effector/target ratio (20:1). In contrast, neither Strep-tag II CAR nor hIgG CAR resulted in significant T cell activation when co-cultured with cells harboring a natural *KRAS* G12V mutation, including NCI-H441, CFPAC-1, and PresentER- KRAS^{G12V} cells.

In summary, KRAS^{G12V} dependent IFN-γ production suggesting anti-tumor cytotoxicity of T cells (Burkea & Young, 2019) was clearly confirmed by cytolytic activity to KRAS^{G12V} peptide loaded onto T2 targets as shown by bioluminescence-based killing assays but not to KRAS^{G12V} positive tumors in line with previous publications reporting that apparently the either no endogenous KRAS^{G12V} peptide is processed or presented by HLA-A*0201(Douglas et al., 2021).

5.4 Anti-tumor activity of CAR NK-92 cell upon exposure to cells loaded with KRAS peptide

After having shown that KRAS CAR T cells elicit an anti-KRAS^{G12V} response we next tested whether NK cells transduced with a KRAS CAR would also elicit KRAS^{G12V} reactivity. The level of IFN-γ released by TCRm-modified NK-92 cells exposed to KRAS^{G12V} peptide-loaded T2 cells was threefold greater than when T2 cells were pulsed with wild-type KRAS peptides, demonstrating the functional capability of re-engineering NK-92 cells against KRAS^{G12V}/HLA-A*0201. Additionally, this finding supported the utility and specificity of TCRm CARs reprogrammed NK-92 cells to recognize mutant KRAS peptides bound to HLA-A2 molecules on target cells. In line with results described above, CAR-mediated activation against naturally presented KRAS^{G12V} pHLA-A2 complexes was not observed in T2 PresentER-G12V target cells, suggesting that this observation was not only attributable to T cells but reflects a general defect in recognition of endogenous KRAS^{G12V} peptide.

5.5 CAR-J reporter cell is a predictive indicator for TCRm CAR properties

One of the major challenges in developing pHLA-specific TCR-mimic CARs is to identify single-chain variable fragments that are capable to recognize specific pHLA complexes (for example peptides within the context of the HLA-A2 allotype) while excluding nonspecific binding to unrelated pHLAs (Christian et al., 2020). There is also the challenge of converting TCRm scFv into CAR formats with optimal biological activity. In order to optimize the selection of candidates, we used the CAR-J reporter assay, which is based on the interaction of TCR-mimic CARs (expressed on Jurkat-NFAT-luciferase reporter cells) with peptides bound to either HLA molecules. The transient interaction results in cell-cell proximity and the activation of the reporter T cell, which can be measured by luciferase activity (Van der Stegen et al., 2015; Davis & van der Merwe, 1996). One of the purposes of this study was to identify and characterize TCRm CAR candidates using Jurkat reporter cells prior to their implementation into T cells, for early functional screening.

In our studies, we assumed that upon recognition of a target antigen, CAR crosslinking would lead to downstream luciferase expression, which would then be measured by the addition of luciferin substrate. Both hIgG-based CAR and Strep-tag II-derived CAR exhibited this activation when co-cultured with T2 cells pulsed with peptides. Strep-tag II CAR gave a stronger signal in the presence of $KRAS^{G12V}$ peptide-pulsed T2 cells than hIgG CAR, suggesting that CAR targeting mutant KRAS peptide-HLA molecules actually needs a short spacer like Strep-tag II (comprising of 60 amino acids) instead of IgG-Fc (239 amino acids). Of note, a number of groups have found that short spacer CARs, which were designed to target epitopes within tyrosine kinase-like orphan receptor 1 (ROR1), interleukin 13 receptor alpha-2 (IL-13Rα2), and CD19, were more effective at activating T cells than CARs with long spacer domains (Stoiber et al., 2019). As to be expected, no signal was observed upon exposure of CAR-J reporter cells with wild-type KRAS peptide-pulsed T2 cells. These data confirmed that recognition of mutant KRAS peptide/HLA-A2 complexes requires specific binding of TCRm scFv to produce activation and downstream luciferase signaling.

Qing Ge et al. demonstrated that soluble peptide-MHC monomers can activate $CD8^+$ T-cells either directly by engaging T-cell receptors (TCRs) or by presenting cognate peptides derived from soluble peptide-MHC monomers on T cells own MHC molecules

(Ge et al., 2002). We performed a signaling assay with a MHC tetramer loaded with KRAS peptides in order to demonstrate that the CAR-J reporter assay consistently gives a robust signal only in the presence of mutant KRAS^{G12V} pHLA-A2 molecules. The incubation of CAR-J reporter cells with soluble KRAS^{G12V} peptide-MHC tetramer led to activation of cells; however, no activation was observed with soluble KRAS^{G12WT} peptide-containing MHC, supporting the notion that mobilized KRAS^{G12V} peptide-containing MHC facilitates CAR-crosslinking and downstream activation of CAR-J reporter cells.

The generated CAR-J reporter cells were further tested by targeting the hIgG and Strep-tag II spacer domains, respectively, with anti-hIgG and anti-Strep-tag II antibodies. The level of luciferase signal induced by anti-Strep-tag II antibody was greater than induction by anti -hIgG mAb, indicating that CARs with short spacers are more effective in CAR-J reporter cells than CARs with long spacers, supporting of our previous CAR-J signaling results. Furthermore, when PresentER-G12V-bearing T2 cells were co-incubated with CAR-J reporter cells, CAR-J signaling failed to be activated, again indicating that CAR-J reporter cells could not recognize KRAS^{G12V} pHLA-A2 molecules naturally formed through endogenous processing. Since these reporter cells express CD3 and CD28 antigens (data not shown), as a positive control, we decided to activate CAR-J reporter cells with application of soluble anti-CD3/CD28 antibodies. As expected, soluble anti-CD3 plus anti-CD28 induced luciferase expression, showing that these reporter cells retain their luciferase expression even after being transduced with our TCR-mimic CARs.

The comparison of CAR candidates' performance in CAR-J assay and killing assay indicates that CAR-J assay can not only be used to detect target antigens on tumor cells, but also as a potential screening assay for development of TCRm CARs prior to converting single-chain variable fragments into CAR format to perform functional in vitro assays by CAR-modified T cells.

5.6 Detection of (m) KRAS^{G12V} peptide-HLA-A2 molecules on cancer cells

We next determined whether the scFv-10-7-UCHT1 BiTE derived from scFv D10-7 could recognize mutant KRAS^{G12V} peptide-pulsed T2 cells. The analysis of KRAS^{G12V} peptide-pulsed T2 cells by flow cytometry after incubation with BiTE demonstrated that

recombinant protein bound to KRAS^{G12V} peptide-pulsed T2 cells, while no binding to KRAS^{G12WT} peptide-pulsed T2 cells was observed. Therefore, this study suggested that TCRm bispecific antibodies derived from scFv D10-7 were capable of specifically recognizing exogenous mutant peptides bound to HLA-A2 on T2 cells. We then further tested scFv-10-7-UCHT1 for its ability to recognize KRAS^{G12V} pHLA-A2 complexes formed by endogenous antigen processing using G12V-expressing cells, including parental NCI-H441 and CFPAC-1 cell lines. Like the CAR scFv-D10-7-UCHT1 also failed to recognize the cognate mutant pHLA-A2 derived from KRAS protein. In an effort to analyze whether this failure was due to a processing defect in the tumor cell lines tested, we developed a mammalian minigene-based method (called PresentER) that is capable of encoding HLA class I-presented peptides without undergoing typical processing for HLA class I peptides presentation (Gejman et al., 2020). Therefore, we generated T2 cells transduced with plasmid PresentER encoding mutant KRAS^{G12V}. To demonstrate that our BiTE was capable of binding to PresentER-driven KRAS^{G12V} peptide, we stained PresentER G12V-expressing T2 cells with scFv-D10-7-UCHT1. Again, BiTE did not bind to cells expressing PresentER-encoded G12V.

In conclusion, we were unable to detect HLA-A2-related KRAS^{G12V} $_{(5\text{-}14)}$ peptides expressed by G12V-expressing cells, and our results suggest that is not due to a processing defect. In line with our results a recent study published by Douglass et al., who used mass spectrometry (MS) to analyze the KRAS^{G12V} peptide bound to HLA-A*0201 reported that they were not able to detect KRAS^{G12V} peptides bound to HLA-A2 (Douglas et al., 2021). Considering these results, it is likely that KRAS^{G12V} $_{(5\text{-}14)}$ (KLVVVGAVGV) is not naturally expressed or only in very low amounts by HLA-A*201 molecules.

5.7 scFv-D10-7-UCHT1 antibody-mediated T cell activation upon exposure to mutant KRAS peptide-pulsed T2 cells

Upon co-culturing KRAS^{G12V} peptide loaded T2 cells with T cells and scFv-D10-7-UCHT1, we could show a specific activation of T cells in response to an exogenous mutant peptide-pulsed target cell, mediated by our TCRm BiTE and measured by IFN-γ ELISpot analysis. In contrast, there were no detectable IFN-γ spots in co-cultures of T cells with PresentER-G12V expressing T2 cells in comparison to the equivalent

control cells, indicating that scFv-D10-7-UCHT1 was not able to activate T cells in the presence of cells harboring endogenous mutant *KRAS* genes.

Next, our IFN-γ ELISpot results were validated by conducting cell-killing assays. We observed strong scFv-D10-7-UCHT1 mediated cell killing of T2 cells pulsed with exogenous mutant peptide; whereas no cell killing was observed with T2 cells transduced with PresentER-G12V, (the result of this experiment is not included in this thesis). Given these data, T cells exposed to $KRAS^{G12V}$ elicited scFv-D10-7-UCHT1 mediated cell death to peptide-pulsed T2 cells but not endogenous $KRAS^{G12V}$ positive target in a time-dependent manner and target-dependent fashion We further confirm these results using Jurkat reporter cells and scFv-D10-7-UCHT1 BiTE as previously shown by Xiong et al (Xiong et al., 2021). Our results showed a low background luciferase signal in the presence of Jurkat incubated only with scFv-D10-7-UCHT1. The addition of BiTE to $KRAS^{G12V}$ peptide-pulsed T2 cells co-cultured with Jurkat significantly enhanced luciferase expression in effector cells, whereas T2 cells pulsed with wild-type peptide caused no appreciable increase in luciferase signal, representing specific interaction of scFv-D10-7 to exogenous mutant peptide on the surface of target cells. There was no increase in luciferase signal with PresentER-G12V expressing T2 cells when compared to controls. Thus, the potency of scFv-D10-7-UCHT1 could also be determined by a reporter gene assay and data were in perfect line with those of the bioluminescence-based killing assay and the ELISpot assay.

5.8 LH-UCH1 antibody-mediated T cell cytotoxicity in response to mutant *KRAS* gene-harboring HLA-A*0301 target cells

Since we were not able to observe activation of T cells in co-cultures with scFv-D10-7-UCHT1 and cells carrying endogenous HLA-A*0201 and $KRAS^{G12V}$ mutations, we next focused on targeting cells with HLA-A*0301 and $KRAS^{G12V}$ mutations. A study by Douglass et al. reported a low level of $KRAS^{G12V}{}_{(7\text{-}16)}$ peptide (VVVGAV GVGK) naturally present in HLA-A3 molecules on the surface of cells with KRAS mutation, such as NCI-H441 and CFPAC-1. They also reported that COS-7 cells transfected with plasmids encoding HLA-A3 and *KRAS* genes produce high levels of $KRAS^{G12V}{}_{(7\text{-}16)}$ pHLA-A3 complexes formed via antigen processing (Douglass et al., 2021).

For assessment of the potential ability of LH-UCHT1 to activate T cells in the presence of cells containing mutated *KRAS* gene and HLA-A*0301, we first performed an ELISpot assay to measure IFN-γ. In this test, generated scFv LH-UCHT1 BiTE induced IFN-γ release by T cells exposed to either NCI-H441 or CFPAC-1. In the absence of BiTE, there were negligible levels of IFN-γ in equivalent co-cultures. The number of IFN-γ spots produced by scFv LH-UCHT1 in co-cultures of T cells with NCI-H441 target cells was greater than that of CFPAC-1 cells, indicating that LH-UCHT1 caused a stronger response of T cells to antigens on the surface of NCI-H441 cells as compared to CFPAC-1 cells. These differences in T cell immune response against corresponding target cells may be attributable to the density of $KRAS^{G12V}{}_{(7\text{-}16)}$ pHLA-A3 molecules on the surface of these two cell lines. In line with our observations, Douglass et al. reported that the number of copies of $KRAS^{G12V}{}_{(7\text{-}16)}$ pHLA-A3 present on the surface of NCI-H441 cells is threefold greater than that of CFPAC-1 cells (Douglas et al., 2021). In addition, we found that scFv LH-UCHT1 was not capable of inducing IFN-γ release from T cells when no target cells were present, demonstrating that this BiTE cannot activate T cells in an antigen-independent manner. These data further support previous results that BiTE cannot activate T cells independently of their target cells (Wu & Cheung, 2018).

To determine the lytic potency of LH-UCHT1 targeting cells with HLA-$A3^{+}$ and G12V mutation, we next conducted a crystal violet staining assay and a bioluminescence-based killing assay. The crystal violet results demonstrated that the scFv LH-UCHT1 BiTE was able to efficiently lyse both NCI-H441 and CFPAC-1 target cells in the presence of T effector cells. The cell death of both target cells was minimal in the absence of LH-UCHT1. In addition, T cells co-cultured with either NCI-H441 or CFPAC-1 cells exhibited BiTE-dependent lysis and with increasing the effector-to-target ratio, T cells showed greater cytotoxicity against target cells. Thus, at an effector-to-target ratio of 20:1, LH-UCHT1 was most effective in mediating killing of both NCHI-H441 and CFPAC-1 target cells, exhibiting 81% and 75% cytotoxicity, respectively. As shown before, the higher lytic potency observed for NC-H441 as compared to CFPAC-1 is likely to be a result of the greater density of the HLA-A3-presented $KRAS^{G12V}{}_{(7\text{-}16)}$ peptide complexes in NCI-H441 versus CFPAC-1 (Douglass et al., 2021).

We further applied a cell-based luciferase reporter gene assay to test whether LH-UCHT1 specifically activated Jurkat reporter cells in the presence of target cells carrying the endogenous HLA-A3 allele and the $KRAS^{G12V}$ mutation. There was no luciferase signal when Jurkat reporter cells were combined with target cells in the absence of LH-UCHT1, whereas luciferase expression increased by adding BiTE. Likewise, we found that when the number of effector versus target cells was equal, the signal reached its highest peak and as the number of target cells decreased, the luminescence signal intensity declined. This indicates a positive correlation between LH-UCHT1-mediated activation of Jurkat reporter cells and the number of target cells expressing copies of $KRAS^{G12V}$ pHLA-A3 on their cell surface. The signal intensity illuminated by LH-UCHT1 activated-reporter cells combined with NCI-H441 was greater than that shown for CFPAC-1, supporting published observations (Douglass et al., 2021).

5.9 LH-UCHT1 antibody triggers $CD3^+$ NK-92 cell activation upon exposure to HLA-A*0301 cells with *KRAS* G12V mutation

We finally evaluated whether the cytotoxicity of NK-92 cells may also be enhanced by LH-UCHT1 BiTE using CD3 engineered NK-92 cells. In a similar manner to what we observed with T cells, CD3-positive NK-92 cells ($CD56^+$ $CD3^+$) showed little IFN-γ upon exposure to target cells in the absence of LH-UCHT1. Contrary to this, the addition of BiTE led to a marked increase in the production of IFN-γ. These results indicate that recombinant LH-UCHT1 is specifically bound to $KRAS^{G12V}$ pHLA-A3 neoantigens on target cells, thereby crosslinking CD3-positive NK-92 cells to G12V-bearing target cells. Moreover, we found that the amount of IFN-γ secreted from $CD56^+$ $CD3^+$ cells exposed to NCI-H441 was significantly higher than that produced by CFPAC-1 in the presence of bispecific antibodies. Moreover, our results demonstrated that LH-UCHT1 binding alone to target antigen was insufficient to activate wild-type NK-92 cells ($CD56^+$ $CD3^-$), which lack human CD3 antigen.

In this line, results of our cytotoxicity experiments demonstrated that LH-UCHT1 markedly enhanced the killing activity of CD3-positive NK-92 cells against NCI-H441. In this study, cytotoxicity of CD3-modified NK-92 cells ($CD56^+$ $CD3^+$) increased significantly with increasing incubation time, demonstrating the time-dependent fashion of bispecific-mediated cytotoxicity of $CD56^+$ $CD3^+$ cells. The activation and

cytolytic abilities of T cells towards NCI-H441, however, was more pronounced than that of CD3-expressing NK-92 cells ($CD56^+$ $CD3^+$) in the presence of LH-UCHT1. Different receptor signaling mechanisms and co-receptor expression could explain the difference between these two effector cells (Narni-Mancinelli et al., 2011). Co-receptor molecules that bind independently from TCR to the region of pHLA can enhance the recognition mechanism TCR-pHLA-mediated T cell activation. An example of such a co-receptor, which is present on the surface of nearly 90% of all cytotoxic lymphocytes, is the CD8-αβ heterodimer (Norment & Littman, 1988). In addition to increasing antigen sensitivity, this co-receptor also stabilizes the TCR-pHLA class I interaction at the cell surface (Holler & Kranz, 2003; Janeway, 1992; Wooldridge et al., 2005). In response to this activation, signaling molecules are recruited to the TCR-CD3 complex, which results in enhancement and amplification of T cell activation signals (Laugel et al., 2007). In fact, a few studies have shown that T cell activation can be abolished by disrupting the pHLA-CD8 interaction (Sewell et al., 1999; Choksi et al., 1998). We assume that the lack of interaction between pHLA and CD8 in CD3-positive NK-92 effector cells and target cells may influence partially the activation of CD3-modified NK-92 cells upon recognition of $KRAS^{G12V}$ neoantigens.

Taken together, our results suggest that the LH-UCHT1 BiTE redirected CD3-reprogrammed NK-92 effector cells ($CD56^+$ $CD3^+$) to target cells expressing $KRAS^{G12V}$ neoantigens and resulted in an antitumor response. Further, it is feasible to combine BiTE with CD3-modified NK-92 cells in order to increase NK-92 cytotoxicity and specifically target tumor cells expressing endogenous *KRAS* G12V mutations.

5.10 Summary and outlook

The presented data herein are novel findings that led to the establishment of several important principles. In the current study, we sought to target protein products originating from mutant *KRAS* oncogene. From previous findings' report, we identified TCRm scFvs capable of binding to $KRAS^{G12V}$ neoantigens. As a first step, we validated specific binding capability of selected scFvs to target antigens using fluorescently labeled HLA-peptide tetramer staining assays. To target tumor cells expressing mutant $KRAS^{G12V}$ peptide complexed with HLA-A*0201, we then developed CARs derived from TCR-mimic single-chain variable fragments. Our CAR formats were optimized with an optimal and effective anti-tumor efficiency through the use of Jurkat-NFAT

reporter cells. One important factor to consider regarding our study is the fact that signaling assays performed with reporter cells expressing TCRm CARs revealed distinct luminescence intensities due to the fact that CARs contain distinct spacer domain regions. Compared to CAR with a long spacer domain containing hIgG, CAR with a shorter spacer domain derived from Strep-tag II exhibited greater potency against $KRAS^{G12V}$ pHLA-A2 complexes. The results of our experiments indicate that the length of the CAR hinge region is important for cytotoxicity. As a result, CAR-J assays allowed us to determine the performance of respective CAR formats before they were expressed in T cells.

We next demonstrated the efficacy of optimized CARs generated from TCRm scFv in inducing T cell activation and subsequent cytotoxic activity against targets expressing exogenous $KRAS^{G12V}$ pHLA-A2 complexes. A significant finding of this study is that TCRm CARs recognized and lysed cells pulsed with exogenous mutant $KRAS^{G12V}$ peptide, but did not recognize or lyse $KRAS^{G12V}$ pHLA-A2 molecules formed by natural processing on tumor cells with endogenous *KRAS* mutation and HLA-A2 allele. Due to this fact, it was not possible to perform any in vivo studies in a clinically relevant autochthonous NSCLC mouse model despite the fact that mice harboring a lung epithelial cell-specific $KRAS^{G12V}$ mutation and p53 deletion had been crossed with HLA-A*0201 transgenic littermates for over 5 generations to provide a HLA-$2K^b$ restriction element and were ready to be used. We also expressed a hIgG-containing CAR version of the TCR-mimic scFv in NK-92 cells, resulting in CAR-mediated activation upon exposure to exogenous $KRAS^{G12V}$ peptide complexed with HLA-A2 molecules. When comparing the IFN-γ production of effector cells exposed to target cells containing $KRAS^{G12V}$ pHLA-A2 neoantigen, we found that CAR can activate T cells against this neoantigen more successfully than NK-92 cells.

To recognize the $KRAS^{G12V}$ peptide bound to HLA-A2 molecules and not the wild-type form on the target cell in the subsequent experiments, we converted our TCRm scFv into a TCRm-BiTE. Antibody created from TCRm scFv was unable to activate T cells exposed to target cells harboring endogenous *KRAS* G12V mutation. Furthermore, bispecific antibody-mediated T cell killing was not observed. Similar to CAR constructs, T cell activation is affected by BiTE in the presence of exogenous $KRAS^{G12V}$ pHLA–A2 on artificial antigen-presenting T2 cells. Flow cytometry staining with BiTE confirmed our previous findings. In our study, $KRAS^{G12V}$ complexed to HLA-

A2 molecules could not be detected on target cells with endogenous *KRAS* G12V mutations and HLA-A2^{+}, even on one overexpressing model T2 cell line transduced with plasmid encoding PresentER-G12V minigene.

It was found that the KRAS^{G12V} peptide derived from codon 5 to 14 (KLVVVGAVGV) is not produced naturally by proteolytic processing; however, this 10 mer-peptide can be bound to HLA-A2 molecules exogenously. In addition to NetMHC prediction of binding affinity of the KRAS^{G12V} peptide to HLA-A2 molecules, our data from HLA-staining assays also support that the mutant peptide binds with evident up-regulation in HLA-A2 molecules compared to its control counterpart. Furthermore, we were able to identify KRAS^{G12V} complexed with HLA-A2 molecule using bispecific antibodies on the surface of T2 cells pulsed with exogenous KRAS^{G12V}.

Douglas et al. isolated and detected a peptide derived from codons 7-16 (VVVGAV GVGK) containing G12V mutations in cell lines. This peptide (VVVGAVGVGK) was predicted to bind to HLA-A3 molecules using the NetMHC algorithm. A TCRm scFv was developed that binds to KRAS^{G12V} pHLA-A3 molecules. In collaboration with this laboratory, we focused our efforts on developing another BiTE, LH-UCHT1, which would recognize KRAS^{G12V} in the context of HLA-A3. In the presence of T cells expressing endogenous G12V mutations and HLA-A3 positive targets, this BiTE enhanced cytotoxic killing. Furthermore, LH-UCHT1-mediated activation of T cells was induced by exposure to target cells that presented endogenous KRAS^{G12V} neoantigen. The results presented here represent the first report of the therapeutic efficacy of TCRm-BiTE in combination with CD3-expressing NK-92 cells (CD56^{+} CD3^{+}) against endogenous *KRAS* G12V expressing target cells. The LH-UCHT1, recombinant KRAS^{G12V} BiTE, markedly enhanced the killing activity of NK-92 cells carrying CD3 molecules. In spite of the fact that CD3-positive NK-92 cells and T cells through bispecific antibodies lysed tumor cells expressing *KRAS* mutation and HLA-A3^{+}, BiTE-mediated T cell cytotoxicity was more effective than cytolytic activity of CD3-positive NK-92 cells (CD56^{+} CD3^{+}) toward target cells.

Data presented here are restricted to preclinical studies. Further research is needed to determine whether BiTEs or CARs based on TCRm scFv are feasible for targeting genetically altered KRAS^{G12V} protein products in vivo. Moreover, this would have to assessed in clinical trials to evaluate efficacy and toxicity.

The results of our study indicate that it is possible to effectively target the $KRAS^{G12V}$ pHLA complex on the cell surface. From creating TCRm scFv, we can develop bispecific antibodies and CARs to detect epitopes of proteins encoded by other mutant driver cancer genes.

6. References

Abraham RT and Weiss A (2004). Jurkat T cells and development of the T-cell receptor signaling paradigm. Nat Rev Immunol 4, 301–308.

Akbar AN, Terry L, Timms A, Beverley PC, Janossy G (1988). Loss of CD45R and gain of UCHL1 reactivity is a feature of primed T cells. J Immunol 140 (7), 2171–2178.

Alberts B, Johnson A, Lewis J, Raff M, Roberts K, and Walter P (2002). Molecular Biology of the Cell (New York: Garland Science Press)

Almåsbak H, Walseng E, Kristian A, Myhre MR, Suso EM, Munthe LA, …, and Kyte JA (2015). Inclusion of an IgG1-Fc spacer abrogates efficacy of CD19 CAR T cells in a xenograft mouse model. Gene Ther 22, 391–403.

Andreatta M, Nielsen M (2016). Gapped sequence alignment using artificial neural networks: application to the MHC class I system. Bioinformatics 32(4), 511-7.

Ataie N, Xiang J, and Cheng N (2015). Structure of a TCR mimic antibody with target predicts pharmacogenetics. J Mol Biol.

Bacik I, Cox JH, Anderson R, Yewdell JW, and Bennink JR (1994). TAP (transporter associated with antigen processing)-independent presentation of endogenously synthesized peptides is enhanced by endoplasmic reticulum insertion sequences located at the amino- but not carboxyl-terminus of the peptide. J Immunol 152, 381–7.

Bardi MS, Jarduli LR, Jorge AJ, Camargo RB, Carneiro FP, and Gelinski JR (2012). HLA-A, B and DRB1 allele and haplotype frequencies in volunteer bone marrow donors from the north of Parana State. Rev Bras Hematol Hemoter 34, 25–30.

Bassani-Sternberg M, Bräunlein E, Klar R, Engleitner T, Sinitcyn P, Audehm S, ... , and Krackhardt AM (2016). Direct identification of clinically relevant neoepitopes presented on native human melanoma tissue by mass spectrometry. Nat Commun 7, 13404.

Bassani-Sternberg M, Pletscher-Frankild S, Jensen LJ, and Mann M (2015). Mass spectrometry of human leukocyte antigen class I peptidomes reveals strong effects of protein abundance and turnover on antigen presentation. Mol Cell Proteomics 14(3), 658–673.

Brentjens RJ, Davila ML, and Riviere I (2013). CD19-targeted T cells rapidly induce molecular remissions in adults with chemotherapy-refractory acute lymphoblastic leukemia. Sci Transl Med 5(177), 177ra38.

Bridgeman JS (2010). The optimal antigen response of chimeric antigen receptors harboring the CD3ζ transmembrane domain is dependent upon incorporation of the receptor into the endogenous TCR/CD3 complex. J Immunol 184, 6938–6949.

Brocker T (2000). Chimeric Fv-ζ or Fv-ε receptors are not sufficient to induce activation or cytokine production in peripheral T cells. Blood 96, 1999–2001.

Burkea JD, and Young HA (2019). IFN-γ: A cytokine at the right time, is in the right place. Semin Immunol 43, 101280.

Cabrera T, Angustias Fernandez M, and Sierra A (1996). High frequency of altered HLA class I phenotypes in invasive breast carcinomas. Hum Immunol 50(2), 127–134.

Carbone DP (2017). First-line nivolumab in stage IV or recurrent non-small-cell lung cancer. N Engl J Med 376, 2415–2426.

Chames P (2000). Direct selection of a human antibody fragment directed against the tumor T-cell epitope HLA-A1–MAGE-A1 from a nonimmunized phage-Fab library. Proc Natl Acad Sci 97(14), 7969–74.

Chan BA and Hughes BG (2015). Targeted therapy for non-small cell lung cancer: current standards and the promise of the future. Transl. Lung Cancer Res 4(1), 36-54.

Chang AY, Gejman RS, Brea EJ, Oh CY, Mathias MD, Pankov D, …, and Scheinberg DA (2016 Aug). Opportunities and challenges for TCR mimic antibodies in cancer therapy. Expert Opin Biol Ther 16(8), 979-87.

Choksi S, Jameson BA, and Korngold R (1998). A structure-based approach to designing synthetic CD8a peptides that can inhibit cytotoxic T-lymphocyte responses. Nat Med 4, 309–14.

Cohen CJ (2002). Direct detection and quantitation of a distinct T-cell epitope derived from tumor-specific epithelial cell-associated mucin using human recombinant antibodies endowed with the antigen-specific, major histocompatibility complex-restricted specificity of T cells. Cancer Res 62(20), 5835–44.

Cox AD, Fesik SW, Kimmelman AC, Luo J, Der CJ (2014). Drugging the undruggable RAS: Mission possible? Nat. Rev. Drug Discov 13(11), 828-851.

Croce CM (2008). Oncogenes and cancer. The New England Journal of Medicine 358 (5), 502–511.

Croft M and Dubey C (2017). Accessory molecule and costimulation requirements for CD4 T cell response. Crit Rev Immunol 37(2-6), 261-290.

Curran KJ and Brentjens RJ (2015). Chimeric Antigen Receptor T Cells for Cancer Immunotherapy. J ClinOncol 33(15), 1703–1706.

Dahan R and Reiter Y (2012). T-cell-receptor-like antibodies-generation, function and applications. Expert Rev Mol Med 14(February), e6.

Danilova L, Anagnostou V, Caushi JX, Sidhom JW, Guo H, Chan HY, …, and Smith KN (2018). The Mutation-Associated Neoantigen Functional Expansion of Specific T Cells (MANAFEST) Assay: A Sensitive Platform for Monitoring Antitumor Immunity. Cancer Immunol Res 6(8), 888-899.

Dao T (2015). Therapeutic bispecific T-cell engager antibody targeting the intracellular oncoprotein WT1. Nat Biotechnol 33(10), 1079–86.

Davis SJ and van der Merwe PA (1996). The structure and ligand interactions of CD2: implications for T-cell function. Immunol Today 17, 177–87.

Denkberg G, Cohen CJ, Lev A, Chames P, Hoogenboom HR, and Reiter Y (2002). Direct visualization of distinct T cell epitopes derived from a melanoma tumor-associated antigen by using human recombinant antibodies with MHC-restricted T cell receptor-like specificity. Proc Natl AcadSci U S A 99(14), 9421–9426.

Di Magliano MP and Logsdon CD (2013). Roles for KRAS in pancreatic tumor development and progression. Gastroenterology 144(6), 1220-1229.

Dotti G, Gottschalk S, Savoldo B, and Brenner MK (2014). Design and development of therapies using chimeric antigen receptor-expressing T cells. Immunol. Rev. 257, 107–126.

Douglass J, Hsiue EH, Mog BJ, Hwang MS, DiNapoli SR, and Pearlman AH (2021). Bispecific antibodies targeting mutant RAS neoantigens. Sci Immunol 6, eabd5515.

Draper LM, Kwong MLM, and Gros A (2015). Targeting of HPV-16+ epithelial cancer cells by TCR gene engineered T cells directed against E6. Clin Cancer Res 21(19), 4431–4439.

Duan Z and Ho M (2021). T-Cell Receptor Mimic Antibodies for Cancer Immunotherapy. Mol Cancer Ther 20(9), 1533-1541.

Engelman JA, Chen L, Tan X, Crosby K, Guimaraes AR, Upadhyay R, …, and Wong KK (2008). Effective use of PI3K and MEK inhibitors to treat mutant Kras G12D and PIK3CA H1047R murine lung cancers. Nat Med 14(12), 1351-1356.

Fernández-Medarde A, Santos E (2011). Ras in cancer and developmental diseases. Genes Cancer 2(3), 344-358.

Finney HM, Akbar AN, and Lawson AD (2004). Activation of resting human primary T cells with chimeric receptors: costimulation from CD28, inducible costimulator, CD134, and CD137 in series with signals from the TCR ζ chain. J Immunol 172, 104–113.

Fioretti D, Iurescia S, Fazio VM, and Rinaldi M (2010). DNA vaccines: developing new strategies against cancer. J Biomed Biotechnol, 2010174378.

Fujiwara K, Tsunei A, Kusabuka H, Ogaki E, Tachibana M, and Okada N (2020). Hinge and Transmembrane Domains of Chimeric Antigen Receptor Regulate Receptor Expression and Signaling Threshold. Cells 9(5):1182.

Garrido F, Aptsiauri N, Doorduijn EM, Garcia Lora AM, and van Hall T (2016). The urgent need to recover MHC class I in cancers for effective immunotherapy. Curr Opin Immunol 39, 44–51.

Ge Q, Stone JD, Thompson MT, Cochran JR, Rushe M, Eisen HN, Chen J, and Stern LJ (2002). Soluble peptide-MHC monomers cause activation of CD8+ T cells through transfer of the peptide to T cell MHC molecules. Proc Natl Acad Sci U S A 99(21), 13729-34.

Gejman RS, Jones HF, Klatt MG, Chang AY, Oh CY, Chandran SS, …, and Scheinberg DA (2020). Identification of the Targets of T-cell Receptor Therapeutic Agents and Cells by Use of a High-Throughput Genetic Platform. Cancer Immunol Res 8(5), 672-684.

Gill S and June CH (2015). Going viral: chimeric antigen receptor T-cell therapy for hematological malignancies. Immunol Rev 263(1), 68–89.

Goffin J, Lacchetti C, Ellis PM, Ung YC, and Evans WK (2010). Lung cancer disease site group of cancer care Ontario's program in evidence-based care. First-line systemic chemotherapy in the treatment of advanced non-small cell lung cancer: a systematic review. J Thorac Oncol 5(2), 260-274.

Guedan S (2018). Enhancing CAR T cell persistence through ICOS and 4-1BB costimulation. JCI Insight 3, 96976.

Guest RD, Hawkins RE, Kirillova N, Cheadle EJ, Arnold J, O'Neill A, …, and Shaw DM (2005). The role of extracellular spacer regions in the optimal design of chimeric immune receptors: evaluation of four different scFvs and antigens. J Immunother 28, 203–211.

Gutcher I and Becher B (2007). APC-derived cytokines and T cell polarization in autoimmune inflammation. J Clin Invest 117 (5), 1119–1127.

Hansen TF and Jakobsen A (2011). Clinical implications of genetic variations in the VEGF system in relation to colorectal cancer. Pharmacogenomics 12(12), 1681-1693.

Hata A.N, Yeo A, Faber AC, Lifshits E, Chen Z, Cheng KA, ..., and Engelman JA (2014). Failure to induce apoptosis via BCL-2 family proteins underlies lack of efficacy of combined MEK and PI3K inhibitors for KRAS-mutant lung cancers. Cancer Res 74(11), 3146-3156.

Hewitt EW (2003). The MHC class I antigen presentation pathway: strategies for viral immune evasion. Immunology 110,163–9.

Hobbs GA, Der CJ, Rossman KL (2016). RAS isoforms and mutations in cancer at a glance. J Cell Sci 129(7), 1287-1292.

Holler PD and Kranz DM (2003). Quantitative analysis of the contribution of TCR/pMHC affinity and CD8 to T cell activation. Immunity 18, 255–64.

Hombach A, Hombach AA, and Abken H (2010). Adoptive immunotherapy with genetically engineered T cells: modification of the IgG1 Fc 'spacer' domain in the extracellular moiety of chimeric antigen receptors avoids 'off-target' activation and unintended initiation of an innate immune response. Gene Ther, 17(10):1206-13

Hsiue EH, Wright KM, Douglass J, Hwang MS, Mog BJ, and Pearlman AH (2021). Targeting a neoantigen derived from a common TP53 mutation. Science 371, eabc8697.

Hudecek M, Lupo-Stanghellini MT, Kosasih PL, Sommermeyer D, Jensen MC, Rader C, and Riddell SR (2013). Receptor affinity and extracellular domain modifications affect tumor recognition by ROR1-specific chimeric antigen receptor T cells. Clin. Cancer Res 19, 3153–3164.

Hudecek M, Sommermeyer D, Kosasih PL, Silva-Benedict A, Liu L, Rader C, Jensen MC, and Riddell SR (2015). The nonsignaling extracellular spacer domain of chimeric antigen receptors is decisive for in vivo antitumor activity. Cancer Immunol. Res 3, 125–135.

Hui Xiong, Fengyan Luo, Pengfei Zhou, and Jizu Yi (2021). Development of a reporter gene method to measure the bioactivity of anti-CD38 × CD3 bispecific antibody. Antib Ther 4(4), 212–221.

Imai C (2004). Chimeric receptors with 4-1BB signaling capacity provoke potent cytotoxicity against acute lymphoblastic leukemia. Leukemia 18, 676–684.

James SE, Greenberg PD, Jensen MC, Lin Y, Wang J, Till BG, Raubitschek AA, Forman SJ, and Press OW (2008). Antigen sensitivity of CD22-specific chimeric TCR is modulated by target epitope distance from the cell membrane. J. Immunol 180, 7028–7038.

Jancík S, Drábek J, Radzioch D, and Hajdúch M (2010). Clinical relevance of KRAS in human cancers. J Biomed Biotechnol, 2010150960.

Janeway CA Jr (1992). The T cell receptor as a multicomponent signaling machine: CD4/CD8 coreceptors and CD45 in T cell activation. Annu Rev Immunol 10, 645–74.

Jiang X, Wang J, Deng X, Xiong F, Ge J, Xiang B, …, and Zeng Z (2019). Role of the tumor microenvironment in PD-L1/PD-1-mediated tumor immune escape. Mol Cancer 18(1), 10.

Jinesh GG, Sambandam V, Vijayaraghavan S, Balaji K, and Mukherjee S (2018). Molecular genetics and cellular events of K-Ras driven tumorigenesis. Oncogene 37(7), 839-846.

JL Bos, Rehmann H, and Wittinghofer A (2007). GEFs and GAPs: critical elements in the control of small G proteins. Cell 129, 865-877.

Jost C, Darowski D, Challier J, Pulko V, Hanisch LJ, Xu W,… , and Klein C (2020). CAR-J cells for antibody discovery and lead optimization of TCR-like immunoglobulins. MAbs 12(1), 1840709.

June CH, O'Connor RS, Kawalekar OU, Ghassemi S, and Milone MCCAR (2018). T cell immunotherapy for human cancer. Science 359, 1361–1365.

Klebanoff CA and Wolchok JD (2018). Shared cancer neoantigens: Making private matters public. J Exp Med 215, 5–7.

Klichinsky M, Ruella M, Shestova O, Lu XM, Best A, and Zeeman M (2020). Human chimeric antigen receptor macrophages for cancer immunotherapy. Nat Biotechnol 38, 947–53.

Kochenderfer JN, Wilson WH, Janik JE, Dudley ME, Stetler-Stevenson M, and Feldman SA (2010). Eradication of B-lineage cells and regression of lymphoma in a patient treated with autologous T cells genetically engineered to recognize CD19. Blood 116, 4099–102.

Kodaz H, Kostek O, Hacioglu MB, Erdogan B, Kodaz CE, Hacibekiroglu I, et al. (2017). Frequency of ras mutations (KRAS, NRAS, HRAS) in human solid cancer. EJMO 1(1), 1-7.

Kreitman RJ, Tallman MS, Robak T, Coutre S, Wilson WH, and Stetler-Stevenson M (2012). Phase I trial of anti-CD22 recombinant immunotoxin moxetumomab pasudotox (CAT-8015 or HA22) in patients with hairy cell leukemia. J Clin Oncol 30, 1822–8.

Kuwana Y (1987). Expression of chimeric receptor composed of immunoglobulin-derived V regions and T-cell receptor-derived C regions. Biochem Biophys Res Commun 149, 960–968.

Lau TP, Roslani AC, Lian LH, Lee PC, Hilmi I, Goh KL, and Chua KH (2014). Association between EGF and VEGF functional polymorphisms and sporadic colorectal cancer in the Malaysian population. Genet Mol Res 13(3), 5555-5561.

Laugel B, Price DA, Milicic A, and Sewell AK (2007). CD8 exerts differential effects on the deployment of cytotoxic T lymphocyte effector functions. Eur J Immunol 37, 905–13.

Lee A (2022). Sotorasib: A Review in KRAS G12C Mutation-Positive Non-small Cell Lung Cancer. Target Oncol 17(6), 727–733.

Lev A (2002). Isolation and characterization of human recombinant antibodies endowed with the antigen-specific, major histocompatibility complex-restricted specificity of T cells directed toward the widely expressed tumor T-cell epitopes of the telomerase catalytic subunit. Cancer Res 62(11), 3184–94.

Lev A, Denkberg G, and Cohen CJ (2002). Isolation and characterization of human recombinant antibodies endowed with the antigen-specific, major histocompatibility complex-restricted specificity of T cells directed toward the widely expressed tumor T-cell epitopes of the telomerase catalytic sub. Cancer Res 62(11), 3184–3194.

Lin YM, Sung WW, Hsieh MJ, Tsai SC, Lai HW, Yang SM, …, and Chen CJ (2015). High PD-L1 expression correlates with metastasis and poor prognosis in Oral squamous cell carcinoma. PLoS One 10(11), e0142656.

Lito P, Solomon M, Li L-S, Hansen R, and Rosen N (2016). Allele specific inhibitors inactivate mutant KRAS G12C by a trapping mechanism. Science 351(6273), 604-608.

Liu E, Marin D, Banerjee P, Macapinlac HA, Thompson P, and Basar R (2020). Use of CAR-transduced natural killer cells in CD19- positive lymphoid tumors. N Engl J Med 382, 545–53.

Liu H, Xu Y, Xiang J, Long L, Green S, and Yang Z (2017). Targeting Alpha-fetoprotein (AFP)-MHC complex with CAR T-cell therapy for liver cancer. Clin Cancer Res 23, 478–88.

Liu L, Sommermeyer D, Cabanov A, Kosasih P, Hill T, and Riddell SR (2016). Inclusion of Strep-tag II in design of antigen receptors for T-cell immunotherapy. Nat Biotechnol 34(4), 430-4.

Lord RV, Brabender J, and Gandara D (2002). Low ERCC1 expression correlates with prolonged survival after cisplatin plus gemcitabine chemotherapy in non-small cell lung cancer. Clin Cancer Res 8, 2286–2291.

Lu YC, Yao X, Crystal JS, Li YF, El-Gamil M, Gross C, …, and Robbins PF (2014). Efficient identification of mutated cancer antigens recognized by T cells associated with durable tumor regressions. Clin Cancer Res 20(13), 3401-10.

Luckey CJ, King GM, and Marto JA (1998). Proteasomes Can either Generate or Destroy MHC Class I Epitopes: Evidence for Nonproteasomal Epitope Generation in the Cytosol. J Immunol 161, 112–121.

Luft T (2001). Exogenous peptides presented by transporter associated with antigen processing (TAP)-deficient and TAP-competent cells: Intracellular loading and kinetics of presentation. J Immunol 167(5), 2529–2537.

M Maiers, L Gragert, and W Klitz (2007). High-resolution HLA alleles and haplotypes in the United States population. Hum Immunol 68, 779–788.

Ma Q (2016). A novel TCR-like CAR with specificity for PR1/HLA-A2 effectively targets myeloid leukemia in vitro when expressed in human adult peripheral blood and cord blood T cells. Cytotherapy 18(8), 985–94.

Maguire O, Tornatore K.M, O'Loughlin KL, Venuto RC, and Minderman H (2013). Nuclear translocation of nuclear factor of activated T cells (NFAT) as a quantitative pharmacodynamic parameter for tacrolimus. Cytometry A 83, 1096–1104.

Maher J, Brentjens RJ, Gunset G, Rivière I, and Sadelain M (2002). Human T-lymphocyte cytotoxicity and proliferation directed by a single chimeric TCRζ/CD28 receptor. Nat Biotechnol 20, 70-75.

Maiers M, Gragert L, Klitz W (2007). High-resolution HLA alleles and haplotypes in the United States population. Hum Immunol 68(9), 779-88.

Marangoni F, Murooka TT, Manzo T, Kim EY, Carrizosa E, Elpek NM, and Mempel TR (2013). The transcription factor NFAT exhibits signal memory during serial T cell interactions with antigen-presenting cells. Immunity 38, 237–249.

Masoud V and Pagès G (2017). Targeted therapies in breast cancer: New challenges to fight against resistance. World J Clin Oncol 8(2), 120-134.

Maus MV, Fraietta JA, Levine BL, Kalos M, Zhao Y, and June CH (2014). Adoptive immunotherapy for cancer or viruses. Annu Rev Immunol 32,189–225.

Maus MV, Plotkin J, Jakka G, Stewart-Jones G, Rivière I, and Merghoub T (2016). An MHC-restricted antibody-based chimeric antigen receptor requires TCR-like affinity to maintain antigen specificity. Mol Ther Oncol 3, 1–9.

Maverakis E, Kim K, Shimoda M, Gershwin M, Patel F, Wilken R, et al. (2015). "Glycans in the immune system and the altered glycan theory of autoimmunity". J Autoimmun 57 (6), 1–13.

Michaeli Y (2009). Expression hierarchy of T cell epitopes from melanoma differentiation antigens: unexpected high level presentation of tyrosinase /HLA-A2 Complexes revealed by peptide-specific, MHC-restricted, TCR-like antibodies. J Immunol 182(10), 6328–41.

Miyamoto Y, Suyama K, and Baba H (2017). Recent advances in targeting the EGFR signaling pathway for the treatment of metastatic colorectal cancer. Int J Mol Sci 18(4), E752.

Mizukoshi E, Nakamoto Y, Tsuji H, Yamashita T, and Kaneko S (2006). Identification of alpha-fetoprotein-derived peptides recognized by cytotoxic T lymphocytes in HLA-A24+ patients with hepatocellular carcinoma. Int J Cancer 118(5), 1194–1204.

Motonari K (2016). One niche to rule both maintenance and loss of stemness in HSCs. Immunity 45 (6), 1177–1179.

Müller T, Uherek C, Maki G, Chow KU, Schimpf A, Klingemann HG, Tonn T, and Wels WS (2008). Expression of a CD20-specific chimeric antigen receptor enhances cytotoxic activity of NK cells and overcomes NK-resistance of lymphoma and leukemia cells. Cancer Immunol Immunother 57, 411–423.

Nakagawa H and Fujita M (2018). Whole genome sequencing analysis for cancer genomics and precision medicine. Cancer Sci 109, 513–22.

Narni-Mancinelli E, Vivier E, and Kerdiles YM (2011). The 'T-cell-ness' of NK cells: unexpected similarities between NK cells and T cells. Int Immunol 23(7), 427-31.

Neelapu SS (2017). Axicabtagene ciloleucel CAR T-cell therapy in refractory large B-cell lymphoma. N Engl J Med 377, 2531–2544.

Norment AM and Littman DR (1988). A second subunit of CD8 is expressed in human T cells. EMBO J 7, 3433–9.

Oelke M, Moehrle U, Chen JL, Behringer D, Cerundolo V, Lindemann A, and Mackensen A (2000). Generation and purification of CD8+ melan-A-specific cytotoxic T lymphocytes for adoptive transfer in tumor immunotherapy. Clin Cancer Res 6, 1997−2005.

Oiseth SJ and Aziz MS (2017). Cancer immunotherapy: a brief review of the history, possibilities, and challenges ahead. J Cancer Metastasis Treat 3, 250–261.

Olaussen KA, Dunant A, and Fouret P (2006). DNA repair by ERCC1 in non-small-cell lung cancer and cisplatin-based adjuvant chemotherapy.N Engl J Med 355, 983–991.

Ostrem JML and Shokat KM (2016). Direct small-molecule inhibitors of KRAS: from structural insights to mechanism-based design. Nat Rev Drug Discov 15(11), 771-785.

Parkhurst M, Gros A, Pasetto A, Prickett T, Crystal JS, and Robbins P (2017). Isolation of T-cell receptors specifically reactive with mutated tumor-associated antigens from tumor-infiltrating lymphocytes based on CD137 expression. Clin Cancer Res 23, 2491–505.

Patricelli MP, Janes MR, Li LS, Hansen R, Peters U, Kessler LV, …, and Liu Y (2016). Selective inhibition of oncogenic KRAS output with small molecules targeting the inactive state. Cancer Discov 6(3), 316-329.

Pelletier JPR and Mukhtar F (2020). Passive Monoclonal and Polyclonal Antibody Therapies. Immunol Concepts Transfus Med 16, 251–348.

Perica K, Varel JC, Oelke M, and Schneck J (2015). Adoptive T cell immunotherapy for cancer. Rambam Maimonides Med J 6, e0004.

Polakova K, Plaksin D, Chung DH, Belyakov IM, Berzofsky JA, and Margulies DH (2000). Antibodies directed against the MHC-I molecule H-2Dd complexed with an antigenic peptide: similarities to a T cell receptor with the same specificity. J Immunol 165(10), 5703–5712.

Poorebrahim M, Mohammadkhani N, Mahmoudi R, Gholizadeh M, Fakhr E, and Cid-Arregui A (2021). TCR-like CARs and TCR-CARs targeting neoepitopes: an emerging potential. Cancer Gene Ther 28(6), 581-589.

Poorebrahim M, Sadeghi S, Fakhr E, Abazari MF, Poortahmasebi V, and Kheirollahi A (2019). Production of CAR T-cells by GMP-grade lentiviral vectors: latest advances and future prospects. Crit Rev Clin Lab Sci 56, 393–419.

Porru M, Pompili L, Caruso C, Biroccio A, and Leonetti C (2018). Targeting KRAS in metastatic colorectal cancer: current strategies and emerging opportunities. J Exp Clin Cancer Res 37(1), 57.

Porter DL, Levine BL, Kalos M, Bagg A, and June CH (2011). Chimeric antigen receptor modified T cells in chronic lymphoid leukemia. N Engl J Med 365, 725–33.

Qin T, Zeng YD, Qin G, Xu F, Lu JB, Fang WF, ..., and Wang SS (2015). High PD-L1 expression was associated with poor prognosis in 870 Chinese patients with breast cancer. Oncotarget 6(32), 33972–81.

Rajasekharan SK, Raman T (2013). Ras and Ras mutations in cancer. Cent Eur J Biol 8(7), 609-624.

Ranpura V, Hapani S, and Wu S (2011). Treatment-related mortality with bevacizumab in cancer patients: a meta-analysis. JAMA 305(5), 487-494.

Rosenberg SA (1988). Use of tumor-infiltrating lymphocytes and interleukin-2 in the immunotherapy of patients with metastatic melanoma. A preliminary report. N Engl J Med 319, 1676–1680.

Rosenberg SA (1994). Treatment of patients with metastatic melanoma with autologous tumor-infiltrating lymphocytes and interleukin 2. J Natl Cancer Inst 86, 1159–1166.

Rosenberg SA and Restifo NP (2015). Adoptive cell transfer as personalized immunotherapy for human cancer. Science 348(6230), 62–8.

Sadelain M, Brentjens R, and Rivière I (2013). The basic principles of chimeric antigen receptor design. Cancer Discov 3, 388–398.

Sahin U and Tureci O (2018). Personalized vaccines for cancer immunotherapy. Science 359, 1355–60.

Salter RD, Howell DN, and Cresswell P (1985). Genes regulating HLA class I antigen expression in T-B lymphoblast hybrids. Immunogenetics 21(3), 235–246.

Sarkizova S, Klaeger S, Le PM, Li LW, Oliveira G, Keshishian H, …, and Keskin DB (2020). A large peptidome dataset improves HLA class I epitope prediction across most of the human population. Nat Biotechnol 38(2), 199-209.

Schneider U, Schwenk HU, and Bornkamm G (1977). Characterization of EBV-genome negative “null” and “T” cell lines derived from children with acute lymphoblastic leukemia and leukemic transformed non-Hodgkin lymphoma. Int J Cancer 19, 621–626.

Scholtalbers J, Boegel S, Bukur T, Byl M, Goerges S, Sorn P, Loewer M, Sahin U, and Castle JC (2015). TCLP: An online cancer cell line catalogue integrating HLA type, predicted neo-epitopes, virus and gene expression. Genome Med 7, 118.

Schroder K, Hertzog PJ, Ravasi T, and Hume DA (2004). Interferon-gamma: an overview of signals, mechanisms and functions. Journal of leukocyte biology 75, 163–189.

Schumacher TN and Schreiber RD (2015). Neoantigens in cancer immunotherapy. Science 348, 69–74.

Seaman S, Zhu Z, Saha S, Zhang XM, Yang MY, and Hilton MB (2017). Eradication of tumors through simultaneous ablation of CD276/B7-H3-positive tumor cells and tumor vasculature. Cancer Cell 31, 501–15.

Sewell AK, Gerth UC, and Price DA (1999). Antagonism of cytotoxic T-lymphocyte activation by soluble CD8. Nat Med 5, 399–404.

Shaib W, Mahajan R, and El-Rayes B (2013). Markers of resistance to anti-EGFR therapy in colorectal cancer. J Gastrointest Oncol 4(3), 308-318.

Simanshu DK, Nissley DV, and McCormick F (2017). RAS proteins and their regulators in human disease. Cell 170(1), 17-33.

Skora AD, Douglass J, Hwang MS, Tam AJ, Blosser RL, Gabelli SB, …, and Zhou S (2015). Generation of MANAbodies specific to HLA-restricted epitopes encoded by somatically mutated genes. Proc Natl Acad Sci USA 112(32), 9967-72.

Starck L, Popp K, Pircher H, and Uckert W (2014). Immunotherapy with TCR-Redirected T Cells: Comparison of TCR-Transduced and TCR-Engineered Hematopoietic Stem Cell-Derived T Cells. J Immunol 192(1), 206–213.

Stewart-jones G, Hombach A, and Shenderov E (2009). Rational development of high-affinity T-cell receptor-like antibodies. Proc Natl Acad Sci 106(26), 10872–10872.

Stoiber S, Cadilha BL, Benmebarek M-R, Lesch S, Endres S, and Kobold S (2019). Limitations in the Design of Chimeric Antigen Receptors for Cancer Therapy. Cells 8(5), 472.

Sung H, Ferlay J, Siegel RL, Laversanne M, Soerjomataram I, Jemal A, et al.(2021). Global Cancer Statistics 2020: GLOBOCAN Estimates of Incidence and Mortality Worldwide for 36 Cancers in 185 Countries. CA Cancer J Clin 71(3), 209-249.

Swift S, Lorens J, Achacoso P, and Nolan GP (2001). Rapid production of retroviruses for efficient gene delivery to mammalian cells using 293T cell-based systems. Curr Protoc Immuno 10 (10), 17C.

Tran E, Robbins PF, and Rosenberg SA (2017). 'Final common pathway' of human cancer immunotherapy: targeting random somatic mutations. Nat Immunol 18, 255–62.

Tureci O, Lower M, Schrors B, Lang M, Tadmor A, and Sahin U (2018). Challenges towards the realization of individualized cancer vaccines. Nat BioMed Eng 2, 566–9.

Uherek C, Tonn T, Uherek B, Becker S, Schnierle B, Klingemann HG, and Wels W (2002). Retargeting of natural killer-cell cytolytic activity to ErbB2-expressing cancer cells results in efficient and selective tumor cell destruction. Blood 100, 1265–1273.

Van der Stegen SJ, Hamieh M, and Sadelain M (2015). The pharmacology of second-generation chimeric antigen receptors. Nat Rev Drug Discov 14, 499–509.

Varadarajan N, Julg B, Yamanaka YJ, Chen H, Ogunniyi AO, McAndrew E, ... ,and Pereyra F. (2011). A high-throughput single-cell analysis of human CD8+ T cell functions reveals discordance for cytokine secretion and cytolysis. The Journal of clinical investigation 121(11), 4322-4331.

Vrisekoop N, Monteiro JP, Mandl JN, Germain RN (2014). Revisiting thymic positive selection and the mature T cell repertoire for antigen. Immunity 41, 181–190.

Wang Q, Douglass J, Hwang MS, Hsiue EH, Mog BJ, Zhang M, …, and Vogelstein B (2019). Direct Detection and Quantification of Neoantigens. Cancer Immunol Res 7(11), 1748-1754.

Watanabe K, Terakura S, Martens AC, van Meerten T, Uchiyama S, and Imai M (2015). Target antigen density governs the efficacy of anti-CD20-CD28-CD3 ζ chimeric antigen receptor-modified effector CD8+ T cells. J Immunol 194, 911–20.

Weiden PL (1979). Antileukemic effect of graft-versushost disease in human recipients of allogeneic-marrow grafts. N Engl J Med 300, 1068–1073.

Weng TY, Yen MC, Huang CT, Hung JJ, Chen YL, Chen WC, …, and La MD (2014). DNA vaccine elicits an efficient antitumor response by targeting the mutant Kras in a transgenic mouse lung cancer model. Gene Ther 21(10), 888-896.

Willemsen R, Debets R, Hart E, Hoogenboom H, Bolhuis R, and Chames P (2001). A phage display selected fab fragment with MHC class I-restricted specificity for MAGE-A1 allows for retargeting of primary human T lymphocytes. Gene Ther 8, 1601–8.

Wittman VP, Woodburn D, Nguyen T, Neethling FA, Wright S, and Weidanz JA (2006). Antibody Targeting to a Class I MHC-Peptide Epitope Promotes Tumor Cell Death. J Immunol 177(6), 4187–4195.

Wong HS, Germain RN (2021). Mesoscale T cell antigen discrimination emerges from intercellular feedback. Trends Immunol 42(10), 865-875.

Wooldridge L, van den Berg HA, and Glick M (2005). Interaction between the CD8 co-receptor and major histocompatibility complex class I stabilizes T cell receptor–antigen complexes at the cell surface. J Biol Chem 280, 27491–501.

Yang B, Jeang J, Yang A, Wu TC, and Hung C-F (2014). DNA vaccine for cancer immunotherapy. Hum Vaccin Immunother 10(11), 3153-3164.

Yarchoan M, Johnson BA, Lutz ER, Laheru DA, and Jaffee EM (2017). Targeting neoantigens to augment antitumor immunity. Nat Rev Cancer 17, 209–22.

Zamora AE, Crawford JC, and Thomas PG (2018). Hitting the Target: How T Cells Detect and Eliminate Tumors. J Immunol 200, 392–9.

Zarnitsyna VI, Evavold BD, Schoettle LN, Blattman JN, Antia R (2013). Estimating the diversity, completeness, and cross-reactivity of the T cell repertoire. Front Immunol 4, 485.

Zeichner SB, Terawaki H, and Gogineni KA (2016). Review of systemic treatment in metastatic triple-negative breast cancer. Breast Cancer (Auckl.) 10, 25-36.

Zeitouni D, Pylayeva-Gupta Y, Der CJ, and Bryant KL (2016). KRAS mutant pancreatic cancer: no lone path to an effective treatment. Cancers (Basel) 8(4), 45.

Zhang G, Wang L, Cui H, Wang X, Zhang G, and Ma J (2014). Anti-melanoma activity of T cells redirected with a TCR-like chimeric antigen receptor. Sci Rep 4, 3571.

Zhihao Wu and Nai-Kong V Cheung (2018). T cell engaging bispecific antibody (T-BsAb): from technology to therapeutics. Pharmacol Ther 182, 161–175.

Zimmermann R (2011). Protein translocation across the ER membrane. Biochim Biophys Acta 1808(3), 912-24.

7. Appendix

Snapgene® viewer version 6.0.2 was used to generate the following vector maps.

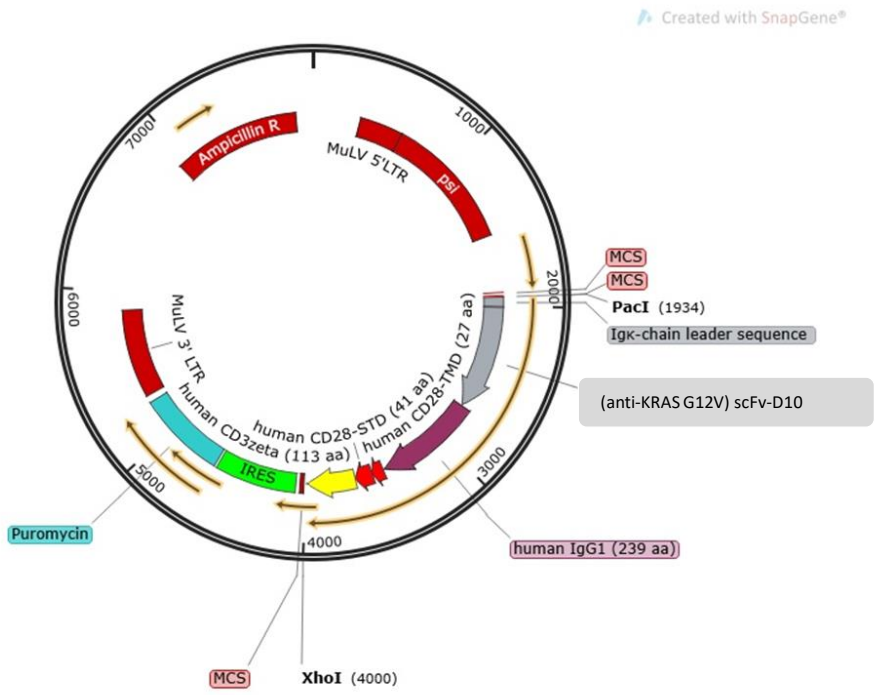

Figure 6.1: Schematic representation of the retroviral vector pMXs-(anti-KRAS^{G12V}) scFv-D10-hIgG-hCD28TMD-hCD28STD-hCD3z-IRES-Puro. A set of oligonucleotides encoding (anti-KRAS^{G12V}) scFv-D10 with L-kappa leader sequence, and hCD28TMD-hCD28STD-hCD3z sequence were amplified using PCR and then subcloned into a retroviral expression vector pMXs-IRES-Puro, which contains an internal ribosome entry site (IRES), puromycin- and ampicillin-resistance genes, Moloney murine leukemia virus long terminal repeats (MulV LTRs), viral package signal (psi), and multi cloning site (MCS) for cloning of a target gene. PCR cloning was performed using the enzyme restriction sites displayed above. The variable light and heavy chains of the scFv are linked by a 12-mer-linker (GGGSGGGGSGGG).

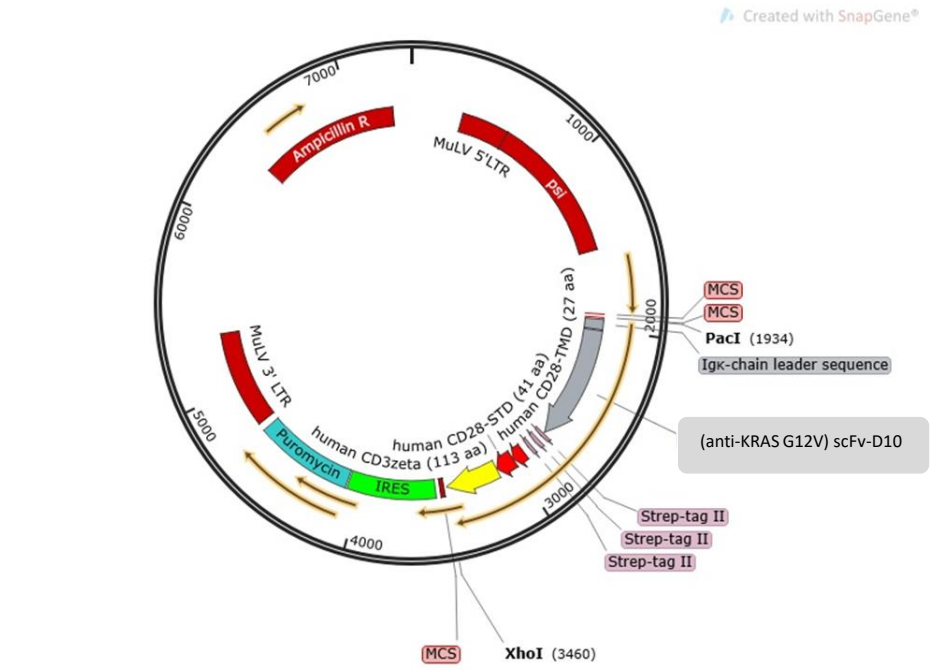

pMXs-(anti-KRAS G12V) scFv-D10-Strep-tag II-hCD28TMD-hCD28STD-hCD3z-IRES-Puro

7362 bp

Figure 6.2: Schematic representation of the retroviral vector pMXs-(anti-KRAS^{G12V}) scFv-D10-Strep-tag II-hCD28TMD-hCD28STD-hCD3z-IRES-Puro. Oligonucleotides encoding (anti-KRAS^{G12V}) scFv-D10 with L-kappa leader sequence, and Strep-tag II- hCD28TMD-hCD28STD-hCD3z sequence were amplified using PCR and then subcloned into a retroviral expression vector pMXs-IRES-Puro, which contains an internal ribosome entry site (IRES), puromycin- and ampicillin-resistance genes, Moloney murine leukemia virus long terminal repeats (MulV LTRs), viral package signal (psi), and multi cloning site (MCS) for cloning of a target gene. The restriction sites displayed by the enzymes were utilized to carry out PCR cloning. A 12mer-linker (GGGSGGGGSGGG) connects the variable light and heavy chains of the scFv. Three Strep-tag II (NWSHPQFEK) sequences connecting with 10mer- linker (GGGGS) 2 were interposed between the scFv and the CD28 transmembrane domain.

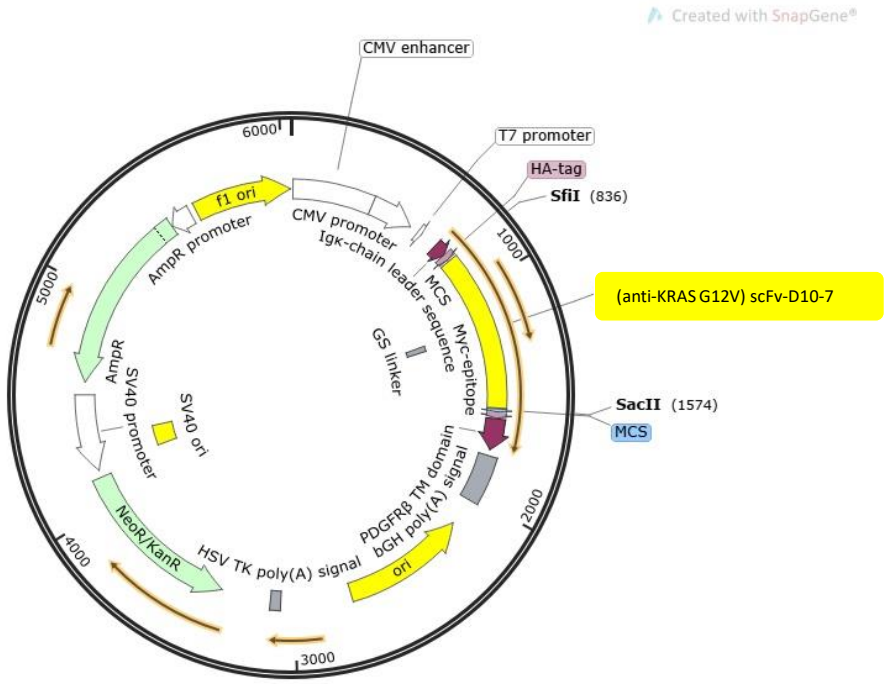

pDisplay-HA-tag-(anti-KRASG12V) scFv-D10-7-Myc-PDGFR-Neo & Kano

6040 bp

Figure 6.3: Diagram of expression vector pDisplay-HA-tag-(anti-KRAS^{G12V}) scFv-D10-7-Myc-PDGFR-Neo & Kano. Oligonucleotides encoding (anti-KRAS^{G12V}) scFv-D10-7 sequence were amplified by PCR and then grafted into pDisplay, which carries at the C-terminus an Igκ-chain leader sequence, followed by a HA epitope tag. At the N-terminus, this vector carries a Myc epitope and the platelet-derived growth factor receptor (PDGFR) transmembrane domain, which anchors the expressed protein to the plasma membrane. A 12mer-linker (GGGSGGGGSGGG) connects the variable light and heavy chains of the scFv.

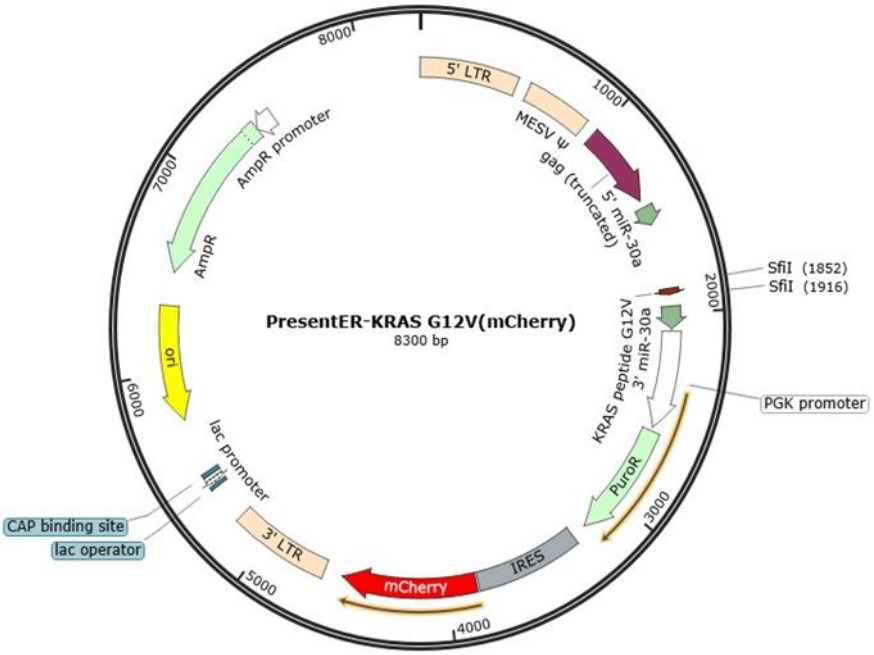

Figure 6.4: Schematic representation of the retroviral transfer vector PresentER-KRAS^{G12V} (mCherry). Oligonucleotides encoding KRAS^{G12V} sequence were amplified using PCR and then fused to the downstream of ER signal sequence of a retroviral expression vector PresentER, which contains puromycin- and ampicillin-resistance genes, an internal ribosome entry site (IRES), red fluorescent protein (mCherry), long terminal repeats (LTRs), and viral package signal (ψ). The restriction sites displayed by the enzymes were used for PCR cloning**.**

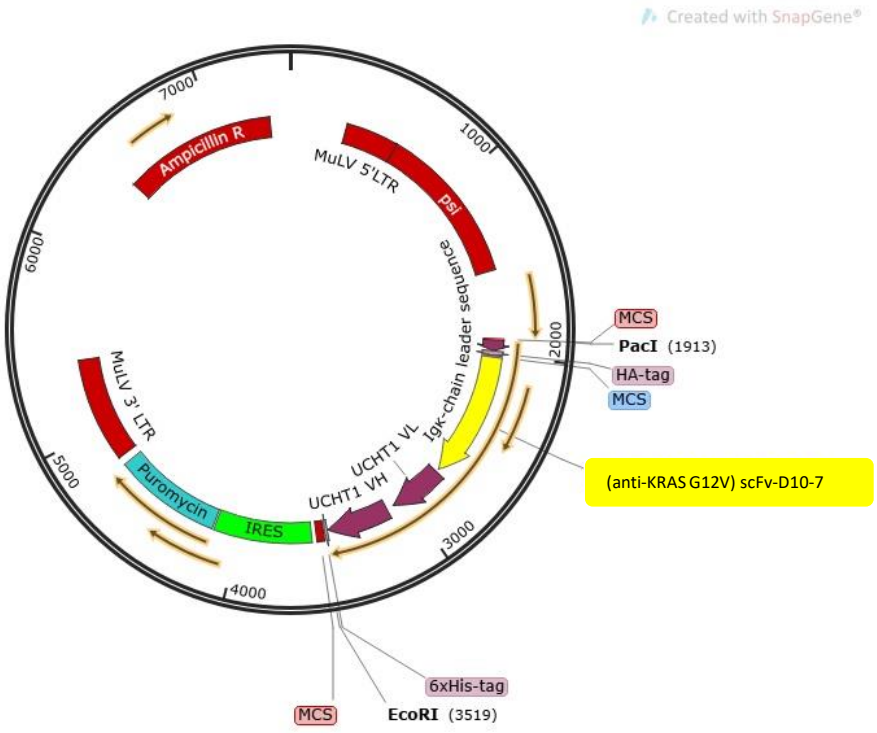

Figure 6.5: Diagram of the retroviral transfer vector pMXs-(anti-KRAS^{G12V}) scFv-D10-7-UCHT1-IRES-Puro. Oligonucleotides encoding (anti-KRAS^{G12V}) scFv-D10-7, and UCHT1 (an anti-CD3 clone) sequences were amplified using PCR and then subcloned into a retroviral expression vector pMXs-IRES-Puro, which contains an internal ribosome entry site (IRES), puromycin- and ampicillin-resistance genes, Moloney murine leukemia virus long terminal repeats (MulV LTRs), viral package signal (psi), and multi cloning site (MCS) for cloning of a target gene. Displayed enzymes restriction sites were used for PCR based cloning. An Igκ-chain leader sequence, which followed by hemagglutinin A (YPYDVPDYA) epitope tag was placed upstream of the scFv. A 12mer-linker (GGGSGGGGSGGG) connects the variable light and heavy chains of the scFv-D10-7 bound to the UCHT1 sequence by a short linker (GGGGS). A long linker $(GGGGS)_3$ connects VL $_{UCHT1}$-VH $_{UCHTI}$ sequence followed a 6 × His-tag at the C-terminus.

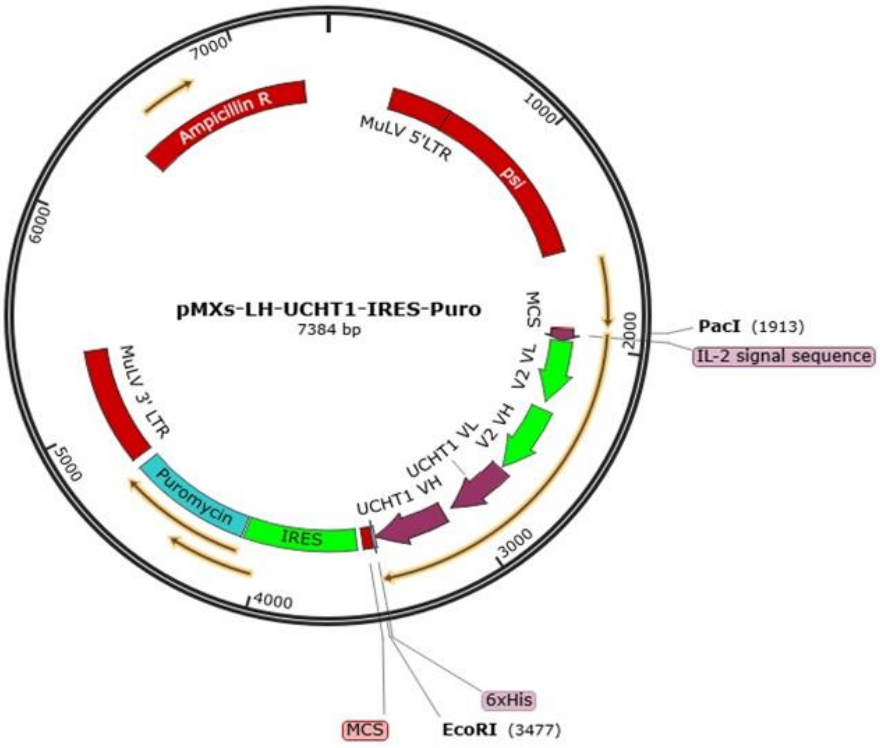

Figure 6.6: Schematic illustration of the retroviral transfer vector pMXs-LH-UCHT1-IRES-Puro. Oligonucleotides encoding LH- UCHT1 sequence bearing C-terminal 6 × His-tag were amplified using PCR and then subcloned into a retroviral expression vector pMXs-IRES-Puro, which contains an internal ribosome entry site (IRES), puromycin- and ampicillin-resistance genes, Moloney murine leukemia virus long terminal repeats (MulV LTRs), viral package signal (psi), and multi cloning site (MCS) for cloning of a target gene. Enzyme restriction sites shown on the map were used for PCR cloning. A signal sequence for IL-2 was incorporated upstream of the scFv. A short linker (GGGGS) connects the variable light and heavy chains of V2 and UCHT1. A long linker $(GGGGS)_3$ connects V2 to UCHT1 sequence.

Table 6.1: Sequences of the scFv amino acids. Sequence of $KRAS^{G12V}$ scFvs and anti-CD3 scFv used to generate TCRm CARs and bispecific antibodies.

scFv name	antigen	amino acid sequence
D10	$KRAS^{G12V}$ pHLA-A2	DIQMTQSPSSLSASVGDRVTITCRASQDVNT AVAWYQQKPGKAPKLLIYSASFLYSGVPSR FSGSRSGTDFTLTISSLQPEDFATYYCQQYY YYPPTFGQGTKVEIKRTGGGSGGGGSGGG ASEVQLVESGGGLVQPGGSLRLSCAASGF NINGSYIHWVRQAPGKGLEWVAYIDPETGY SRYADSVKGRFTISADTSKNTAYLQMNSLR AEDTAVYYCSRDSASDAMDVWGQGTLVTVSS
D10-7	$KRAS^{G12V}$ pHLA-A2	DIQMTQSPSSLSASVGDRVTIACRASQDVNT AVAWYQQKPGKAPKLLIYSASFLYSGVPSR FSGSRSGTDFTLTISSLQPEDFATYYCQQYY YYPPTFGQGTKVEIKRTGGGSGGGGSGGG ASEVQLVESGGGLVQPGGSLRLSCAASGF HINGSYIHWVRQAPGKGLKWVAYIDPETGY SRYADSVKGRFAISADMSKNTAYLQMNSLR AEDTAVYYCSRDSASDAMDVWGQGTLVTVSS
LH	$KRAS^{G12V}$ pHLA-A3	DIQMTQSPSSLSASVGDRVTITCRASQDVNT AVAWYQQKPGKAPKLLIYSASFLYSGVPSR FSGSRSGTDFTLTISSLQPEDFATYYCQQSYY YFRPITFGQGTKVEIKGGGGSGGGGSGGGG SEVQLVESGGGLVQPGGSLRLSCAASGFNLS YSDIHWVRQAPGKGLEWVAVVMPDSGHTNYA DSVKGRFTISADTSKNTAYLQMNSLRAEDTAV YYCSRATNIPVYAFDYWGQ GTLVTVSS
UCHT1	Human CD3	DIQMTQTTSSLSASLGDRVTISCRASQDIRN YLNWYQQKPDGTVKLLIYYTSRLHSGVPSK FSGSGSGTDYSLTISNLEQEDIATYFCQQGNT LPTFAGGTKLEIKGGGGSGGGGSGGGG SEVQLQQSGPELVKPGASMKISCKASGYSFT GYTMNWVKQSHGKNLEWMGLINPYKGVSTYN QKFKDKATLTVDKSSSTAYMELLSLTSEDSAV YYCARSGYYGDSDWYFDVW GAGTTVTVSS

CURRICULUM VITAE

Saber Ebrahimi

Address:

University Medical Center of the Johannes Gutenberg- University of Mainz
III. Dept. of Medicine - Hematology, and Medical Oncology
Bld. for R&D, Obere Zahlbacherstr. 63
D-55131 Mainz / Germany
✉ sebrahim@uni-mainz.de
✆ +49(0) 6131 17-9686

Education and Qualifikation:

2019 – 2024	Ph.D. Studentship in Translational Biomedicine Programme (**TRANSMED**), University Medical Center (UMC) Mainz, Mainz, Germany.
2017 – 2019	German Language Institute Tehran (**DSIT**), Tehran, Iran.
2011 – 2014	M.Sc. in Laboratory Hematology and Blood Banking, Tehran University of Medical Sciences (No. 1 National Medical University in Iran), Tehran, Iran.
2009 – 2011	B.Sc. Medical Laboratory Sciences, Shahid Beheshti University of Medical Sciences (2nd top National Medical University in Iran), Tehran, Iran.
2007 – 2009	A.D. Medical Laboratory Sciences, Tehran University of Medical Sciences (1st top National Medical University in Iran), Tehran, Iran.
2002 – 2005	High School Studies, Experimental Sciences, Alborz, Iran.

List of own publications

- Tavasoli B, **Ebrahimi S**, Manafi R, Kiani F, Safa M, Kazemi A. Indole3-carbinol Induces G1 cell cycle arrest in Pre-B acute lymphoblastic leukemia cell line. Arak Medical University Journal (AMUJ) 2014; 17(7): 30-40. Cited by: 1

- Safa M, Tavasoli B, Manafi R, Kiani F, Kashiri M, **Ebrahimi S**, Kazemi A. Indole-3-carbinol suppresses NF-κB activity and stimulates the p53 pathway in pre-B acute lymphoblastic leukemia cells. Tumor Biology 2015; 36(5): 3919-3930. IF: 3.65, Cited by: 49

Acknowledgement

I would like to thank the following individuals, without whom I would not have been able to complete this research and without whom I would not have completed my PhD.

First and foremost, I would like to express my sincere gratitude to my first supervisor PD Dr. Udo Hartwig (III. Department of Medicine, University Medical Center of Johannes Gutenberg University Mainz) for his consistent support and guidance during the running of this project. Thanks for giving me the opportunity to participate in his scientific working group on such a relevant and interesting topic!

In addition, I would like to acknowledge PD Dr. Ernesto Bockamp (Institute for Translational Immunology, University Medical Center of Johannes Gutenberg University Mainz) as the second supervisor of this thesis.

I would also like to thank the following experts that participated in this study: Jacqueline Douglass (John Hopkins University School of Medicine, USA), Prof. Dr. Bert Vogelstein (John Hopkins University School of Medicine, USA), Prof. Dr. Matthias Peipp (University Medical Center Schleswig-Holstein, Germany), Dr. Christian Klein (Roche Innovation Center Zurich, Switzerland), and Prof. Dr. Hinrich Abken (University Hospital Regensburg, Germany). My gratitude and indebtedness to them goes beyond words for sharing expertise, as well as for their sincere and helpful guidance and encouragement.

I am grateful to all the lab members who have taught me a great deal about scientific research and life in general. A special thank you goes out to our technical assistant Shamsul Khan for his technical assistance, guidance, and valuable suggestions throughout the project.

In the pursuit of this project, nobody has been more important to me than the members of my family. It is my privilege to express my gratitude to my parents, whose love and guidance remain with me throughout my life. My parents have been my role models throughout my life. In particular, I am grateful for my amazing brother, who provides me with endless inspiration.

Declarations

I hereby certify that I have written the dissertation independently. Additionally, no academic degree has been awarded to this scientific work by any other German or foreign university or any comparable institution.

Furthermore, I confirm that I have not previously completed another doctoral or equivalent program in the subject area of this doctoral program.

I hereby declare that I wrote the dissertation submitted without any unauthorized external assistance and used only sources acknowledged in the work. All textual passages which are appropriated verbatim or paraphrased from published and unpublished texts as well as all information obtained from oral sources are duly indicated and listed in accordance with bibliographical rules. In carrying out this research, I complied with the rules of standard scientific practice as formulated in the statutes of Johannes Gutenberg University Mainz to insure standard scientific practice.

____Mainz, 22.07.2024_____ ____Saber Ebrahimi_____

Place, Date Signature